RIGID FRAME STUDIES

Progress Report

Development of Simplified Design Methodology for Tapered Beams

Submitted to

Star Manufacturing Co.
Oklahoma City, Oklahoma

by

Priscilla Nelson

and

Thomas M. Murray, P.E.
Associate Professor

School of Civil Engineering and Environmental Science
University of Oklahoma
Norman, Oklahoma

August, 1979

TABLE OF CONTENTS

LIST OF ILLUSTRATIONS

LIST OF TABLES

ABSTRACT

This study is concerned with the elastic stability analysis of simply supported tapered members loaded by end moments. The governing differential equations are derived and a numerical solution technique is described. A computer program was developed to perform the analysis and solutions are presented for both singly - and doubly - symmetrical tapered and prismatic members. The results are compared to closed-form and finite difference solutions available in the literature. The finite element method was used to compare the results for tapered and prismatic members. Agreement of solutions shows the proposed analysis technique to be accurate in determining the buckling loads of tapered elastic members.

Using solutions generated with this program, and a multiple linear regression technique, a simplified precedure for the calculation of critical buckling loads is presented. This procedure is statistically verified and, within the noted limitations, will be accurate to ±8% for tapered beams in single curvature and ± 12% for double curvature.

RIGID FRAME STUDIES

CHAPTER I

INTRODUCTION

1.1 General

Prismatic structural steel beams with H-shaped cross-sections are commonly used in conventionally designed frames. The cross-section is usually selected to resist a maximum stress at a single location along the member, although the stresses elsewhere may be considerably lower. Noting such inherent inefficiency, Aminikian (1), in 1952, suggested the use of tapered beams in which the web and/or flange dimensions are varied along a member to provide only the strength required at any location. Following his suggestion, much experimental and theoretical work has been reported on, resulting in the adoption of a recommended design procedure for doubly symmetric web-tapered or "wedge" beams into the American Institute of Steel Construction Specification for the Design, Fabrication, and Erection of Structural Steel for Buildings (2) (henceforth referred to as the AISC Specification). This procedure, included as Supplement No. 3, was adopted in 1974, and represents the

first time provisions for the design of tapered members were included in North American specifications. Appendix D of the 1979 AISC Specification covers the design of doubly symmetric web-tapered members satisfying certain requirements (3).

The current use of high strength steels, together with the emphasis placed on material optimization, results in flexural members with high flange stresses. These higher stresses result in an increased potential for failure by elastic lateral-torsional buckling. For wedge beams, with higher average flange stresses, elastic lateral-torsional buckling becomes an increasingly likely failure mode. Since design equations including inelastic effects are traditionally based on modifications of equations derived for elastic behavior, an understanding of elastic buckling is first necessary to develop a complete design procedures.

The purpose of this study is to develop a rational, simplified procedure for the design of tapered beams with doubly or singly symmetrical cross-sections where lateral torsional stability is the assumed failure mode. A literature survey of previous investigations is first presented. Papers and texts giving historical perspective of stability in general and lateral torsional buckling in particular are cited. The governing differential equations for beam stability are derived and a solution technique presented. A design methodology for simply supported flexural members which uses basic equations from classical stability analysis but modified to account for taper and varying end moments is proposed. Consideration is extended to sections with only one plane of symmetry with respect to the axis of bending.

1.2 Historical Perspective and Recent Literature

1.2.1 Elastic Instability of Prismatic Beams

The problem of elastic instability was first discussed in conjunction with lateral buckling of compression members. In the 18th Century, Euler presented a theoretical treatment of the elastic stability of concentrically loaded compression members and van Musschenbrock performed several experiments to determine the elastic capacity of columns with solid rectangular cross-sections (discussed in Ref. 4). At that time, the principal structural materials were wood and stone which exhibit low strength and unpredictable behavior, resulting in the use of stocky members for which yielding or bearing failure occurs before elastic instability. Thus, the theories developed in the 18th century found little application until the introduction of wrought iron and steel in the 19th Century. These higher strength materials allowed the use of more slender members to resist both concentric compressive and flexural loadings and interest in buckling increased. In the late 19th and early 20th Centuries much experimental and theoretical work was conducted, resulting in the currently accepted procedures for column stability consideration. A complete account of the development of column stability analysis is found in the texts by Bleich (5), Timoshenko (6), Timoshenko and Gere (7), Galambos (8) and in the Structural Stability Research Council's Guide to Stability Design Criteria for Metal Structures (9).

The combined mode of failure, lateral-torsional buckling was first considered in 1899 by Prandtl (9). In this failure mode, a critical magnitude of the applied loading is reached when a bifurcation of

the equilibrium is possible and out-of-plane lateral deflections occur simultaneously with twist about the deflected shear center. Torsional buckling, as a distinct mode of failure of compression members was investigated by Wagner (10) in 1929. Wagner explained that initial deflections cause axial compressive stresses to exert a disturbing torque. This explanation has been referred to as the Wagner effect (21) and is discussed in detail in Chapter II.

The analysis of beam failure by lateral-torsional buckling has historically been made with one of three approaches. Timoshenko (11) derived the pertinent differential equations describing the instability of thin walled members by considering the equilibrium of a finite portion of the buckled beam. This procedure leads to three simultaneous equations, two of which are second order and one third order. These equations are coupled for the general case of unspecified symmetry of the cross-section. Vlasov (12) has derived similar equations by considering the equilibrium of an infinitesimally small element of the buckled beam. This procedure leads to three fourth order differential equations, again coupled for the unsymmetrical case and is more general than the equations derived by Timoshenko in that the statical boundary conditions are not used in the derivation. F. Bleich and H. Bleich (13) derived the differential equations from the theorem of stationary potential energy and established the generality of the equations provided the axis defined by the cross-section shear center is chosen as the reference coordinate for displacements (5). These differential equations can only be uncoupled if symmetry of the cross-section and location of the applied load is specified.

Each of these approaches involve the assumption that while plane cross-sections warp, their geometric shape does not change during buckling. Additional simplification is possible when it is assumed that shear strains have no effect on the deformations. The incorporation of solutions of these differential equations into the design process is discussed in Section 1.2.3.

1.2.2 Elastic Stability of Tapered Beams

Research into the elastic instability of tapered beams has only recently been conducted. Lee (11) in 1956 derived equations for non-uniform torsion of tapered I-beams, ignoring the effect of web deformation. By specifying double symmetry of the cross-section Lee found that the equations become uncoupled. Lee noted that the beam acts as two flanges in bending and torsion, and that the web is ineffective in resistance to out-of-plane bending. He also demonstrated experimentally that the term concerned with torsionally induced shear stresses remains unchanged in tapered beams from that derived by Timoshenko for prismatic beams.

Culver and Preg (15,16) derived differential equations for tapered beam stability using the Vlasov's approach (12), and used the finite difference method to evaluate critical moments for beams of varying web tapers, support conditions, and end moments.

Lee, Morrell and Ketter (17) investigated the stability of doubly symmetric tapered members under varying end moments using a minimum potential energy approach. Only members linearly tapered in depth were considered. The strain energy functional was derived from potential energy considerations, and the Rayleigh-Ritz Method was

employed for the solution. Chi (18) performed a similar study but included singly symmetrical tapered members. In both of these studies, polynomial displacement functions were chosen for use in an approximate solution. As is discussed in Chapter II, the functional derived in the above studies does not include all natural boundary conditions required by the statics of the problem, and it appears that the conclusions drawn in these two studies are valid only for the case of a uniform moment.

Trahair and his research team (19,20,21) have investigated the lateral stability of stepped and uniformly tapered, singly and doubly symmetric beams. In Ref. 21, Trahair and Kitipornchai note that for an arbitrary tapering of any cross-section dimension, the loci of shear center and centroid locations are inclined toward each other and the out-of-plane bending action and the torsion action are interdependent. Trahair and Kitipornchai derived a set of differential equations which are valid for tapered beams with at least one plane of symmetry in the cross-section. These equations were solved by the finite integral method for the case of a beam with flange width taper and the solutions were verified experimentally. The approach of Trahair and Kitipornchai will be used in deriving the differential equations used in this study.

1.2.3 Suggested Design Procedures

An exact solution of the governing differential equations for lateral-torsional buckling of beams is only available for prismatic beams under uniform moment. In 1943, Winter (22) presented approximate equations for the calculation of critical moments of singly symmetrical I-beams, derived using Rayleigh's energy method. de Vries (23) presented several empirical equations to deal with cases of transverse loadings

and Hall (24) in a discussion of de Vries' article recommended that the case of uniform moment be used as a basic case for further simplifications. Salvadori (25,26), using an approach similar to that of Lee (17) and Chi (18) but with trigonometric series as displacement functions, calculated the critical buckling moment for cases of varying end moments applied to doubly symmetric prismatic beams. The results and recommendations of Salvadori (26) have been incorporated into the AISC Specification as the multiplying factor, C_b. This factor, a function of end moment magnitudes, is applied to the critical moment as calculated from an equation which represents the closed form solution for the case of uniform moment along the member.

Clark and Hill (27) obtained solutions in a similar manner for both singly and doubly symmetrical beams subjected to a variety of support and loading conditions. They obtained separate modifying factors, for use with the closed form solution mentioned previously. This procedure allows the designer to include effects of unequal end moments, location of transverse load with respect to the centroidal axis, load distribution and end restraint. A summary of their findings is included in the Structural Stability Research Council Guide (9).

Morrell and Lee (28) used the results presented in a previous paper (17) to develop allowable stress formulas for the proportioning of doubly symmetrical web tapered members. Their approach was to modify existing AISC design equations for prismatic members by adjusting the length of a prismatic beam having the same cross-section dimensions as the smaller end of the tapered member. Their goal was to invent a prismatic beam with a critical stress equal to the critical stress of

the tapered beam. This approach has been adopted in Appendix D of the current AISC Specification (3).

The simplicity of the use of modifying factors, such as suggested by Salvadori, as compared to the Lee and Morrell approach, is immediately appreciated. It is the aim of this study to determine analogous modifying factors to permit a simplified design procedure for tapered beams under moment gradient.

1.3 Scope of Study

The design rules provided in the AISC specification are limited to tapered members with at least one axis of symmetry perpendicular to the plane of bending and the flanges must be of equal and constant area. Because local buckling considerations may require greater area in the compression flange than is needed in the tension flange, economy in tapered members may frequently be achieved through the use of different flange sizes. For this reason, this study is undertaken to extend the basic theory for the stability analysis of tapered doubly symmetrical beams to singly symmetric tapered beams.

Current AISC design proceedings for the design of tapered beams incorporate the use of length modification factors in conventional AISC prismatic member design formulas. Two equations are required for these factors as thin, deep sections are distinguished from thick, shallow sections in the calculation of allowable stresses. These length modification factors introduce design complication, and make it difficult for the designer to develop an appreciation of the effect of various parameters on buckling strength.

The study described here is an investigation of the lateral-torsional stability of tapered sections under stress gradients induced by unequal applied end moments. Cross-sections included in this study are restricted to built-up members composed of relatively thin plates and with one axis of symmetry in the plane of bending. The governing differential equations are derived using the method of Trahair and Kitipornchai (21) and solved using a Galerkin series approximation. The critical buckling solutions obtained are verified using a finite element procedure. Individual modifying coefficients to account for taper and moment gradient are then developed from these results using a multiple linear regression technique. The work of Galambos (8), Vlasov (12), Trahair and Kitipornchai (21), and Trahair (29) are freely consulted in the derivation and solution of the governing differential equations.

CHAPTER II

THEORETICAL ANALYSIS

2.1 Differential Equations of Bending and Torsion

Only web-tapered beams with uniform web thickness and flanges of constant dimensions are included in this study. The tapering is assumed to be linear and only simply supported beams loaded by end moments are considered. Reactions, induced in the cases of unequal end moments, are assumed to act through the shear center.

Defining a centroidal coordinate system as shown in Figure 2.1, where the z-axis is the locus of centroids and the y-axis is the plane of symmetry, all cross-section properties are then functions of the distance z from the origin of the coordinate system. For the linearly tapered member shown in Figure 2.2, the depth of any distance z from the left end can be expressed as:

$$d_z = d_L + \alpha z \tag{2.1}$$

where α is the taper given by

$$\alpha = \frac{d_R - d_L}{\ell} \tag{2.2}$$

where d_R and d_L are the depths at the left and right ends of the member and ℓ is the member length. Thus α is positive if the small end is located at the origin and negative if the large end is located at the origin.

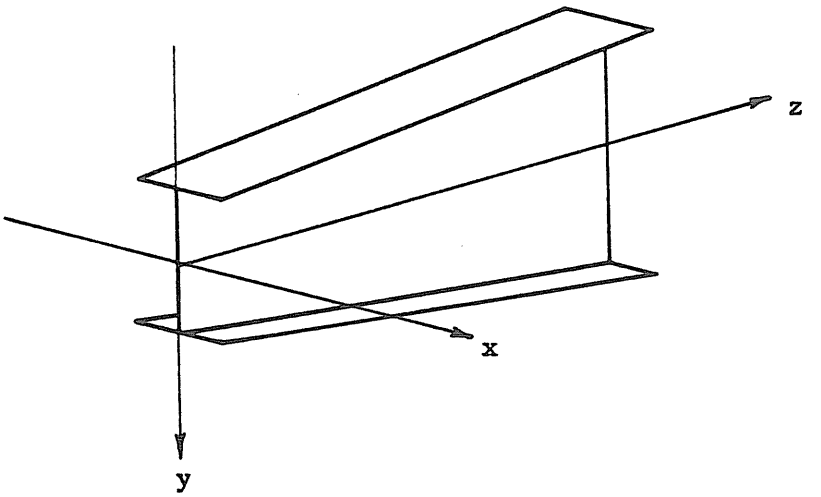

Fig 2.1 Centroidal Coordinate System

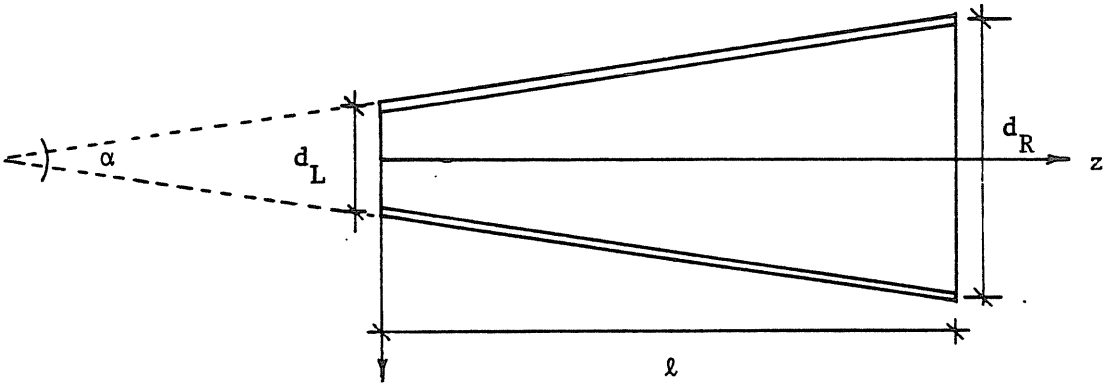

Fig. 2.2 Tapered Beam Geometry

The following assumptions are made:

1) the material behaves elastically;

2) there are no residual stresses;

3) the member is initially straight and untwisted;

4) the moment of inertia about the x-axis is significantly larger than that about the y-axis;

5) the external moments are applied about the x-axis of the member;

6) the member has a taper less than 10^{o};

7) plane cross-sections do not change in geometric shape during buckling;

8) shear strains have no effect on the deformations and may be disregarded.

Assumption 4 was made by Salvadori (25) and allows deflections in the plane of the web to be neglected when considering lateral stability. Assumption 6 is made in conjunction with the findings of Boley (30). By restricting beams to a maximum of 10^{o} taper (1 in 12 slope for each flange), less than a 2% error may be expected when using standard flexural formulas for the calculation of normal stresses. Assumptions 7 and 8 are consistant with the assumptions of Vlasov (12). By using these assumptions, it is possible to separate the combined bending and torsion of a member into two independent bending actions.

2.1.1 Major Axis Bending

In accordance with assumption 6, the differential equation for major axis bending of nonprismatic beams is assumed to be of the same form as for a uniform beam (14), i.e.,

$$M_x = -EI_x(z)v'' \tag{2.3}$$

where $I_x(z)$ is the major axis moment of inertia which varies along the beam and v is the y-axis or in-plane deflection. Here, and elsewhere in this paper, the primes refer to differentiation with respect to z. This equation is independent of the minor axis (out-of-plane) deflection, u, and the angle of twist, ϕ.

2.1.2 Minor Axis Bending

In general, out-of-plane displacement will be accompanied with rotation, as shown in Figure 2.3. With the subscripts t and b referring to the top and bottom flanges and assuming no distortion of the cross-section, the displacements of the flanges are related to u and ϕ as

$$u_t = u + a_t\phi \tag{2.4a}$$

$$u_b = u - a_b\phi \tag{2.4b}$$

where a_t and a_b are the distances from the shear center to the respective flanges and are given by:

$$a_t = \frac{I_{fb}}{I_y} d_z \tag{2.5a}$$

$$a_b = \frac{I_{ft}}{I_y} d_z \tag{2.5b}$$

In these equations, I_{fb} and I_{ft} are the moments of inertia of each flange about the y axis and d_z is the depth at any arbitrary distance from the origin, as specified in Eq. 2.1.

Neglecting the effect of the web on warping, the flange bending moments are related to flange curvatures as:

$$M_{ft} = EI_{ft}u_t'' = EI_{ft}\left[\frac{d^2u}{dz^2} + \frac{d^2(a_t\phi)}{dz^2}\right] \tag{2.6a}$$

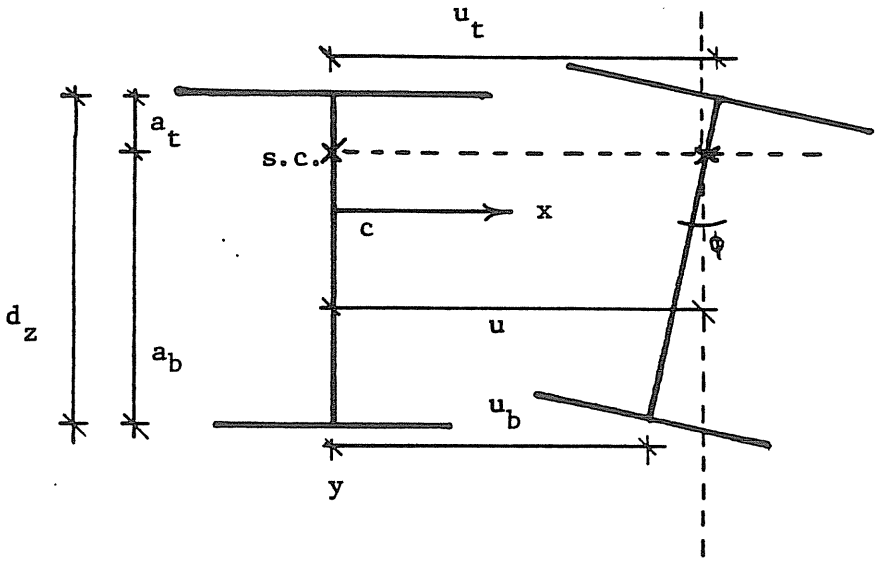

Fig. 2.3 Out-of-Plane Deflection Coupled with Twisting

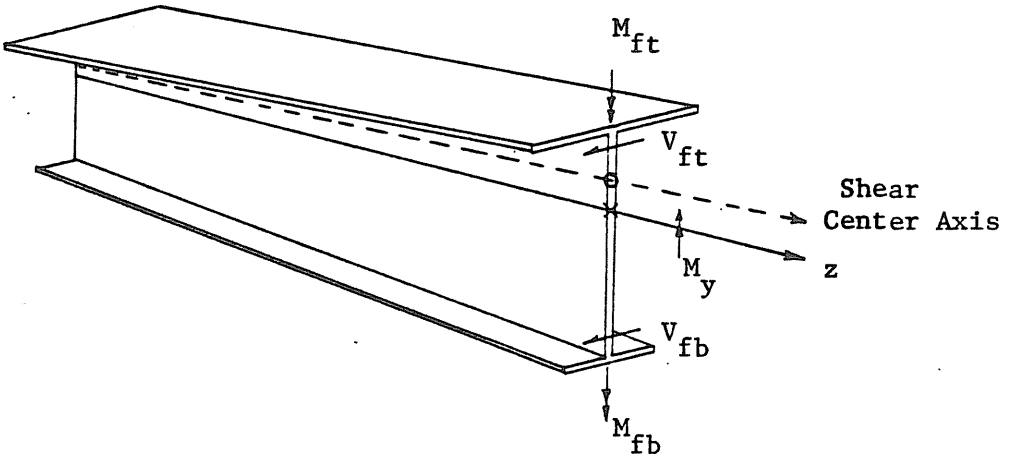

Fig. 2.4 Relationship of Flange Shears and Flange Moments

$$M_{fb} = EI_{fb}u''_b = EI_{fb}[\frac{d^2u}{dz^2} - \frac{d^2(a_b\phi)}{dz^2}] \quad (2.6b)$$

and the total minor axis bending moment is

$$M_y = M_{ft} + M_{fb} \quad (2.7)$$

Substituting Eqs. 2.5 and 2.6 into Eq. 2.7, the minor axis bending moment becomes

$$M_y = E(I_{ft} + I_{fb})u'' + E(a_tI_{ft} - a_bI_{fb})\phi'' + 2E(a'_tI_{ft} - a'_bI_{fb})\phi' + E(a''_TI_{ft} - a''_bI_{fb})\phi \quad (2.8)$$

Neglecting the contribution of the web to the y-axis moment of inertia, I_y can be written as

$$I_y = I_{ft} + I_{fb} \quad (2.9)$$

Neglecting second order derivatives of "a" as small, and noting that

$$a_tI_{ft} = [\frac{I_{fb}}{I_y}(d_L + \alpha z)]I_{ft} = \frac{I_{ft}I_{fb}}{I_y}(d_L + \alpha z) \quad (2.10a)$$

$$a_bI_{fb} = [\frac{I_{ft}}{I_y}(d_L + \alpha z)]I_{fb} = \frac{I_{ft}I_{fb}}{I_y}(d_L + \alpha z) \quad (2.10b)$$

the second term of equation 2.8 is equal to zero and the equation may be rewritten as

$$M_y = EI_yu'' + EI_{\psi x}\phi' \quad (2.11)$$

with the additional beam property, $I_{\psi x}$, defined as

$$I_{\psi x} = a'_tI_{ft} - a'_bI_{ft} \quad (2.12)$$

2.1.3 Torsion

In general, the total torque, T_{sc}, acting about the shear center axis may be considered to be comprised of three components (21),

$$T_{sc} = T_{sv} + T_f + T_w \quad (2.13)$$

where T_{sv} is the Saint Venant torque, T_f is the flange shear or warping torque, and T_w is the torque due to the Wagner effect. It has been demonstrated (14, 31) that the St. Venant component is the same for tapered beams as it is for prismatic members:

$$T_{sv} = GJ(z)\phi' \tag{2.14}$$

where GJ is the torsional rigidity of the section at a distance z, from the origin and ϕ is the angle of twist at a section. The second term in Eq. 2.13 results from the out-of-plane displacements of the flanges which induce flange shears and with reference to Fig. 2.4, these flange shears are expressed as:

$$V_{ft} = \frac{-dM_{ft}}{dz} \tag{2.15a}$$

$$V_{fb} = \frac{-dM_{fb}}{dz} \tag{2.15b}$$

Since the flange moments are inclined at angles to the shear center axis as shown in Fig. 2.5, the warping component of torsion is expressed as:

$$T_f = (a_t V_{ft} - a_b V_{fb}) + (M_{ft} \frac{da_t}{dz} - M_{fb} \frac{da_b}{dz}) \tag{2.16}$$

or, on substitution of Eq. 2.15,

$$T_f = -a_t \frac{dM_{ft}}{dz} + a_b \frac{dM_{fb}}{dz} + M_{ft} \frac{da_t}{dz} - M_{fb} \frac{da_b}{dz} \tag{2.17}$$

which can be rewritten as:

$$T_f = \frac{-d}{dz}(a_t M_{ft} - a_b M_{fb}) + 2(a_t' M_{ft} - a_b' M_{fb}) \tag{2.18}$$

Substituting Eqs. 2.5 and 2.6 into the first term of Eq. 2.18 yields

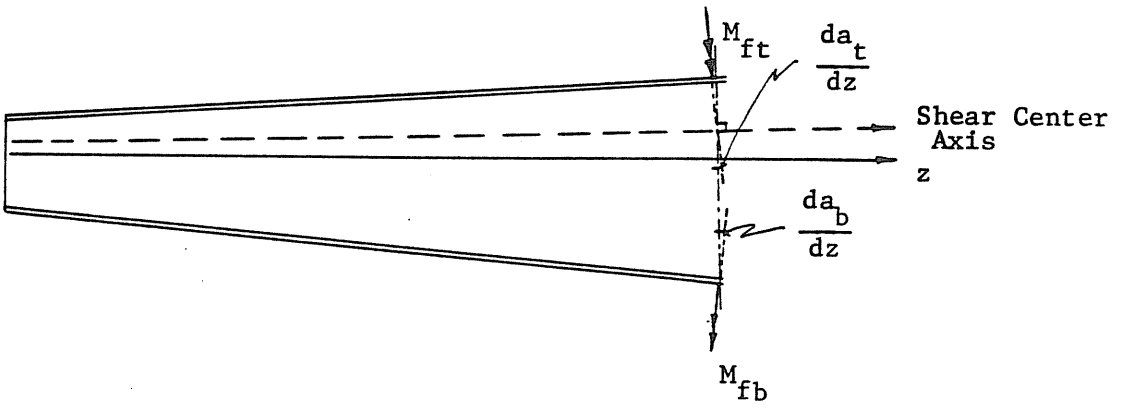

Fig. 2.5 Inclination of Flange Moments

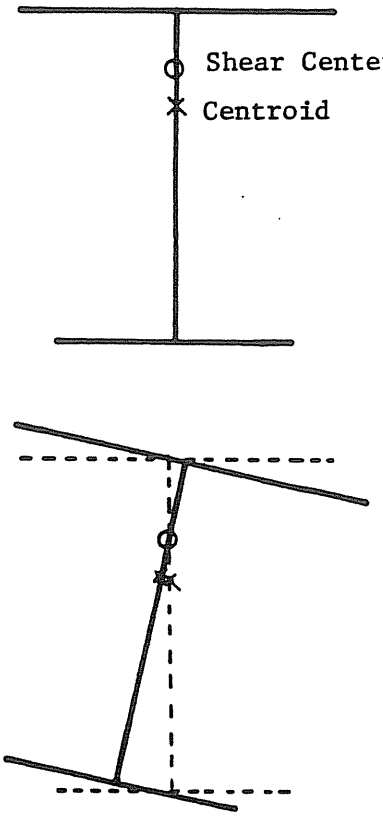

Fig. 2.6 Displacement and Rotation of a Mono-Symmetric Cross Section

$$\frac{-d}{dz}(a_t M_{ft} - a_b M_{fb}) = \frac{-Ed}{dz}[\frac{I_{fb}I_{ft}}{I_y}d_z u'' - \frac{I_{ft}I_{fb}}{I_y}d_z u'' + \frac{I_{fb}d_z}{I_y}\frac{d^2}{dz^2}(a_t\phi) + \frac{I_{ft}d_z}{I_y}\frac{d^2}{dz^2}(a_b\phi)] \quad (2.19)$$

Noting that the u" terms cancel, expanding and neglecting second order derivatives of "a" as small, this term becomes

$$\frac{-d}{dz}(a_t M_{ft} - a_b M_{fb}) = \frac{-Ed}{dz}[a_t^2 I_{ft}\phi'' + a_b^2 I_{fb}\phi'' - 2(a_t I_{ft}a_t' + a_b I_{fb}a_b')\phi'] \quad (2.20)$$

A similar sequence of substitutions into the second term of equation 2.18 results in the following equation for the flange warping component of torsion,

$$T_f = \frac{-d}{dz}(EI_w\phi'')\ \frac{-d}{dz}(EI_{w\psi}\phi') + EI_{\psi x}u'' + EI_{w\psi}\phi'' + EI_\psi\phi' \quad (2.21)$$

where the additional beam properties are defined as

$$I_w = a_t^2 I_{ft} + a_b^2 I_{fb} \quad (2.22a)$$

$$I_{w\psi} = 2(a_t I_{ft}a_t' + a_b I_{fb}a_b') \quad (2.22b)$$

$$I_{wx} = a_t' I_{ft} - a_b' I_{fb} \quad (2.22c)$$

$$I_\phi = 4[(a_t')^2 I_{ft} + (a_b')^2 I_{fb}] \quad (2.22d)$$

When a monosymmetric thin-walled beam loaded in its plane of symmetry is twisted, as in the case of lateral torsional buckling, normal stresses present will exert an additional disturbing torque.

This occurs because the shear center axis, or center of twist, does not coincide with the centroidal axis and any twisting which occurs causes the centroidal axis to deflect, as shown in Figure 2.6. As a result, portions of the section are further strained by the small additional bending while other parts experience unloading. In singly symmetric sections, these effects will cancel out. In addition, the longitudinal flange force vectors are rotated such that components transverse to the shear center axis are developed as shown in Figure 2.7. These components produce a net torque on the beam.

The effect of this disturbing torque was first explained by Wagner (7) and can be thought of as reducing the torsional stiffness of compression elements and increasing the torsional stiffness of tension elements (21). In doubly symmetric beams without residual stresses, the effect of these tension and compression flange torques cancel. In a singly symmetric beam, the small flange is the farther from the shear center and the stresses and torque resulting from the small flange force are greater. Thus, the state of stress in the small flange predominates in the Wagner effect. When the small flange is in tension the torsional stiffness is increased; when the small flange is in compression the torsional stiffness is reduced.

For tapered, singly symmetric beams, the distance ρ, Fig. 2.8, from any fiber to the shear center varies along the beam. When the cross section twists and warps, any longitudinal stresses develop components transverse to the shear center line and, in general, these transverse force components are

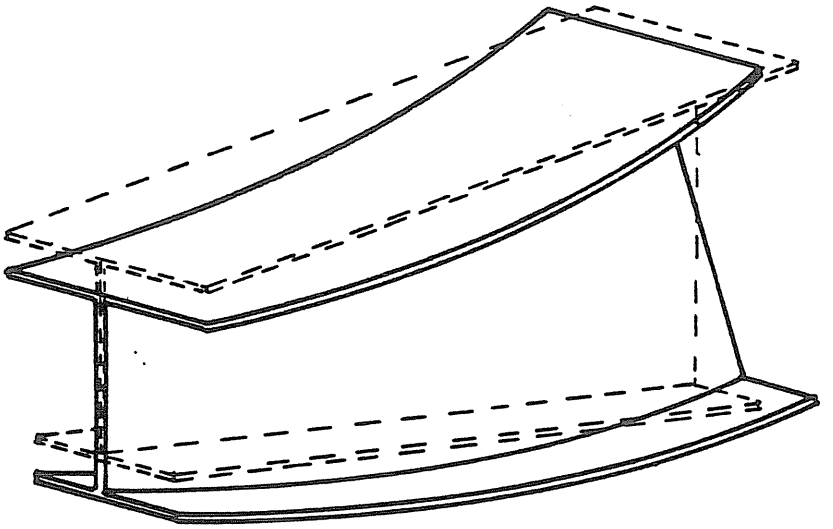

Fig. 2.7a The Wagner Effect - Major Axis Bending of a Singly Symmetric Beam

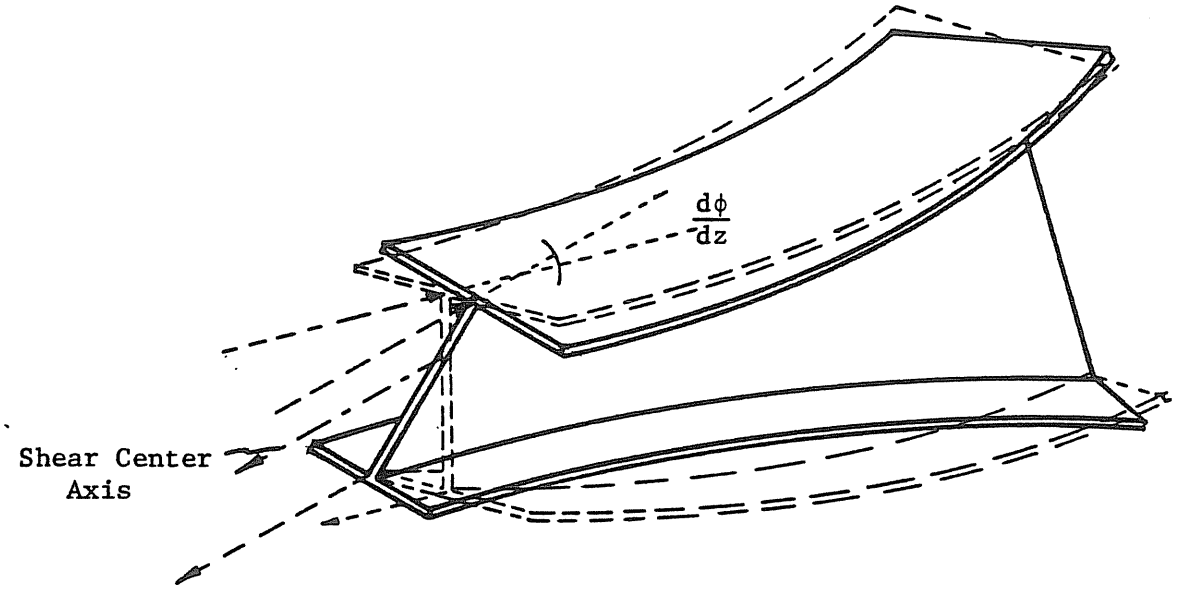

Fig. 2.7b The Wagner Effect - Shear Center Twist Producing a Disturbing Torque as Flange Force Vectors Are Rotated

$$dF = f \frac{d(\rho\phi)}{dz} dA \tag{2.23}$$

The resulting torque is then

$$T_w = \int_A \rho dF = \int_A \rho f \frac{d}{dz}(\rho\phi) dA \tag{2.24}$$

where

$$f = \pm \frac{M_x y}{I_x} \pm \frac{M_y x}{I_y} \pm \text{Residual Stresses} \tag{2.25}$$

Since residual stresses are ignored in this analysis and the cross-section is assumed to be symmetric with respect to the y-axis so that the effects of the minor axis bending moments cancel, the torsion equation may be rewritten as

$$T_w = \int_A \frac{M_x y}{I_x} \frac{d}{dx}(\rho\phi) dA \tag{2.26}$$

or

$$T_w = M_x \beta_x \phi' + M_x \bar{\beta}_x \phi \tag{2.27}$$

where the additional section properties are defined as

$$\beta_x = \frac{1}{I_x} \int_A \rho^2 y dA \tag{2.28a}$$

$$\bar{\beta}_x = \frac{1}{I_x} \int_A \rho \frac{d\rho}{dz} y dA \tag{2.28b}$$

The differential equation for torsion with respect to the shear center is then

$$T_{sc} = GJ(z)\phi' - \frac{d}{dz}(EI_w(z)\phi'') - \frac{d}{dz}(EI_{w\psi}(z)\phi') - EI_{\psi x}(z)u'' + EI_{w\psi}(z)\phi'' +$$

$$EI_{\psi}(z)\phi' + M_x(z)\beta_x(z)\phi' + M_x(z)\bar{\beta}_x(z)\phi \tag{2.29}$$

For the mono-symmetric cross-section, shown in Fig. 2.9, distances from points on the flanges to the shear center are

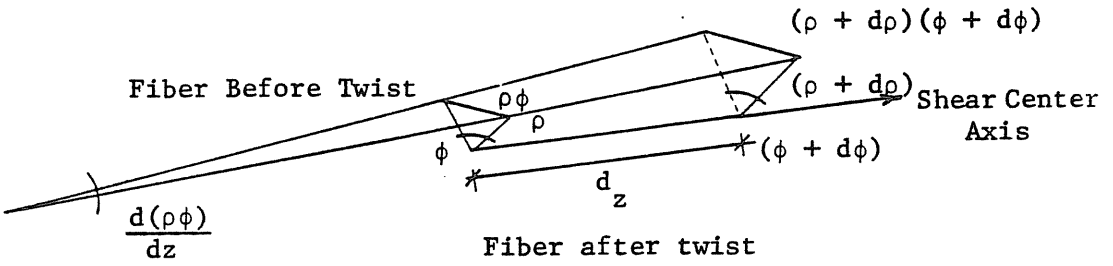

Fig. 2.8 Displacement of Longitudinal Fiber During Twisting (after Trahair, (21))

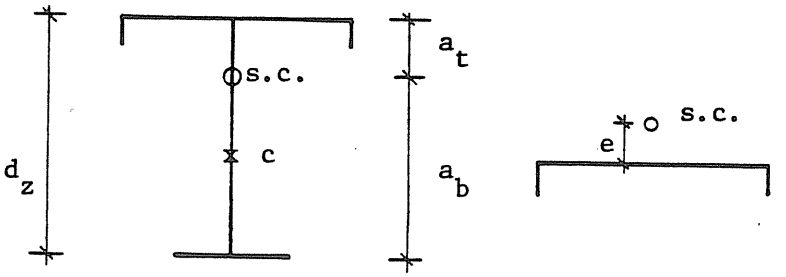

Fig. 2.9 Generalized Mono-Symmetric Cross-Section

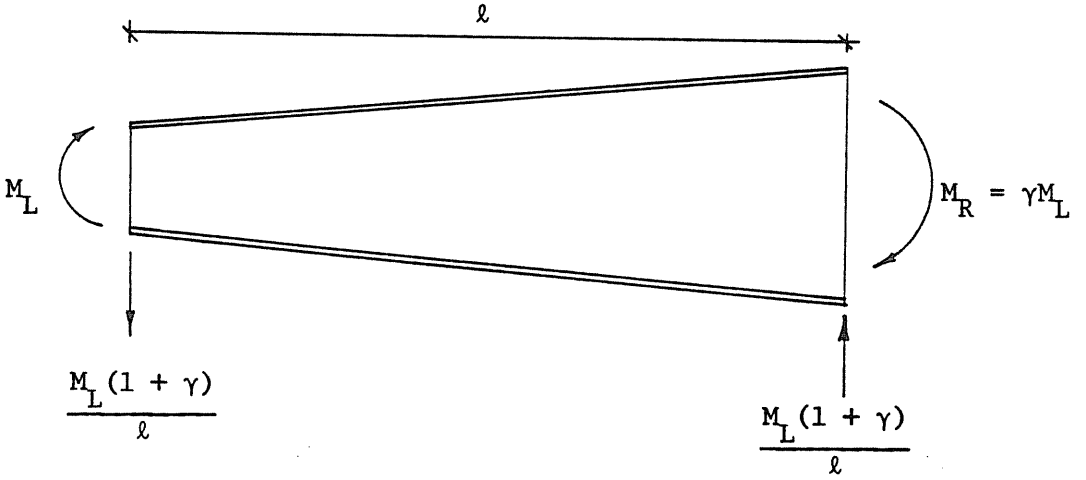

Fig. 2.10 Applied Major Axis Loading Condition

$$a_t = \frac{I_{fb}}{I_y}(d_L + \alpha z + e) \tag{2.30a}$$

$$a_b = \frac{I_{ft}}{I_y}(d_L + \alpha z + e) \tag{2.30b}$$

where e is the distance from the channel web line element to the channel shear center along the axis of symmetry. Other section properties are

$$I_w = (d_L + \alpha z + e)^2 \frac{I_{fb}I_{ft}}{I_y} \tag{2.31}$$

$$I_{w\psi} = \frac{2I_{fb}I_{ft}}{I_y} \alpha(d_L + \alpha z + e) \tag{2.32}$$

$$I_\psi = 4\alpha^2 \frac{I_{fb}I_{ft}}{I_y} \tag{2.33}$$

$$I_{\psi x} = 0 \tag{2.34}$$

Thus, the differential equation for torsion about the shear center is

$$T_{sc} = GJ(z)\phi' - \frac{d}{dz}(EI_w(z)\phi'') - \frac{d}{dz}(EI_{w\psi}(z)\phi') + EI_{w\psi}(z)\phi'' + EI_\psi(z)\phi' +$$

$$M_x\beta_x(z)\phi' + M_x\bar{\beta}_x(z)\phi \tag{2.35}$$

2.1.4 External Moments and Torques

Equations 2.3, 2.11 and 2.35 are general equations valid for any support conditions or loadings. The external moments and torques are now evaluated for the specific case of a simply supported tapered beam loaded only by end moments.

Using the sign convention for the applied moments shown in Fig. 2.10, the moment at any section z from the origin is

$$M_x(z) = M_L(1 - (1 + \gamma)\frac{z}{\ell}) \tag{2.36}$$

where γ is the end moment ratio

$$\gamma = \frac{M_R}{M_L} \tag{2.37}$$

Referring to Fig. 2.11, and assuming that ϕ is small, so that $\sin\phi$ may be approximated as ϕ, the y-axis moment can be written as

$$M_y(z) = -M_x(z)\phi = -M_L\phi(1 - (\gamma + 1)\frac{z}{\ell}) \tag{2.38}$$

With reference to Fig. 2.12, it can be seen that external torque is supplied from two sorces: (1) The reaction, indicated in Fig. 2.10, produces a torsional component as it acts through the out-of-plane displacement, u. (2) This displacement also generates a torsional component from the major axis bending. Thus, the total external torque, again assuming small angles so that cos u' may be approximated as 1.0, may be written as

$$T_{sc} = M_L(1 - (1 + \gamma)\frac{z}{\ell})u' + M_L(\frac{1 + \gamma}{\ell})u \tag{2.39}$$

and if I_y is assumed constant for a beam tapered in depth only, the complete equations become:

In-plane Bending

$$M_L(1 - (1 + \gamma)\frac{z}{\ell}) = -EI_x(z)v'' \tag{2.40}$$

Out of Plane Bending

$$-M_L\phi(1 - (1 + \gamma)\frac{z}{\ell}) = EI_y u'' \tag{2.41}$$

Torsion

$$M_L u'(1 - (1 + \gamma)\frac{z}{\ell}) + M_L(\frac{1 + \gamma}{\ell})u = GJ(z)\phi' - \frac{d}{dz}(EI_w(z)\phi'') - \frac{d}{dz}(EI_{w\psi}(z)\phi')$$

$$+ EI_{w\psi}(z)\phi'' + EI_\psi(z)\phi' + M_L(1 - (1 + \gamma)\frac{z}{\ell})\,[\beta_x(z)\phi' + \bar{\beta}_x(z)\phi] \tag{2.42}$$

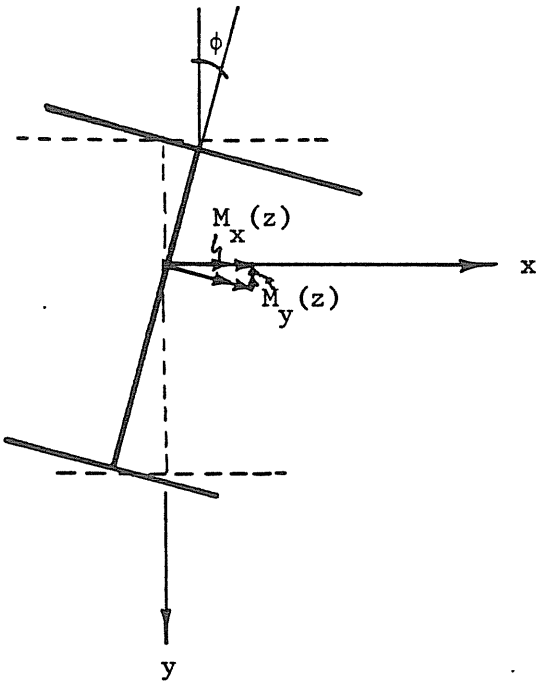

Fig. 2.11 Applied Minor Axis Moment

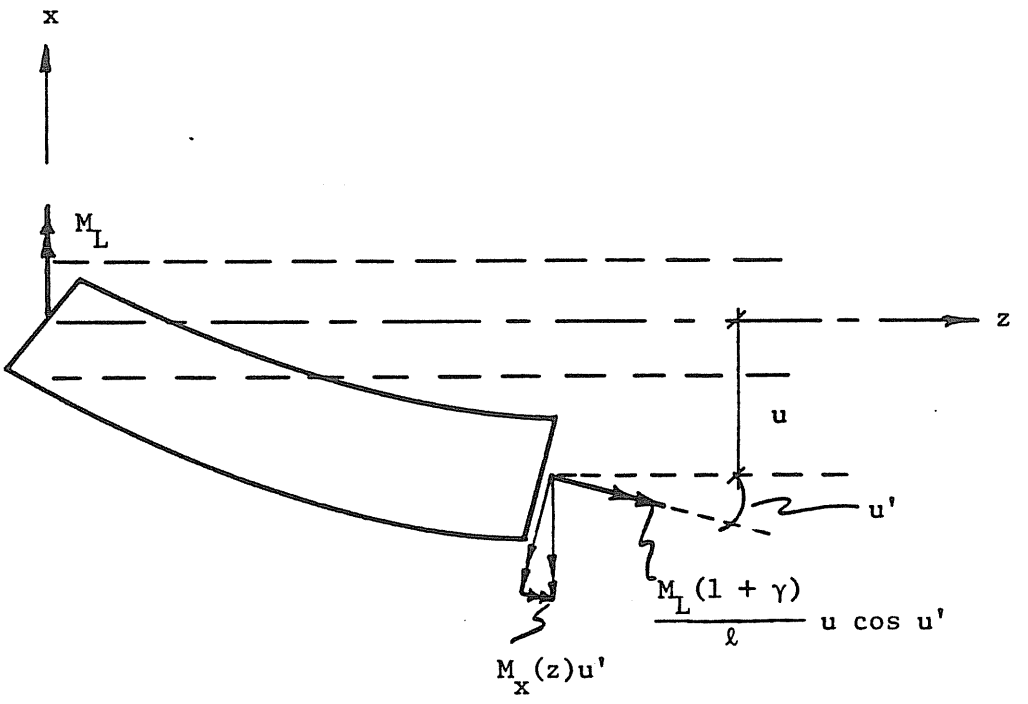

Fig. 2.12 External Applied Torque (plan view)

2.2 Solution of the Differential Equations

Taking two derivatives of Eqs. 2.40 and 2.41, and one derivative of Eq. 2.42, the corresponding fourth order differential equations are

$$\frac{d^2}{dz^2}(EI_x(z)v'') + \frac{d^2}{dz^2}(M_x) = 0 \tag{2.43}$$

$$\frac{d^2}{dz^2}(EI_y u'') + \frac{d^2}{dz^2}(M_x\phi) = 0 \tag{2.44}$$

$$\frac{d}{dz}(M_x u') + \frac{d}{dz}(Ru) - \frac{d}{dz}(GJ(z)\phi') + \frac{d^2}{dz^2}(EI_w(z)\phi'') + \frac{d^2}{dz^2}(EI_{w\psi}(z)\phi') -$$

$$\frac{d}{dz}(EI_{w\psi}(z)\phi'') - \frac{d}{dz}(EI_\psi(z)\phi') - \frac{d}{dz}\left\{M_x[\beta_x(z)\phi' + \bar{\beta}_x(z)\phi]\right\} = 0 \tag{2.45}$$

with abbreviations

$$M_x = M_L(1 - (1 + \gamma)\frac{z}{\ell}) \tag{2.46a}$$

$$R = (\frac{1 + \gamma}{\ell})M_L \tag{2.46b}$$

Noting that

$$\frac{d^2}{dz^2}(M_x\phi) = M_x''\phi + 2M_x'\phi' + M_x\phi'' \tag{2.47}$$

$$M_x' = -\frac{(1 + \gamma)}{\ell}M_L \tag{2.48}$$

$$M_x'' = 0 \tag{2.49}$$

Eq. 2.44 can be rewritten as

$$\frac{d^2}{dz^2}(EI_y u'') - 2R\phi' + M_x\phi'' = 0 \tag{2.50}$$

Noting that, with reference to Eq. 2.45,

$$\frac{d}{dz}(M_x u') = M_x' u' + M_x u'' = -Ru' + M_x u'' \tag{2.51}$$

$$R' = 0 \tag{2.52}$$

$$\frac{d}{dz}(Ru) = R'u + Ru' = Ru' \tag{2.53}$$

the reaction terms cancel and Eq. 2.45 becomes

$$M_x u'' - \frac{d}{dz}(GJ(z)\phi') + \frac{d^2}{dz^2}(EI_w(z)\phi'') + \frac{d^2}{dz^2}(EI_{w\psi}(z)\phi') - \frac{d}{dz}(EI_{w\psi}(z)\phi'') -$$

$$\frac{d}{dz}(EI_\psi(z)\phi') - \frac{d}{dz} M_x\left\{\beta_x(z)\phi' + \bar{\beta}_x(z)\phi\right\} = 0 \tag{2.54}$$

comparing Eqs. 2.43, 2.50 and 2.54 with Preg's (15) differential equations for bending of a doubly symmetric beam with linear taper, the last two terms in Eq. 2.54 are the only additional terms due to asymmetry of the cross-section. It should be noted that the cross-sectional properties are not constant, but are functions of the coordinate z.

Equation 2.43 represents in-plane bending, and is independent of Eqs. 2.50 and 2.54 as a consequence of excluding the effect of in-plane pre-buckling deformations from lateral and torsional stability. Eqs. 2.50 and 2.54 are simultaneous differential equations which are solved to determine the critical buckling moment. The method of solution used here is the construction of the first variation of the corresponding functional using the calculus of variations and employing the method of Galerkin to find a stationary value. This approach is analogous to the statement that the first variation of the total energy of a system must vanish.

The first variation of the functional associated with Eqs. 2.50 and 2.54 is

$$\delta I(u,) = \int_{\ell} \left\{ \frac{d^2}{dz^2}(EI_y u'')\delta u - 2R\phi'\delta u + M_x\phi''\delta u + M_x u''\delta\phi - \frac{d}{dz}(GJ(z)\phi')\delta\phi + \right.$$

$$\frac{d^2}{dz^2}(EI_w(z)\phi'')\delta\phi + \frac{d^2}{dz^2}(EI_{w\psi}(z)\phi')\delta\phi - \frac{d}{dz}(EI_{w\psi}(z)\phi'')\delta\phi - \frac{d}{dz}(EI_{\psi}(z)\phi')\delta\phi$$

$$\left. - \frac{d}{dz}\{M_x(\beta_x(z)\phi' + \bar{\beta}_x(z)\phi)\}\delta\phi \right\} dz \qquad (2.55)$$

The essential boundary conditions of this problem are (32):

$$u = 0 \text{ at } z = 0, \ell \qquad (2.56a)$$

$$\phi = 0 \text{ at } z = 0, \ell \qquad (2.56b)$$

The natural boundary conditions of this problem are (32, 14)

$$u'' = 0 \text{ at } z = 0, \ell \qquad (2.57a)$$

$$z\phi'' + 2\phi' + 0 \text{ at } z = 0, \ell \qquad (2.57b)$$

Equation 2.57b is obtained from Lee (14) and is based in zero warping normal stress at the end of a tapered member. Applying integration by parts to distribute the differentiation to the variations and then using Green's theorem, the first variation of the function is rewritten as:

$$\delta I = \int_{\ell} \left\{ EI_y u''\delta u'' + M_x\delta v'' - 2R\phi'\delta u + M_x\phi''\delta u + M_x u''\delta\phi + GJ(z)\phi'\delta\phi' + \right.$$

$$EI_w(z)\phi''\delta\phi'' + EI_{w\psi}(z)\phi'\delta\phi'' + EI_{w\psi}(z)\phi''\delta\phi' + EI_{\psi}(z)\phi'\delta\phi' +$$

$$\left. M_x\beta_x\phi'\delta\phi' + M_x\bar{\beta}_x\phi\delta\phi' \right\} dz \qquad (2.58)$$

The boundary integrals produced in the use of Green's theorem can be evaluated and all vanish. Thus the first variation of the functional is complete.

The Galerkin method of approximate solution requires that displacement functions be chosen which satisfy the boundary conditions of the problem and which have continuous derivatives up to one order less than present in the equation. Satisfactory functions may, in general, be written as

$$u(z) = \sum_{m=0}^{\infty} a_m u_m(z) \tag{2.59a}$$

$$\phi(z) = \sum_{m=0}^{\infty} b_m \phi_m(z) \tag{2.59b}$$

Preg (15) has noted that the approximating functions may be of the form

$$u_m(z) = f(z)(1 + z + z^2 + \ldots + z^m) \tag{2.60}$$

The function f(z) is then chosen to satisfy the boundary conditions.

The displacement functions chosen must also be capable of representing the true buckled configuration. As noted by Barta (33), Chwalla has assumed the first buckling mode to be valid for lateral buckling. Barta has noted that his assumption of the similarity of the torsional deformation and the first buckling mode gives reasonable results for a doubly symmetric cross-section even under double curvature.

For this study, a trial coordinate function series is chosen as

$$u(z) = \sum_{m=0}^{\infty} a_m z^m \sin \frac{\pi z}{\ell} \tag{2.61a}$$

$$\phi(z) = \sum_{m=0}^{\infty} b_m z^m \sin \frac{\pi z}{\ell} \tag{2.61b}$$

Since consideration of the natural boundary conditions are included in Eq. 2.58, these functions should be admissible, but solutions will be verified and convergence confirmed.

Substituting Eqs. 2.61 into Eq. 2.58, and noting that δa_m and δb_m are arbitrary, two simultaneous equations are obtained:

$$\delta a_m : \int_\ell \left\{ EI_y(\Sigma a_m u_m'')u_n'' + M_x(\Sigma c_m \phi_m'')u_n - 2R(\Sigma c_m \phi_m')u_n \right\} dz = 0 \qquad (2.62a)$$

$$\delta b_m : \int_\ell \Big\{ M_x(\Sigma a_m u_m'')\phi_n + GJ(z)(\Sigma c_m \phi_m')\phi_n' + EI_w(z)(\Sigma c_m \phi_m'')\phi_n'' +$$

$$EI_{w\psi}(z)(\Sigma c_m \phi_m')\phi_n'' + EI_{w\psi}(z)(\Sigma c_m \phi_m'')\phi_n' + EI_\psi(z)(\Sigma c_m \phi_m')\phi_n' + M_x \beta_x (\Sigma c_m \phi_m')\phi_n'$$

$$+ M_x \bar{\beta}_x (\Sigma c_m \phi_m)\phi_n' \Big\} dz = 0 \qquad (2.62b)$$

or, introducing a short hand rotation, for equation 2.62a,

$$\Sigma a_m A_{mn} + \Sigma b_m C_{mn} = 0 \qquad (2.63a)$$

$$\text{where } A_{mn} = \int_\ell EI_y u_m'' u_n'' dz \qquad (2.63b)$$

$$C_{mn} = \int_\ell \left\{ M_x \phi_m'' u_n - 2R\phi_m' u_n \right\} dz \qquad (2.63c)$$

and for equation 2.62b,

$$\Sigma b_m [H_{mn} + G_{mn}] + \Sigma a_m B_{mn} = 0 \qquad (2.64a)$$

$$\text{where } H_{mn} = \int_\ell \Big\{ GJ(z)\phi_m'\phi_n' + EI_w(z)\phi_m''\phi_n'' + EI_{w\psi}(z)(\phi_m''\phi_n' + \phi_m'\phi_n'')$$

$$+ EI_\psi(z)\phi_m'\phi_n' \Big\} dz \qquad (2.64b)$$

$$G_{mn} = \int_\ell M_x(\beta_x \phi_m'\phi_n' + \bar{\beta}_x \phi_m \phi_n')dz \qquad (2.64c)$$

$$B_{mn} = \int_\ell M_x u_m'' \phi_n dz \qquad (2.64d)$$

For ease in numerical computation, it is advantageous to non-dimensionalize the longitudinal coordinate. Defining a non-dimensional coordinate as

$$\bar{z} = \frac{z}{\ell} \tag{2.65}$$

then

$$M_x(\bar{z}) = M_L(1 - (1 + \gamma)\bar{z}) \tag{2.66}$$

and

$$u_m(z) = u_m(\bar{z})\ell^m \tag{2.67a}$$

$$u'_m(z) = u'_m(\bar{z})\ell^{m-1} \tag{2.67b}$$

$$u''_m(z) = u''_m(\bar{z})\ell^{m-2} \tag{2.67c}$$

Since identical displacement functions are chosen for u and ϕ, equations similar to Eqs. 2.67 can be written for ϕ. Substitution of Eqs. 2.65, 2.66 and 2.67 into Eqs. 2.63 and 2.64 results in

$$\Sigma \bar{a}_m \bar{A}_{mn} + \Sigma \bar{b}_m M_L \bar{C}_{mn} = 0 \tag{2.68a}$$

where $$\bar{A}_{mn} = \int_{\ell} \frac{EI_y}{\ell^3} u''_m u''_n d\bar{z} \tag{2.68b}$$

$$\bar{C}_{mn} = \int_{\ell} \left\{ (1 - (1 + \gamma)\bar{z})\left(\frac{1}{\ell}\right)\phi_m u''_n - \frac{2(1 + \gamma)}{\ell}\phi'_m u'_n \right\} d\bar{z} \tag{2.68c}$$

and

$$\Sigma \bar{b}_m \bar{H}_{mn} + \Sigma \bar{b}_m M_L \bar{G}_{mn} + \Sigma \bar{a}_m M_L \bar{B}_{mn} = 0 \tag{2.69a}$$

where $$\bar{H}_{mn} = \int_{\ell} \left\{ \frac{GJ(\bar{z})}{\ell} \phi'_m \phi'_n + \frac{EI_w(\bar{z})}{\ell^3} \phi''_m \phi''_n + \frac{EI_{w\psi}(\bar{z})}{\ell^2}(\phi''_m \phi'_n + \phi'_m \phi''_n) \right.$$

$$\left. + \frac{EI_\psi(\bar{z})}{\ell} \phi'_m \phi'_n \right\} d\bar{z} \tag{2.69b}$$

$$\bar{G}_{mn} = \int_{\ell} \left\{ (1 - (\gamma + 1)\bar{z}) \left[\frac{\beta_x}{\ell} \phi'_m \phi'_n + \bar{\beta}_x \phi_m \phi'_n \right] \right\} d\bar{z} \qquad (2.69c)$$

$$\bar{B}_{mn} = \int_{\ell} (1 - (\gamma + 1)\bar{z}) \left(\frac{1}{\ell}\right) u''_m \phi_n d\bar{z} \qquad (2.69d)$$

In matrix form,

$$\begin{bmatrix} \bar{A}_{mn} & 0 \\ 0 & \bar{H}_{mn} \end{bmatrix} + M_L \begin{bmatrix} 0 & \bar{C}_{mn} \\ \bar{B}_{mn} & \bar{G}_{mn} \end{bmatrix} \begin{Bmatrix} \bar{a}_m \\ \bar{b}_m \end{Bmatrix} = \begin{Bmatrix} 0 \\ 0 \end{Bmatrix} \qquad (2.70)$$

The integrals of matrix elements $\bar{C}_{mn}$ and $\bar{B}_{mn}$ are identical except for the reaction term. This term is included in the functional as the essential boundary condition of zero out-of-plane displacement at the beam supports. Since the coordinate functions satisfy this condition, inclusion of the reaction term is redundant and may be deleted from $\bar{B}_{mn}$. Thus

$$\bar{B}_{mn} = \bar{C}_{mn} = \int_{\ell} (1 + (\gamma + 1)\bar{z} \left(\frac{1}{\ell}\right) u''_m \phi_n dz \qquad (2.71)$$

Eq. 2.70 is then simplified to

$$\begin{bmatrix} \bar{A}_{mn} & 0 \\ 0 & \bar{H}_{mn} \end{bmatrix} + M_L \begin{bmatrix} 0 & \bar{C}_{mn} \\ \bar{C}_{mn} & \bar{G}_{mn} \end{bmatrix} \begin{Bmatrix} \bar{a}_m \\ \bar{b}_m \end{Bmatrix} = \begin{Bmatrix} 0 \\ 0 \end{Bmatrix} \qquad (2.72)$$

Eq. 2.72 is homogeneous, with the characteristic equation

$$\left| \begin{bmatrix} \bar{A}_{mn} & 0 \\ 0 & \bar{H}_{mn} \end{bmatrix} + M_L \begin{bmatrix} 0 & \bar{C}_{mn} \\ \bar{C}_{mn} & \bar{G}_{mn} \end{bmatrix} \right| = 0 \qquad (2.73)$$

The critical load for lateral torsional buckling under the specified moment gradient is determined as the minimum eigenvalue of Eq. 2.73.

2.3 Numerical Solution Technique

For solution of equation 2.73, a computer program was written in the Fortran IV language for the IBM System 370 computer. This program integrates the elements of the matrices in Eq. 2.73 and determines the eigenvalues of the characteristic equation. The required section properties are calculated as detailed in Appendix B using line element idealizations.

A macro-flow chart of the program is shown in Fig. 2.13 and a complete listing is given in Appendix A. The program consists of three main sections: The first section includes data input and echo, and the calculation and output of pertinent section properties. The second section involves the required integrations and matrix formulation. Subroutine DCADRE of the IBM Subroutine Library (IMSL) is employed to integrate the elements of the matrices using the trapezoidal rule (18). The third section involves the calculation of the roots of the characteristic equation and utilizes the IMSL subroutine EIGZF which uses the power method. Typical input for and output from this program are included in Appendix A.

Input data for the program consists of cross-section dimensions, beam length and taper, and stress ratio information. The stress ratio, r, is defined as

$$r = \frac{Z_R}{Z_L} \tag{2.74}$$

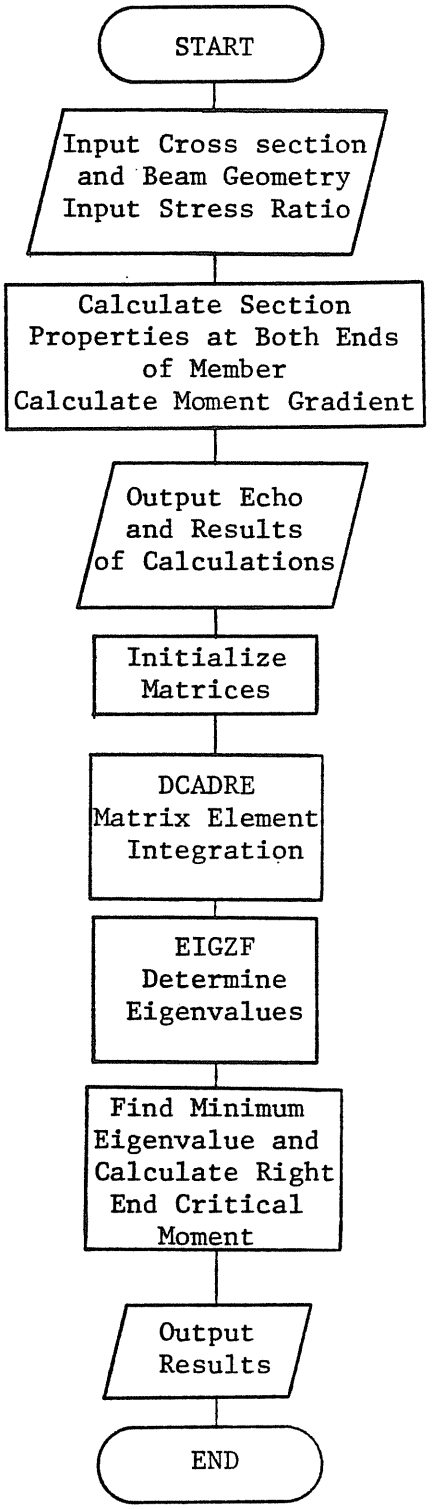

Fig. 2.13 Macro-Flowchart for Computer Program

where Z_R and Z_L are the relative magnitudes of the stresses developed in the flange extreme fibers. A reference end of the beam is determined as the end with the largest flange compressive fiber stress. This end is oriented at the left and Z_L assigned the value +1.0 if the top flange is in compression, and -1.0 if the bottom flange is in compression. If Z_L is equal to +1.0, then the state of stress at the right end, top flange, is described by Z_R, e.g., if the right end top flange is in compression, Z_R is a positive number equal in magnitude to the ratio of the top flange extreme fiber stresses at the beam ends and is less than or equal to +1.0, and the right end top flange is in tension, Z_R is a negative number equal in magnitude to the ratio of the top flange extreme fiber stresses at the beam ends and is greater than or equal to -1.0. If Z_L is equal to -1.0, then the state of stress at the right end, bottom flange is similarly described by Z_R. It is seen that a positive stress ratio corresponds to single curvature, a negative stress ratio to double curvature.

The magnitude of the critical buckling moment of a singly symmetric beam depends on which flange is in compression. Thus the end moment ratio, defined in Eq. 2.36, must be clearly redefined with respect to a frame of reference. Considering the discussion in the previous paragraphs, the end moment ratio is redefined as

$$\gamma = \frac{Z_R S_R}{Z_L S_L} \tag{2.75}$$

where Z_R and Z_L are as previously defined and S is the section modulus to the outermost fiber of the referenced flange. If the top flange is in compression at the referenced end, then S_R and S_L are determined with

respect to the top flange extreme fiber at the right and left ends, respectively. If the bottom flange is in compression at the referenced end, then S_R and S_L are determined with respect to the bottom flange extreme fibers.

It is noted that the end moment ratio could, alternatively, be defined with respect to tension flange stresses and section moduli. The critical moments calculated with either frame of reference are identical for cases of zero taper. As taper increases for a singly symmetric beam, however, the ratio of section moduli to the top flange at the beam ends differs increasingly from the ratio of section moduli to the bottom flange at beam ends. Since the stability of the compression flange is of greater importance than the tension flange in lateral-torsional buckling, all solutions generated in this study are referenced to the flange in compression at the left end of the beam.

2.4 Verification of Results

2.4.1 Convergence of the Method

The trigonometric power series used as displacement functions converges to an acceptable point with the use of four terms of the series. To illustrate this convergence, five H-shaped cross sections were selected and solutions obtained for various stress ratios, tapers and lengths. Solutions obtained using four and five terms to the displacement function are given in Appendix C and summarized in Table 2.1. Differences between the two solutions are less than 1.0%, and the average difference is 0.20%. Since computing time is approximately 50%

TABLE 2.1

Percent Differences Between Computer Solutions Obtained with Four and Five Term Displacement Functions

Section	I		II		III		IV		V	
Top Flange	4 x .25		5 x .3125		6 x .3125		6 x .25		6 x .1799	
Small End Web	6 x .1875		10 x .375		14 x .400		18 x .4375		18 x .4375	
Bottom Flange	4 x .25		5 x .1799		6 x .3125		6 x .1799		6 x .25	
Length	60"	180"	120"	120"	180"	180"	240"	240"	240"	240"
Taper	0.00	0.01	0.00	0.05	0.00	0.05	0.00	0.05	0.00	0.05
Stress Ratio	PERCENT DIFFERENCE									
+1.0	0.00	0.00	0.00	0.05	0.00	0.01	0.00	0.02	0.00	0.00
+.5	0.00	0.00	0.00	0.01	0.00	0.00	0.00	0.00	0.00	0.00
0,0	0,02	0,09	0,02	0,13	0,02	0,12	0,03	0,13	0.05	0.14
-.5	0.20	0.51	0.24	0.34	0.28	0.62	0.34	0.66	0.48	0.96
-1.0	0.38	0.30	0.85	0.10	0.52	0.01	0.80	0.47	0.81	0.19

Avg. % difference = 0.20%

greater if five terms are used, solutions generated in the remainder of this study are for four terms of the displacement function series.

2.4.2 Comparison with Alternate Methods of Solution

Closed-form solutions of the governing differential equations are available for prismatic beams under uniform moment only. For doubly symmetric beams (8),

$$M_{cr} = \sqrt{\frac{\pi^4 E^2 I_y I_w}{L^4} + \frac{\pi^2 EI_y GJ}{L^2}} \tag{2.76}$$

where M_{cr} is the critical buckling load and the cross-sectional properties are as previously defined. For singly symmetric beams (8),

$$M_{cr} = \pm \frac{\pi^2 EI_y \beta_x}{2L^2} \left[1 \pm \sqrt{1 + \frac{4}{\beta_x^2} \left(\frac{I_w}{I_y} + \frac{GJL^2}{\pi^2 EI_y} \right)} \right] \tag{2.77}$$

In this equation, the positive root is taken when the larger flange is in compression; the negative root is taken when the small flange is in compression.

The results of calculations using Eqs. 2.75 and 2.76 are compared with those obtained using the proposed method with four terms of displacement function in Table 2.2. In all cases the critical buckling moments agree to within 0.1%.

Equation 2.73 is identical to the characteristic equation for tapered beams under moment gradient as derived by Chi (18) using the minimum potential energy approach. Chi used a polynomial power series for the displacement functions as recommended by Lee, Morrell and Ketter (17),

$$u_m(z) = z(z - \ell)z^m \tag{2.78}$$

TABLE 2.2

Percent Differences Observed Between the Proposed Method, Exact Solutions and the Method of Chi (18).

	Section	Taper	Length	Stress Ratio	% Differences* Exact.	% Differences* Chi	Taper	Length	Stress Ratio	% Differences* Chi
	4 x .25			+1.0	0.00	+0.05			+1.0	+0.38
				+0.5		-0.11			+0.5	-0.88
I	6 x .1875	0.0	60"	0.0		-1.17	0.01	180"	0.0	-7.42
				-0.5		-4.79			-.5	-24.27
	4 x .25			-1.0		-9.37			-1.0	-25.55
	5 x .3125			+1.0	0.00	+0.04			+1.0	+2.73
				+0.5		-0.57			0.5	-0.06
II	10 x .375	0.0	120"	0.0		-3.54	0.05	120"	0.0	-8.39
				-0.5		-13.66			-0.5	-17.56
	5 x .1799			-1.0		-20.29			-1.0	-3.68
	6 x .3125			+1.0	0.00	+0.05			+1.0	+2.47
				+0.5		-0.38			+0.5	+0.01
III	14 x .400	0.0	180"	0.0		-2.99	0.05	180"	0.0	-7.64
				-0.5		-11.00			-0.5	-18.62
	6 x .3125			-1.0		-20.02			-1.0	-3.24
	6 x .25			+1.0	0.00	+0.04			+1.0	+2.68
				+0.5		-0.70			+0.5	+0.52
IV	18 x .4375	0.0	240"	0.0		-5.17	0.05	240"	0.0	-9.41
				-0.5		-17.87			-0.5	-23.83
	6 x .1799			-1.0		-28.05			-1.0	-7.69
	6 x .1799			+1.0	-0.02	+0.04			+1.0	+2.07
				+0.5		-0.69			+0.5	+0.38
V	18 x .4375	0.0	240"	0.0		-4.81	0.05	240"	0.0	-8.45
				-0.5		-15.41			-0.5	-26.61
	6 x .25			-1.0		-28.05			-1.0	-10.52

*% Differences based on comparison of 4-term displacement function solutions. Minus sign indicates solution less than proposed method solution.

To compare solutions obtained using the trigonometric series proposed here and the polynomial series proposed by Chi, the computer program in Appendix A was rewritten to calculate the matrix elements of Eq. 2.73 using Eq. 2.78 as the displacement function. The solutions obtained are given in Appendix C and summarized in Table 2.2.

The critical buckling moments calculated using trigonometric and polynomial displacement functions agree only for the case of prismatic beams under uniform moment. The solutions are not in agreement for other stress ratios; the differences between the solutions become more pronounced for beams subjected to double curvature loading.

The results obtained with the proposed method do, however, agree with those obtained by Culver and Preg (16), who used the finite difference method to obtain critical buckling loads for doubly symmetric tapered beams under moment gradients. Comparison of results is made on the basis of a factor, C, defined by Culver and Preg as

$$C = \frac{M_{cr}^*}{M_{cr_2}} \tag{2.79}$$

where M_{cr}^* is the critical moment of the tapered beam under a moment gradient developed at the large end of the beam and M_{cr_2} is the critical moment of a prismatic beam identical in cross section to the large end of the tapered beam, both loaded with equal end moments. Culver and Preg use M_{cr_2} as the "basic case" critical moment. Values of C calculated using the proposed method and the method of Chi with polynomial displacement functions are given in Table 2.3. In all cases there is excellent agreement between results obtained by the proposed method and by Culver and Preg. The results obtained using polynomial displacement

TABLE 2.3

"C" Values for Prismatic
Doubly Symmetric Members

Section	Stress Ratio	Chi(18)	Culver and Preg(10)	Proposed
I 4 x .25 6 x .1875 4 x .25 Length = 60"	+1.0	1.00	1.00	1.00
	+0.5	1.32	1.32	1.32
	0.0	1.83	1.85	1.85
	-0.5	2.48	2.60	2.61
	-1.0	2.49	2.74	2.75
III 6 x .3125 14 x .400 6 x .3125 Length = 180"	+1.0	1.00	1.00	1.00
	+0.5	1.32	1.32	1.32
	0.0	1.79	1.84	1.84
	-0.5	2.29	2.57	2.58
	-1.0	2.19	2.72	2.72

functions differ significantly for stress ratios less than 0.0, when the beam is in double curvature and significant reactions develop at the beam supports. In Chi's derivation, the reaction term included in the $\bar{B}_{mn}$ integral is neglected, which is acceptable if the displacement function chosen satisfies the natural boundary conditions of the problem. The polynomial series used by Chi does not satisfy the natural boundary conditions, and the error involved increases as the induced reaction increases.

The finite element method has also been used to determine the buckling strength of structural members. In this method, a structural member is divided into a number of finite-sized and conveniently shaped sub-regions or elements. Typical elements are isolated and the variational problem is formulated for arbitrary boundary conditions employing only simple polynomials. Inter-element continuity is preserved by the appropriate choice of these polynomials. A final matrix equation is assembled from the individual element equations, preserving the geometry of the system, and boundary conditions are imposed upon this final matrix. Points of element interconnection, or nodes, serve as locations for force applications and specified displacement boundary conditions.

The program, BASP15, developed at the University of Texas, uses the finite element method and was specifically developed to analyze the stability of H-shaped sections with one axis of symmetry perpendicular to the bending axis (34). The web is idealized using two-dimensional quadrilateral elements while the flanges are idealized by one-dimensional elements.

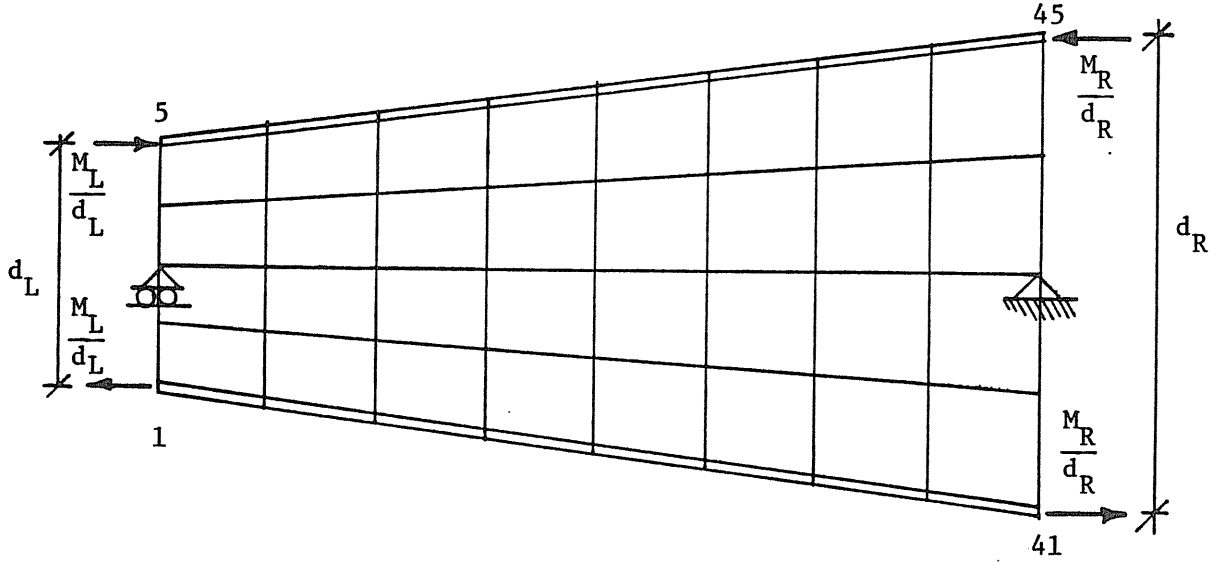

In-plane Boundary Conditions
at 3 u = 0

at 43 u = 0

v = 0

Out-of-Plane Boundary Conditions at
1, 2, 3, 4, 5, 41, 42, 43, 44, 45 w = 0

$\theta_k = 0$

Fig. 2.14 4 x 8 Finite Element Mesh

The program consists of two types of analyses: the first is an in-plane stress analysis under the applied loads, the second uses these stresses in an out-of-plane buckling analysis. For in-plane analysis, eighteen degree-of-freedom plane stress elements are used for the web and truss elements are used for the flanges (18). For the out-of-plane analysis, nineteen degree-of-freedom plate bending elements are used for the web and beam elements are used for the flanges. The characteristic equation of the final matrix formulation is solved using inverse iteration.

To obtain comparison results for critical buckling loads of tapered and prismatic members under stress gradients, the program BASP15 was used. The beams chosen were discretized into a finite element mesh as shown in Fig. 2.14. Convergence of the finite element solutions is confirmed by repeating the analysis with different meshes of finite elements. Three different modeling meshes were used in this study to verify convergence of the solution: 4 x 16, 2 x 25, 4 x 8. The most coarse mesh, 4 x 8, is shown in Fig. 2.14. Using the previous five cross-sections, solutions were obtained for the critical buckling moments. Some difficulty in achieving satisfactory solutions was encountered since the use of flexural plate elements in the web allows consideration of web distortion and local buckling in overall beam stability. For this study, local buckling of the web is not an admissible failure mode and web distortions are neglected. Thus, for sections with very slender web plates, it was found that a mid-span stiffening element was needed to ensure elastic lateral-torsional buckling before web failure.

TABLE 2.4

Percent Differences* Between the Proposed Method and Finite Element Solutions

Section	I	II	III	IV	V
Top Flange	4 x .25	5 x .3125	6 x .3125	6 x .25	6 x .1799
Small End Web	6 x .1875	10 x .375	14 x .400	18 x .4375	18 x .4375
Bottom Flange	4 x .25	5 x .1799	6 x .3125	6 x .1799	6 x .25
Length	60" 180"	120" 120"	180" 180"	240" 240"	240" 240"
Taper	0.00 0.01	0.00 0.05	0.00 0.05	0.00 0.05	0.00 0.05
Stress Ratio		Percent Difference			
+1.0	+0.46 +1.79	+2.92 +2.95	+2.27 +1.96	+3.64 +3.54	+3.77 +3.53
+0.5	+0.21 +2.10	+2.92 +2.86	+2.24 +1.96	+3.66 +3.54	+3.75 +3.57
0.00	+0.12 +1.25	+2.87 +2.26	+2.16 +1.50	+3.69 +3.40	+3.75 +3.42
-0.5	+0.67 -0.99	+2.08 -1.39	+1.67 -1.02	+3.66 +2.59	+3.43 +2.81
-1.0	+1.85 +2.33	+0.29 +0.24	+1.12 +0.59	+3.32 +2.90	+3.32 +3.40

*Calculations based on solution by the proposed method with four terms of displacement function. Minus sign corresponds to a finite element solution less than the proposed method solution.

The critical moments calculated by the proposed method and the finite element method are in close agreement. The results of these calculations are shown in Appendix C, and the differences observed between the solutions are summarized in Table 2.4. The critical moments calculated by the two methods never differed by more than 4% with an average difference of 1.18%. Comparisons are based on solutions obtained using four terms of the displacement function in the proposed method, and the minimum finite element solution from the meshes considered. Convergence of the finite element solutions can be seen with reference to Appendix C.

Thus it is shown that the trigonometric displacement function used in the proposed method is adequate. Solutions calculated by the proposed method are in excellent agreement with those obtained from closed-form, finite difference and finite element solutions for doubly and singly symmetric beams with less than 10^{o} of taper and loaded by end moments of varying magnitude.

CHAPTER III

DEVELOPMENT OF PROPOSED DESIGN METHODOLOGY

3.1 Introduction

Solution of the governing differential equations for cases involving taper and unequal end stresses is not possible in closed form, and numerical techniques such as the proposed method are too involved for use on a design basis. Equations 2.76 and 2.77 provide closed form solutions of the critical lateral-torsional buckling load for prismatic beams under uniform moment. This loading case, a prismatic beam loaded by equal and opposite end moments, is defined as the "basic case." To account for taper, it is proposed that the basic case solution be modified as follows:

$$(M_{cr})_s = C_a M_{cr} \tag{3.1}$$

where C_a is a modifying factor to be determined and M_{cr} is the critical moment of a prismatic beam with cross-section identical with that at the small end of the tapered beam, and is calculated by Eq. 2.76 for doubly symmetric sections or by Eq. 2.77 for singly symmetric sections. The moment, $(M_{cr})_s$, corresponds to the critical moment developed at the small end of a tapered beam subjected to end moments producing approximately uniform flange stress along the member, the "basic case" for tapered members. The critical moment at the large end is then

$$(M_{cr})_L = R(M_{cr})_S = RC_a M_{cr} \qquad (3.2)$$

where R is the ratio of the section moduli, to the extreme fiber of the compression flange, at the large end to that of the small end.

For the case of varying flange stress, it is proposed that these equations be further modified to

$$(M_{cr})_S = C_b C_a M_{cr} \qquad (3.3)$$

$$(M_{cr})_L = C_b R C_a M_{cr} \qquad (3.4)$$

where C_b is a modifying factor, to be determined, for cases of stress gradients.

The multiplying factors, C_a and C_b, will be determined using multiple linear regression analysis of theoretically correct values of M_{cr}, calculated by the method discussed in Chapter II. The development of these two factors is described in the following sections.

3.2 Discussion of Regression Analysis Technique

Data generated in this portion of the study are treated statistically in a stepwise regression search method. This technique economizes on computational efforts and computes a sequence of regression equations by successively entering or removing independent variables. Selection of variables is determined by the ability to explain the variation in the dependent variable, but independent variables which are too highly correlated with independent variables already selected are screened out (35).

The BMDP series of computer programs, developed at the Health Sciences Computing Facility, UCLA, which is sponsored by NIH Special Research Resources Grant RR-3, was used for the data analysis (36). In

particular, the multiple linear regression computer program BMDP2R was used to develop the prediction equations. The output of the analyses are equations which include one or more independent variables, and the coefficients to be applied to these variables are statistically determined to minimize the errors of prediction. The program output also includes statistics to aid in the evaluation of the equations. The R statistic is a multiple correlation coefficient and is the correlation between the dependent variable and the predicted value from the multiple regression. The term, R^2, is the proportion of the variance of the dependent variable explained by the multiple regression relating it to the other variables. The nearer R is to 1.0, the stronger the linear correlation.

The standard error of estimate, S, is analgous to the standard deviation from the mean of a population, and is a measure of the scatter of data points about the regression line. A small value of S reflects the goodness of fit of the equation.

3.3 C_a Modification for Taper

This study is limited to cross-sections, taper ratios and unbraced lengths normally found in rigid frames of pre-engineered metal buildings. Cross-sections sections were selected with the following limitations:

$$1.5 \leq \frac{\text{minimum depth}}{\text{flange width}} \leq 3.0$$

$$24 \geq \frac{\text{length}}{\text{minimum depth}}$$

$$15 \leq \frac{\text{flange width}}{\text{flange thickness}} \leq 50$$

6 in. $\leq$ depth of small end $\leq$ 24 in.

3 in. $\leq$ flange width $\leq$ 12 in.

3/16 in. $\leq$ flange thickness $\leq$ 3/4 in.

Tapers were taken as 0.00, 0.01, 0.05, or 0.10 and unbraced lengths as 60, 120, 180, or 240 inches. The web thickness was 1/4 in. for sections with a flange thickness greater than or equal to 3/4 in., and 3/16 in., otherwise. Both singly and doubly symmetric sections were included, and a listing of the sections and beam geometries considered is presented in Tables 3.1a and 3.1b. In all, a total of 941 cross-section, length and taper combinations were generated.

The factor C_a is defined as the ratio of the critical moment at the small end of a tapered beam subjected to "basic case" loading, e.g. approximately uniform stress throughout the length of the compression flange to the critical moment of a prismatic beam with the same cross section as the small end of the tapered beam, that is,

$$C_a = \frac{(M_{cr})_S}{M_{cr}} \tag{3.5}$$

with terms as previously defined. Solutions for the 941 cases were obtained and regression analysis performed.

The selection of independent variables to be included in the regression is often the most difficult problem in regression analysis. A preliminary investigation of the data provides some insight. Figure 3.1 shows the variation of C_a versus α for a beam with 18 in. small end depth, and 12 in. wide flanges with thicknesses of 0.375 in. and 0.25 in. The results are shown for both the large and small flange in compression.

Table 3.1a

Symmetrical Section Data
for
Determining C_a

Small End Depth in	Flange Width in	Flange Thickness, in							Taper α radians	Unbraced Length, in			
		3/16	1/4	5/16	3/8	1/2	5/8	3/4		60	120	180	240
6.0	3.0	X							0.00	X	X		
									0.01	X	X		
									0.05	X			
	4.0	X	X						0.00	X	X		
									0.01	X	X		
									0.05	X	X		
8.0	3.0	X							0.00	X	X	X	
									0.01	X			
	4.0	X	X						0.00	X	X	X	
									0.01	X	X	X	
									0.05	X			
	5.0	X	X	X					0.00	X	X	X	
									0.01	X	X	X	
									0.05	X	X		
									0.10	X			
12.0	4.0	X	X						0.00	X	X	X	X
	5.0	X	X	X					0.00	X	X	X	X
									0.01	X	X	X	X
									0.05	X			
	6.0	X	X	X	X				0.00	X	X	X	X
									0.01	X	X	X	X
									0.05	X	X		
									0.10	X			
	8.0	X	X	X	X	X			0.00	X	X	X	X
									0.01	X	X	X	X
									0.05	X	X	X	X
									0.10	X	X		
18.0	6.0	X	X	X	X				0.00	X	X	X	X
	8.0	X	X	X	X	X			0.00	X	X	X	X
									0.01	X	X	X	X
									0.05	X	X		
									0.10	X			
	10.0		X	X	X	X	X		0.00	X	X	X	X
									0.01	X	X	X	X
									0.05	X	X	X	X
									0.10	X	X		
	12.0		X	X	X	X	X	X	0.00	X	X	X	X
									0.01	X	X	X	X
									0.05	X	X	X	X
									0.10	X	X	X	
24.0	8.0	X	X	X	X	X			0.00	X	X	X	X
	10.0		X	X	X	X	X		0.00	X	X	X	X
									0.01	X	X	X	X
									0.05	X	X		
									0.10	X			
	12.0		X	X	X	X	X	X	0.00	X	X	X	X
									0.01	X	X	X	X
									0.05	X	X	X	X
									0.10	X	X		

Table 3.1b

Unsymmetrical Section Data
for
Determining C_a

Small End Depth in	Flange Width in	Large Flange Thickness, in				Small Flange Thickness, in				Taper α Radians	Unbraced Length, in			
		3/16	1/4	5/16	3/8	3/16	1/4	5/16	3/8		60	120	180	240
8.0	5.0		X			X				0.00	X	X	X	
										0.01	X	X	X	
										0.05	X	X		
										0.10	X			
12.0	5.0		X			X				0.00	X	X	X	X
										0.01	X	X	X	X
										0.05	X			
	6.0		X			X				0.00	X	X	X	X
										0.01	X	X	X	X
										0.05	X	X		
										0.10	X			
	8.0		X			X				0.00	X	X	X	X
										0.01	X	X	X	X
										0.05	X	X	X	X
										0.10	X	X		
18.0	6.0		X			X				0.00	X	X	X	X
	8.0		X			X				0.00	X	X	X	X
										0.01	X	X	X	X
										0.05	X	X		
										0.10	X			
	10.0				X		X	X		0.00	X	X	X	X
										0.01	X	X	X	X
										0.05	X	X	X	X
										0.10	X	X		
	12.0				X		X	X		0.00	X	X	X	X
										0.01	X	X	X	X
										0.05	X	X	X	X
										0.10	X	X	X	
24.0	8.0		X			X				0.00	X	X	X	X
	10.0				X		X	X		0.00	X	X	X	X
										0.01	X	X	X	X
										0.05	X	X		
										0.10	X			
	12.0				X		X	X		0.00	X	X	X	X
										0.01	X	X	X	X
										0.05	X	X	X	X
										0.10	X	X		

The coefficient C_a decreases fairly linearly with increasing taper, and with the smaller flange in compression, an increase in taper has a greater effect on C_a.

Figure 3.2 shows the variation of C_a versus length for the same section. It is apparent that C_a varies inversely with the length, and that the effect is again more severe for cases in which the small flange is in compression.

Further insight into possible independent variables is provided by Salvadori (25) and Nethercot (37). Salvadori suggests the use of $\sqrt{JGL^2/EI_w}$ as a nondimensional discriminating variable. Nethercot, citing the work of Kerensky, suggests the use of the ratio $(J_{section}/J_{flanges})$ where J is the St. Venant torsion constant. Nethercot and Rockey (32) suggest that $(I_{y,\ comp.\ flange}/I_{y,\ section})$ may be of use in a predictive equation.

Since C_a is dimensionless, only dimensionless combinations of the basic parameters were used to develop trial independent variables. Furthermore, since it is desirable that an expression for C_a default to unity for the case of a prismatic beam with equal and opposite end moments, the dependent variable in the regression was specified to be $(C_a - 1.0)$ and equations were regressed with a zero intercept. All compounded independent variables constructed included the taper as a component, and are thus equal to zero for the prismatic basic case.

The compounded dimensionless independent variables created for inclusion in the multiple regression were α, α^2, $\alpha\sqrt{GJL^2/EI_w}$, $\alpha\ell/d$, $\alpha I_y/J$, $\alpha J/I_y$, $\alpha I_{yt}/I_y$, $\alpha I_{yc}/I_y$, $\alpha I_{yc}/I_{yt}$, $\alpha I_{yt}/I_{yc}$, $\alpha J_c/J_s$, $\alpha J_s/J_c$, $\alpha J_s/J_t$, $\alpha J_t/J_s$, $\alpha J_t/J_L$, $\alpha J_c/J_t$, $\alpha\beta_x/d$, $\alpha\beta_x/\ell$, $\alpha\ell/\beta_x$, $\alpha d/\beta_x$ and $\alpha d/\ell$, where d is

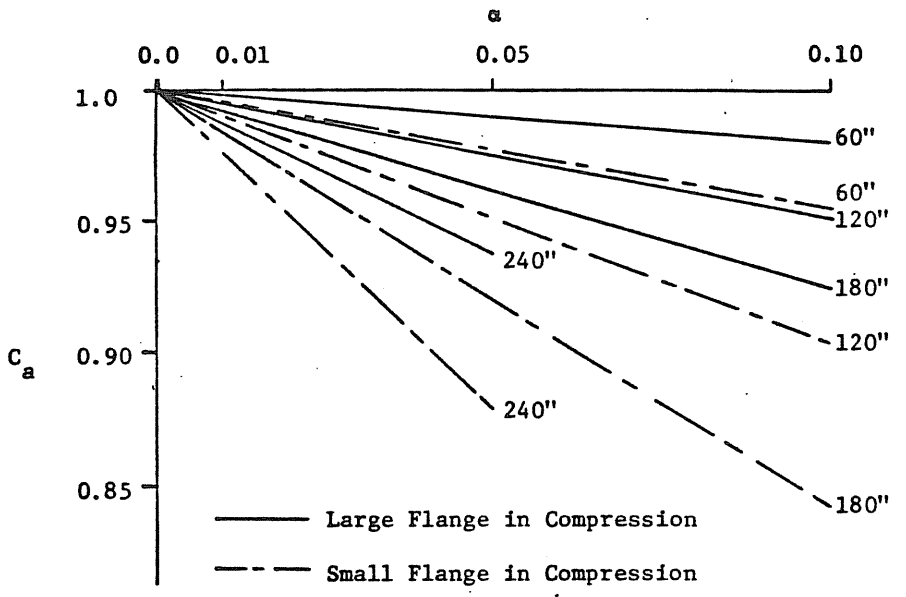

Fig. 3.1 C_α vs. α for Various Lengths, Singly Symmetric 18 in. Deep Section

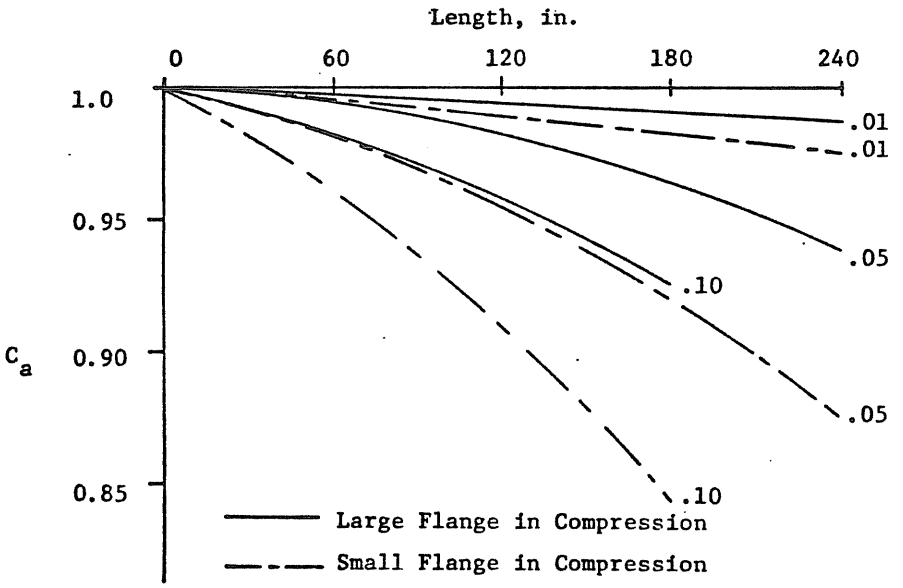

Fig. 3.2 C_α vs. Length for Various Tapers Singly Symmetric Section

the depth at the small end, α is the taper, subscript s refers to the section, subscript c refers to the compression flange, subscript t refers to the tension flange, subscript f refers to both flanges and other terms are as previously defined. Initially, all of these variables were included in the regression analysis, and then the list was selectively reduced. In addition, originally, a separate predictive equation was sought for direct calculation of the large end critical moment, but all equations regressed for this case resulted in errors of greater than 15% even with five separate independent variables included. Thus, it was decided to reference the C_a equation to the small end of a tapered beam, and to multiply by R, the ratio of large end to small end section moduli, to obtain the predicted critical moment at the large end of a tapered beam.

The least error of prediction was obtained in the following equations:

$$C_a = 1.0 - 1.0601\ \alpha\sqrt{\frac{GJ\ell^2}{EI_w}} \tag{3.6a}$$

$$C_a = 1.0 - 0.1163\ \alpha\frac{\ell}{d} \tag{3.6b}$$

$$C_a = 1.0 - 1.4580\ \alpha\sqrt{\frac{GJ\ell^2}{EI_w}} + 44.6328\ \alpha\frac{J}{I_y} \tag{3.6c}$$

$$C_a = 1.0 - 0.1501\ \alpha\frac{\ell}{d}^2 + 0.2950\alpha \tag{3.6d}$$

$$C_a = 1.0 - 1.4580\ \alpha\sqrt{\frac{GJ\ell^2}{EI_w}} + 44.6328\ \alpha\frac{J}{I_y} + 1.0688\ \alpha\frac{\beta_x}{d} \tag{3.6e}$$

$$C_a = 1.0 - 0.0355\ \alpha\frac{\ell}{d}^2 - 1.0978\ \alpha\sqrt{\frac{GJ\ell^2}{EI_w}} + 38.8956\ \alpha\frac{J}{I_y} \tag{3.6f}$$

The notation in these equations agrees with that previously defined, and all section properties are calculated for the small end. Statistics for

TABLE 3.3

Sections Deviating by More Than 5% from Expected C_a Value

Equation	Depth in.	Taper	Length in.	Symmetry	Flange in Compression	Error
Unconservative Deviations						
3.6a	6	.05	120	Double		7.4
	6	.05	120	Double		5.4
	8	.05	120	Single	Small	6.1
	12	.05	180	Double		5.1
	12	.05	240	Double		8.7
	12	.10	120	Double		5.1
	12	.05	240	Double		6.4
	12	.05	240	Double		5.0
	12	.05	180	Single	Small	6.3
	12	.05	240	Single	Small	11.1
	12	.10	120	Single	Small	6.2
	18	.10	180	Single	Small	5.5
3.6c	12	.05	240	Double		6.0
	12	.05	240	Single	Small	8.1
3.6f	6	.05	120	Double		5.5
	8	.05	120	Single	Small	5.1
	12	.05	240	Single	Small	7.2
Conservative Deviations						
3.6a	8	.10	60	Double		-5.4
	12	.10	60	Double		-5.5
	12	.10	120	Double		-7.7
	18	.10	120	Double		-6.5
	18	.10	120	Double		-5.6
	18	.10	180	Double		-6.7
	18	.10	120	Double		-6.9
	18	.10	180	Double		-8.1
3.6c	12	.10	120	Double		-7.1
	18	.10	180	Double		-5.2
	18	.10	180	Double		-7.3
	18	.10	180	Double		-7.6
3.6f	12	.10	120	Double		-5.7
	18	.10	180	Double		-5.4
	18	.10	180	Double		-6.7
	18	.10	180	Double		-6.2

these equations are summarized in Table 3.2. Equations 3.6a, 3.6c and 3.6f are the best fits for one-, two- and three-parameter equations, respectively. Although a one-parameter equation is preferred for simplicity, Eqs. 3.6c and 3.6f have significantly greater prediction capability than Eq. 3.6a and therefore all three equations are considered in the next part of this study. Cases where critical moments calculated by the proposed method deviated by more than 5% from moments calculated by Eqs. 3.6a, 3.6c and 3.6f are listed in Table 3.3, and each listing corresponds to a beam at the extremes of the study parameters, e.g. greatest taper or length for the beam depth.

3.4 C_b, Modification for Moment Gradient

Using the proposed method, solutions were obtained for the critical moments of beams with singly and doubly symmetric cross sections and varying stress ratios. Four cross-sections, two doubly symmetric and two singly symmetric were chosen and a total of fifty beams were generated by varying taper and unbraced length within the limits described in Section 3.3. Small end cross-section dimensions, beam lengths and tapers are shown in Table 3.4.

Solutions were systematically generated by considering one end of the beam as reference. By varying the relative magnitudes of the top flange stresses at the beam ends, solutions were obtained for beams in single and double curvature. The top flange at the referenced end was maintained at a relative stress magnitude, or stress index, of +1.0 (compression). A stress index of +1.0 (compression) in the top flange at the opposite end of the beam allows a solution for the beam in single curvature with approximately uniform top flange compressive stress. To

Table 3.4

Section Data for Determining C_b

Small End Depth in	Flange Width in	Comp. Flange Thickness in	Tension Flange Thickness in	Taper α radians	Unbraced length, in			
					60	120	180	240
9.5	6.0	0.25	0.25	0.00	X	X	X	X
				0.01	x	X	X	X
				0.05	X	X		
				0.10	X			
9.5	6.0	0.25	0.1875	0.00	X	X	X	X
				0.01	X	X	X	X
				0.05	X	X		
				0.10	X			
9.5	6.0	0.1875	0.25	0.00	X	X	X	X
				0.01	X	X	X	X
				0.05	X	X		
				0.10	X			
17.25	10.0	0.375	0.375	0.00	X	X	X	X
				0.01	X	X	X	X
				0.05	X	X	X	X
				0.10	X	X		
17.375	10.0	0.375	0.25	0.00	X	X	X	X
				0.01	X	X	X	X
				0.05	X	X	X	X
				0.10	X	X		
17.375	10.0	0.25	0.375	0.00	X	X	X	X
				0.01	X	X	X	X
				0.05	X	X	X	X
				0.10	X	X		

obtain solutions for the full range of single and double curvature cases, the stress index for the top flange at the opposite end of the beam from the reference end was varied from +1.0 to -1.0 (tension) in increments of 0.20. Doubly symmetric beams were considered with both the large and small end as reference. Singly symmetric beams were considered similarly, and solutions were generated for both the small and large flange in compression at the referenced end. In total, 1650 cases were generated.

The factor C_b is defined as

$$C_b = \frac{(M_{cr})_r}{(M_{cr})_o} \tag{3.7}$$

where $(M_{cr})_o$ is the critical moment at the referenced end for a stress ratio of +1.0, and $(M_{cr})_r$ is the critical moment at the referenced end for the stress ratio in question. The term $(M_{cr})_o$ defines the "basic case" for C_b of approximately uniform top flange compressive stresses for the beam. It is important to note that $(M_{cr})_r$ and $(M_{cr})_o$ must be determined for the same beam with the same taper. Thus, only changes in the critical moment due to the stress ratio are included in the factor C_b.

The choice of independent variables for the regression analysis was guided by the work of Salvadori (25) and Morrell and Lee (17, 28). For prismatic, doubly symmetric beams, the results of Salvadori's work have been statistically treated and a predictive equation obtained (9) as

$$C_b = 1.75 - 1.05r + 0.3r^2 \tag{3.8}$$

which is written in the notation of this paper. This expression is used by AISC (3) for prismatic beams. Morrell and Lee (17) suggest the use of

$$C_b = \begin{cases} 1.0 & r = +1.0 \\ \dfrac{1.75}{1.0 + .25\sqrt{\dfrac{\alpha \ell}{d}}} & r = 0.0 \end{cases} \qquad (3.9)$$

for simply supported, doubly symmetric tapered beams. They also have determined expressions to be used for continuous doubly symmetric tapered beams which include the terms $(1.0 - r)$ and $\alpha\ell(1.0 - r)/d$ as independent variables (28).

A preliminary investigation of the data reveals some insight. Figure 3.3 shows the variation of C_b versus r for three prismatic and three tapered beams. The beam depth is 9.5 in. and the flanges are 6 in. by 0.25 in. for the symmetrical cross-section and 6 inches by 0.1875 in. and 6 inches by 0.25 in. for the monsymmetric cross-sections. This data was generated for the small end referenced case. It is apparent that C_b does not vary linearly with the stress ratio, and that for beams in double curvature, C_b reaches a maximum and decreases sharply. The stress ratio associated with the maximum value of C_b is not constant but varies with taper. It is also apparent from Fig. 3.3 that the decrease in C_b for double curvature cases is more severe for the case of the large flange in compression at the referenced end. For such a beam in double curvature, the small flange is placed in compression at the opposite end, resulting in reduced stability of the beam and thus a reduced value of C_b.

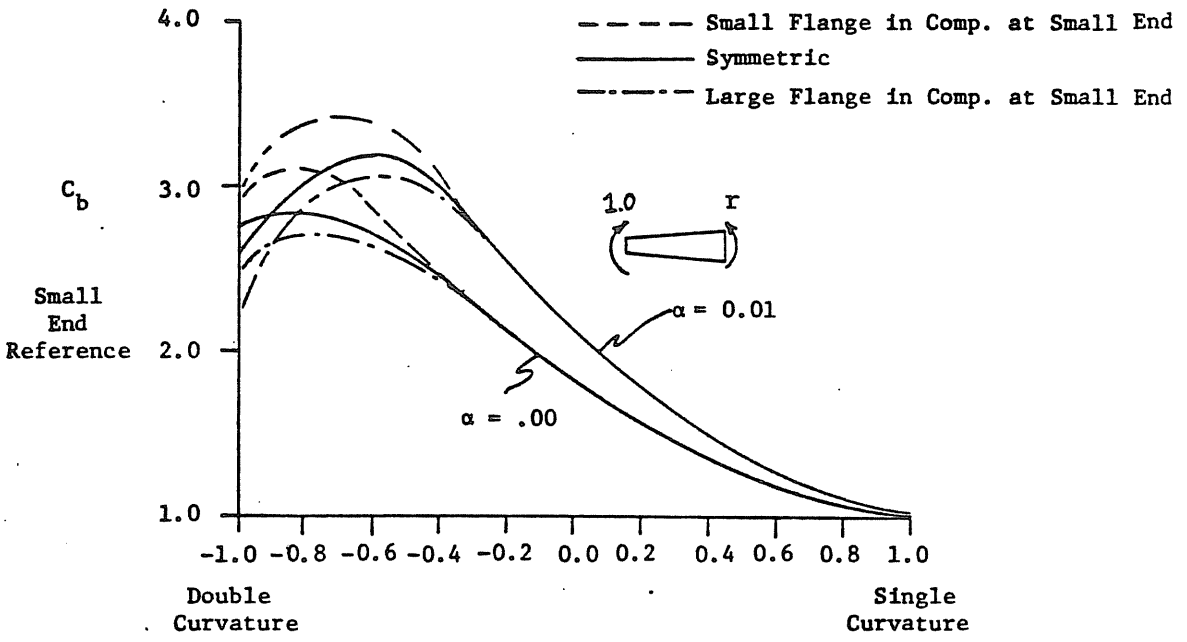

Fig. 3.3 C_b vs. r, 240" beam length

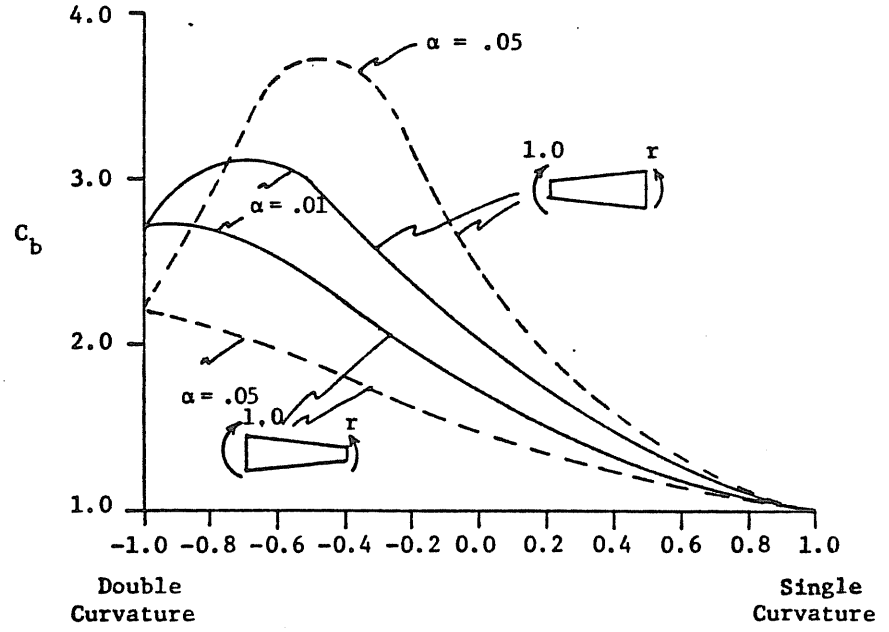

Fig. 3.4 C_b vs. r, 240" Beam Doubly Symmetric Cross Section 17.25 Depth

Inspection of the data also indicates that for a given end-referenced cross-section, C_b is nearly invariant if the magnitude of the product $\alpha\ell$ is constant. Table 3.5 contains data for a 9.5 in. deep symmetric beam illustrating this observation, and the same pattern is also observed for singly symmetric cross-sections.

Figure 3.4 shows the variation of C_b versus r for a 240 in. beam with a doubly symmetric cross section 17.25 in. deep and 10 in. by .375 in. flanges. Data for two tapers are plotted; the upper curves correspond to r varying with the small end reference, and the lower curves to r varying with the large end reference. For cases of small end reference, C_b shows a distinct maximum whereas for large end reference the maximum, if present, is not as clearly defined. Thus C_b varies differently depending upon the referenced end.

Since C_b is dimensionless, only dimensionless combinations of the basic parameters were included in the regression analysis. It is desirable that C_b default to unity for the "basic case" of a stress ratio equal to +1.0. Therefore, the dependent variable was specified to be $(C_b - 1.0)$ and equations were then regressed with a zero intercept. All compounded independent variables included the term $(r - 1.0)$ which is equal to zero for the basic case.

The compounded dimensionless variables initially included in the regression analysis were $(r - 1)$, $(r - 1)^2$, $(r - 1)^3$, $\alpha\ell(r - 1)d$, $\alpha\ell(r - 1)^2/d$, $\alpha\ell(r - 1)^3/d$ and similar terms with higher powers of the factor $\alpha\ell/d$. Preliminary regressions considering the entire data set, i.e. both ends of reference and full range of stress ratio produced equations which yielded predictions up to 75% in error. When the data

TABLE 3.5

C_b Data for Identical Small End Reference Beams, ($\alpha\ell$) Constant

Data for a singly symmetric beam, 9.5" depth.
$\alpha\ell$ = 6.0 in.

r	α = .05 ℓ = 120"	α = .10 ℓ = 60"
+1.0	1.000	1.000
+0.8	1.143	1.143
+0.6	1.330	1.330
+0.4	1.581	1.580
+0.2	1.924	1.923
0.0	2.395	2.392
-0.2	2.985	2.980
-0.4	3.457	3.445
-0.6	3.170	3.155
-0.8	2.399	2.389
-1.0	1.813	1.805

set was divided into two subsets by referenced end, resulting equations were up to 43% in error.

The lack of fit of these equations is largely due to deviations for values of r less than -0.40. Thus it was decided to reduce the initial data set to include only those results corresponding to stress gradients greater than or equal to -0.40, and regress separate equations for large and small end reference. Data corresponding to a stress gradient of -1.0 would be separately regressed, and linear interpolation used to predict a value of C_b for cases with a stress gradient between -0.40 and -1.00. Such an interpolation will generally produce errors on the conservative side. Figure 3.5 illustrates this procedure.

Considering the resulting equations as homologous sets for large and small end reference, the equations representing the best fit are

Small End Reference

2 Parameters

$$C_b = 1 + .7898B^2 + .9379 \frac{\alpha\ell}{d} B^2 \qquad (3.10a)$$

$$C_b = 1 + .7975B^2 - 1.0753 \frac{\alpha\ell}{d}B \qquad (3.10b)$$

$$C_b = 1 + .8069B^2 - .6912 \frac{\alpha\ell}{d}B^3 \qquad (3.10c)$$

3 Parameters

$$C_b = 1 + .4702B^2 - .3812B + .9379 \frac{\alpha\ell}{d}B^2 \qquad (3.10d)$$

$$C_b = 1 - .5949B - .2339B^3 + .9379 \frac{\alpha\ell}{d}B^2 \qquad (3.10e)$$

4 Parameters

$$C_b = 1 - .4200B + .4377B^2 + .6804 \frac{\alpha\ell}{d}B^2 - .2076 \frac{\alpha\ell}{d}B^3 \qquad (3.10f)$$

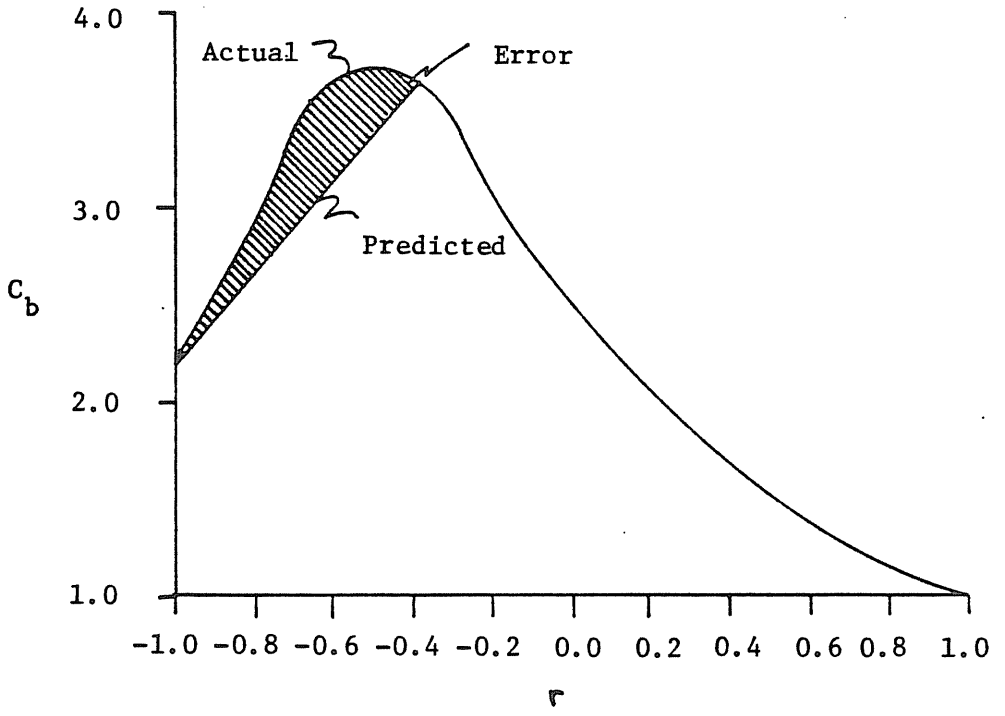

Fig. 3.5 Illustration of the Conservative Nature of the Proposed Interpolation 120" Length Doubly Symmetric Section 9.5" Depth

$$C_b = 1 - .4164B + .4407B^2 + .1653 \frac{\alpha \ell}{d} B + 1.0765 \frac{\alpha \ell}{d} B^2 \qquad (3.10g)$$

Large End Reference

2 Parameters

$$C_b = 1 + .7924B^2 + .8566 \frac{\alpha \ell}{d} B^2 \qquad (3.11a)$$

$$C_b = 1 + .7595B^2 - .7556 \frac{\alpha \ell}{d} B \qquad (3.11b)$$

$$C_b = 1 + .7974B^2 - .7176 \frac{\alpha \ell}{d} B^3 \qquad (3.11c)$$

3 Parameters

$$C_b = 1 + .4638B^2 - .3919B + .8566 \frac{\alpha \ell}{d} B^2 \qquad (3.11d)$$

$$C_b = 1 - .6044B - .2293B^3 + .8524 \frac{\alpha \ell}{d} B^2 \qquad (3.11e)$$

4 Parameters

$$C_b = 1 - .4101B + .4486B^2 - 1.0307 \frac{\alpha \ell}{d} B^2 + .1403 \frac{\alpha \ell}{d} B^3 \qquad (3.11f)$$

$$C_b = 1 - .4139B + .4454B^2 - .1492 \frac{\alpha \ell}{d} B + .7315 \frac{\alpha \ell}{d} B^2 \qquad (3.11g)$$

The variable B in these equations is equal to (r - 1.0), and α and d are determined with respect to the referenced end. Noting the similarity of regression coefficients in homologous pairs, a separate regression was made for the combined data set of small and large end reference cases with stress ratios greater than or equal to -0.40. Using the same notation, the following equation was obtained:

$$C_b = 1 - .3867B + .4739B^2 + .9074 \frac{\alpha \ell}{d} B^2 \qquad (3.12)$$

Statistics generated for Eqs. 3.10, 3.11 and 3.12 are summarized in Table 3.6. The homologous pairs of Eqs. 3.10a and 3.11a, Eqs. 3.10d and 3.11d, Eqs. 3.10g and 3.11g and the single Eq. 3.12 are given

TABLE 3.6

C_b Prediction Equation Statistics

Small End Reference				Large End Reference			
Equation	R	R^2	S	S	R^2	R	Equation
3.10a	.996	.991	.094	.082	.985	.992	3.11a
3.10b	.996	.993	.086	.111	.972	.986	3.11b
3.10c	.993	.985	.121	.069	.989	.995	3.11c
3.10d	.999	.997	.051	.012	1.000	1.000	3.11d
3.10e	.999	.997	.052	.019	.999	1.000	3.11e
3.10f	.998	.997	.050	.012	1.000	1.000	3.11f
3.10g	.998	.997	.050	.012	1.000	1.000	3.11g
Combined Data Set							
3.12	.999	.998	.038				

further consideration as these represent the best fits for two, three and four parameter regressions, and these equations were used along with C_a Eqs. 3.6a, 3.6c and 3.6f to predict the critical moments of the C_b data set for stress ratios greater than or equal to -0.40. The errors observed were statistically treated and this information is summarized in Table 3.7.

It is apparent that the two parameter C_b equations will not be satisfactory design equations, as both the maximum errors and 95% confidence intervals are larger than 10%. The four term C_b equations show little improvement in prediction over three-term equations. For the three term C_b equations, Eqs. 3.10d, 3.11d and 3.12, the two term C_a equation, Eq. 3.6c, provides more accurate prediction than Eq. 3.6a and significantly reduces the number of cases with greater than 5% unconservative error of prediction. The further increase in predictive power associated with the three term C_a equation is minimal, and the use of two individual C_b equations rather than the single Eq. 3.12 is an unwarranted complicating procedure. Thus, the use of Eq. 3.12 for C_b prediction and Eq. 3.6c for C_a prediction is recommended. Cases where critical moments calculated by the proposed method deviated by more than 5% from moments calculated by Eqs. 3.12 and 3.6c are listed in Table 3.8, and each listing corresponds to a beam at the extremes of the study parameters, e.g. greatest taper or length for the beam depth.

Separate regression of a prediction equation for C_b at a stress ratio of -1.0 was slightly less successful. As there is no necessity for C_b to default to unity, C_b served as the dependent variable and a statistically generated constant was included as an intercept.

TABLE 3.7

Summary of Errors Observed and Statictics for C_b Prediction
$-0.40 \leq r \leq 1.00$

C_b Equations	C_a Equation	No. of Cases with >5% Error		Max % Error Observed		Standard Deviation of Error, %	Average Absolute Error, %	Limits of 95% Confidence Interval
		Uncons.	Cons.	Uncons.	Cons.			
3.10a 3.11a	3.6a	58	527	12.93	10.20	4.630	4.693	±12.32
	3.6c	52	539	11.34	10.36	4.562	4.675	±12.25
	3.6f	52	544	10.89	10.87	4.560	4.724	±12.33
3.10d 3.11d	3.6a	30	2	10.18	6.70	1.772	1.220	±3.74
	3.6c	12	3	8.64	6.87	1.581	1.104	±3.30
	3.6f	8	4	8.19	7.39	1.585	1.109	±3.22
3.10g 3.11g	3.6a	26	2	10.75	6.22	1.692	1.154	±3.58
	3.6c	8	4	9.20	6.39	1.514	1.037	±3.17
	3.6f	7	5	8.75	6.91	1.535	1.050	±3.12
3.12	3.6a	19	4	9.40	7.36	1.736	1.225	±3.66
	3.6c	7	6	7.87	7.53	1.562	1.116	±3.25
	3.6f	7	8	7.43	8.05	1.582	1.124	±3.21

TABLE 3.8

Sections Deviating by More Than 5% From
Expected Critical Moment
Equations 3.6c and 3.12

Small End Depth	Taper	Length	Reference End	Symmetry	Flange in Compression	Stress Ratio	Error (+ Uncons.)
9.5	.05	120	Small	Single	Small	-.40	-5.5
9.5	.10	60	Small	Single	Small	-.40	-6.2
9.5	.01	240	Large	Single	Small	0.0	5.1
9.5	.01	240	Large	Single	Small	-.20	5.2
9.5	.01	240	Large	Single	Small	-.40	5.6
17.375	.05	180	Small	Single	Large	-.40	5.9
17.375	.05	240	Small	Single	Large	-.40	7.9
17.375	.10	60	Small	Single	Large	-.40	5.8
17.375	.10	120	Small	Single	Large	-.40	7.8
17.375	.05	180	Small	Single	Small	-.40	-5.3
17.375	.05	240	Small	Single	Small	-.40	-6.2
17.375	.10	120	Small	Single	Small	-.40	-7.5
17.375	.10	120	Large	Single	Large	-4.0	-5.3

Independent variables included $\alpha\ell/d$, ℓ/d, I_c/I_y, $\alpha I_c/I_y$, I_c/I_t, $\alpha I_c/I_t$, β_x/d, $\alpha\beta_x/d$, β_x/ℓ, $\alpha\beta_x/\ell$, J_f/J_s, $\alpha J_f/J_s$, J_t/J_c, $\alpha J_t/J_c$, J_c/J_t, $\alpha J_c/J_t$, J_c/J_s, and $\alpha J_c/J_s$. Regression of a data set composed of both small and large end reference sections produced equations which predicted values of C_b more than 50% in error. Considering the referenced ends individually, the following homologous sets of equations resulted:

Small End Reference

$$C_b = 5.2441 - 4.9677\ I_c/I_y - .6559\ \frac{\alpha\ell}{d} - 15.7893\ \alpha\frac{\beta_x}{d} \qquad (3.13a)$$

$$C_b = 2.7596 - 2.8152\ \frac{\beta_x}{d} - .6562\ \frac{\alpha\ell}{d} - 15.6530\ \alpha\frac{\beta_x}{d} \qquad (3.13b)$$

Large End Reference

$$C_b = 4.7664 - 3.9951\ I_c/I_y + 1.2021\ \frac{\alpha\ell}{d} - 22.2077\ \alpha\frac{\beta_x}{d} \qquad (3.14a)$$

$$C_b = 2.7684 + 1.2025\ \frac{\alpha\ell}{d} - 2.2686\ \frac{\beta_x}{d} - 22.0724\ \alpha\frac{\beta_x}{d} \qquad (3.14b)$$

The statistics for these equations follow

Equation	R	R^2	S
3.13a	.993	.985	.056
3.13b	.993	.986	.055
3.14a	.960	.922	.086
3.14b	.961	.924	.085

The taper and section properties to be used in these equations are taken with respect to the referenced end.

Including the total 1650 cases, Eqs. 3.6c, 3.12, 3.13 and 3.14 were used to predict the critical moments. The interpolation between r values of -.40 and -1.00 yields conservative results as can be seen with reference to Fig. 3.6 which is a relative frequency histogram of

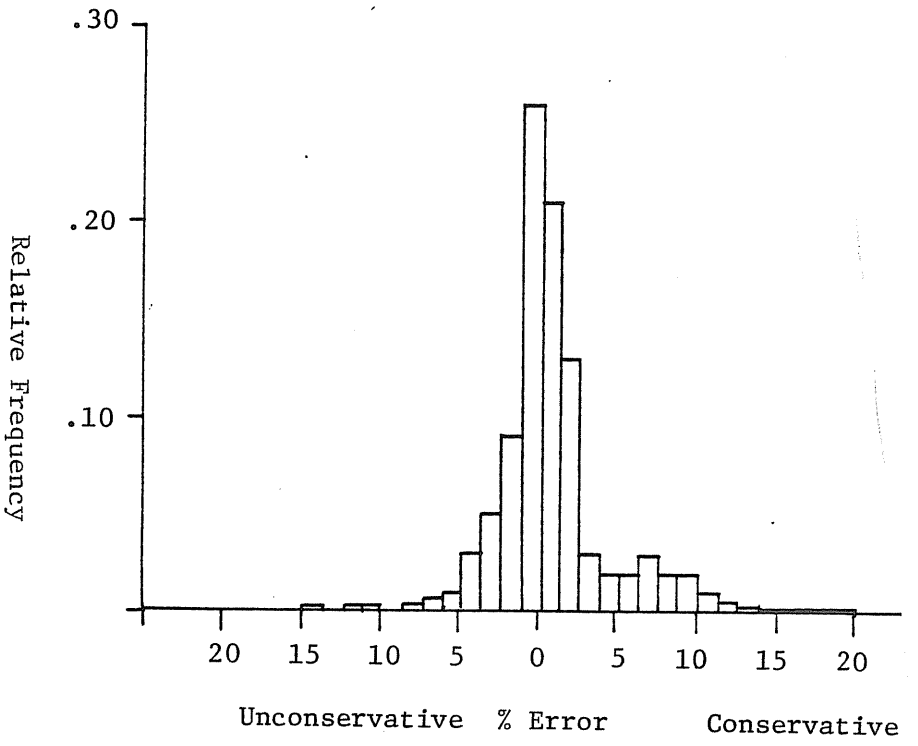

Fig. 3.6 Relative Frequency Histogram of % Errors in Using Eqs. 3.6c, 3.12, 3.13a and 3.14a

the precent error observed in the prediction. The homologous pairs Eqs. 3.13a and 3.14a, Eqs. 3.13b and 3.14b agree to within 0.1% of error. In all cases, the maximum nonconservative errors were observed for beams 240 inches in length, taper of 0.05 and 0.10 and stress ratios of -1.00 with the small flange in compression at the referenced end. At a 95% confidence interval, the estimate provided by these sets of equations will be within 8.1% of the true value.

3.5 Limits of Equation Applicability

The previous equations were regressed for a limited data set, and it is useful to determine extrapolation limits for their use. Eight H-sections were selected, differing only in the thickness of one of the flanges, and eight channel-capped built-up members were chosen, differing only in the thickness of the flange lip. These sections are described in Table 3.9. The column labelled I_{yL}/I_{ys} is the ratio of the moments of inertia of the large flange to the small flange and is a measure of the asymmetry of the section. Solutions were obtained for these sections with length and taper combinations of 120 in. and 0.00, 180 in. and 0.01, 120 in. and 0.05, and 240 in. and 0.05, and for stress ratios of 1.0, 0.5, 0.0, -0.5 and -1.00. Thus 112 data points were generated for each stress ratio.

Using the equations recommended in Section 3.4, the critical moment for each of these cases and stress ratios was predicted. The error statistics observed are summarized in Table 3.10, and it is apparent that for beams in single curvature (r greater than 0.0) these equations retain validity for sections with a I_{yL}/I_{ys} ratio of up to 4.0. All cases of greater than 5% observed error occurred with 240

TABLE 3.9

Wide-Flanged Sections

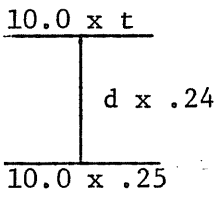

Channel-Capped Sections

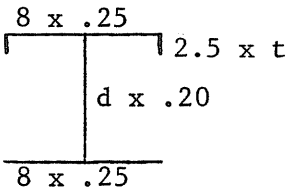

t in.	d in.	Reference End	$\frac{I_{yL}}{I_{yS}}$	t in.	d in.	Reference End	$\frac{I_{yL}}{I_{yS}}$
1.00	24.0	Small	4.0	0.45	14.0	Small	4.375
0.75	24.0	Small	3.0	0.30	14.0	Small	3.250
0.50	24.0	Small	2.0	0.15	14.0	Small	2.125
0.25	24.0	Small	1.0	0.00	14.0	Small	1.00
1.00	30.0	Large	4.0	0.45	26.0	Large	4.375
0.75	30.0	Large	3.0	0.30	26.0	Large	3.250
0.50	30.0	Large	2.0	0.15	26.0	Large	2.125
0.25	30.0	Large	1.0	0.00	26.0	Large	1.00

TABLE 3.10

Summary of Error Statistics
Equations 3.6c, 3.12, 3.13 and 3.14 used in Prediction

Stress Ratio	Equations Used	Average Absolute Error, %	Mean Error, %	Standard Deviation of Error, %	No. of sections with >5% error Unconservative	conservative	Maximum Error, % Unconservative	Conservative
Wide Flange Sections								
1.00		1.89	0.57	3.05	3	3	8.1	10.9
0.50		1.99	-.19	3.32	3	4	10.9	11.0
0.00		2.07	1.10	3.21	3	2	12.7	12.2
-.50	3.13a	5.03	-.62	6.77	7	11	21.1	15.6
-1.00	3.14a	10.69	4.47	15.58	25	9	50.2	46.0
-.50	3.13b	4.92	-.64	6.73	7	11	20.9	15.5
-1.00	3.14b	10.72	4.69	15.66	25	9	49.2	46.0
Channel-Capped Sections								
1.00		2.08	2.08	2.36	9	0	9.4	
0.50		3.08	1.92	3.11	11	0	9.1	
0.00		2.76	2.65	2.41	10	0	9.1	
-.50	3.13a	13.65	8.74	22.87	25	9	100.0	16.7
-1.00	3.14a	18.47	8.85	26.27	27	9	73.8	79.3
-.50	3.13b	11.79	8.46	21.65	22	8	100.0	15.3
-1.00	3.14b	20.15	0.23	36.31	27	11	52.7	100.0

inch beams and 0.05 taper. It is also apparent that the equations used to predict C_b for stress ratios of -1.0 are not valid for large ratios of I_{yL}/I_{yS}. Equations 3.13 and 3.14 are very sensitive to the ratios I_c/I_y and β_x/d, both of which are measures of the asymmetry of the section. The maximum value of I_c/I_y included in the first part of this study was 1.50. As I_c/I_y and β_x/d become large, Eqs. 3.13 and 3.14 predict meaningless, often negative, values for C_b. By study of the data, however, an empirical limit of usefulness can be established.

When the data set is reduced to include only those sections with I_{yL}/I_{yS} less than 2.5, the following error statistics are noted in a data set of 40 cases:

r	Mean Error, %	Standard Deviation of Error, %	No. with >5% Error Conserv.	Uncons.	Maximum Error Conserv.	Uncons.
Equations 3.13a and 3.14a						
-0.5	-2.37	4.02	9	1	15.6	7.5
-1.0	3.79	7.19	2	13	15.3	23.7
Equations 3.13b and 3.14b						
-0.5	-2.57	4.18	9	1	15.5	5.8
-1.0	1.60	5.18	2	10	17.6	11.2

It is apparent that the homologous pair of Eqs. 3.13b and 3.14b has the greater predictive capability, and that predicted critical moments for a stress ratio of -1.0 (double curvature) will be within 10% of the actual moment at a 90% level of confidence when Eqs. 3.13b and 3.14b are used. In addition, it is noted from a study of the data that if the following limitation is observed,

$$\frac{I_{yL}}{I_{yS}}\left(\frac{\alpha\ell}{d}\right) \leq 1.30 \qquad (3.15)$$

the proposed equations can be expected to predict critical moments with less than 8% unconservative error at a 95% confidence level for beams in single curvature and with less than 12% unconservative error at a 95% confidence level for beams in double curvature. In all cases, the error of estimation is reduced as the taper decreases and as the cross-section becomes more nearly doubly-symmetric.

CHAPTER 4

SUMMARY AND CONCLUSIONS

4.1 Summary of Procedure

It is proposed that Eqs. 3.6c, 3.12, 3.13b and 3.14b be used to predict the modifying factors to be used in a simplified design procedure for tapered beams. The following limitations should be observed in the use of this method, in addition to those listed in Section 3.3:

$$\frac{I_{yL}}{I_{yS}}\left(\frac{\alpha \ell}{d_S}\right) \leq 1.30 \qquad (4.1)$$

$$\frac{I_{yL}}{I_{yS}} \leq 2.50 \qquad (4.2)$$

where d_S is the depth at the small end of the beam, I_{yL} and I_{yS} are the moments of inertia of the large and small flange respectively, and the absolute value of the taper is used.

The steps in the proposed procedure are as follows:

(1) Calculate the basic case critical moment for a prismatic beam with the same cross-section as the small end of the beam in question, using Eqs. 2.76 or 2.77. If the cross section is singly symmetrical, the basic case critical moment is calculated for both large and small flanges in compression.

(2) Calculate the modifying factor C_a with reference to the small end section properties, using Eq. 3.6c.

(3) Calculate extreme fiber stresses in the flanges at the beam ends. The end with the largest compressive stress is chosen as the reference end, and the flange with the largest compressive stress is the reference flange.

(4) If the large end is referenced, calculate R, the ratio of section moduli to the extreme fibers of the reference flange at beam ends.

(5) Calculate the stress ratio, r, as the ratio of the beam end stresses in the reference flange. If the beam is in double curvature, r will be less than 0.00.

(6) If r is greater than -0.40, use Eq. 3.12 and the referenced end section properties to calculate C_b.

(7) If r is less than -0.40, calculate C_b for r equal to -0.40 using Eq. 3.12, and C_b for r equal to -1.0 using Eq. 3.13b for small end reference and Eq. 3.14b for large end reference. Use linear interpolation between these two values to determine C_b for the stress ratio in question.

(8) Calculate the tapered beam critical moment using Eq. 3.3 for small end reference and Eq. 3.4 for large end reference.

4.2 Example Calculation

To illustrate the critical moment calculations required in this proposed method, the simple span beams shown in Fig. 4.1 are analyzed.

Figure 4.1. Beam Description and Section Properties for Section 4.2 Example

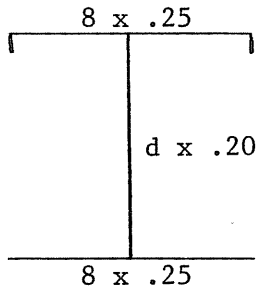

Unbraced length = 120.0 in.
Taper = 0.05
$E = 30 \times 10^3$ ksi
$G = 11.2 \times 10^3$ ksi

Load Case I

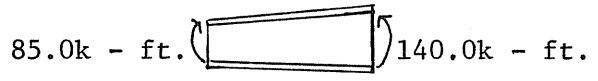

Load Case II

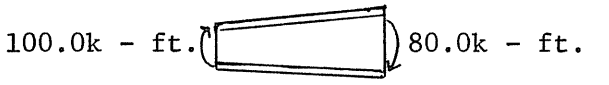

Section Properties:

	Small End	Large End
Depth, in.	14.0	20.0
I_{yL}, in.^{4}	22.67	22.67
I_{yS}, in.^{4}	10.67	10.67
I_y, in.^{4}	33.33	33.33
I_x, in.^{4}	264.48	586.24
$S_{x,top}$, in.^{3}	41.14	63.38
$S_{x,bottom}$, in.^{3}	34.93	54.53
J, in.^{4}	0.126	0.142
I_w, in.^{6}	1559.23	3096.51
β_x, in.	5.763	7.845

The taper and unbraced length are within the ranges listed in Section 3.3 and

$$1.5 \leq \frac{\text{minimum depth}}{\text{flange width}} = \frac{14}{8} = 1.75 \leq 3.0$$

$$24 \geq \frac{\text{length}}{\text{minimum depth}} = \frac{120}{14} = 8.6$$

$$15 \leq \frac{\text{flange width}}{\text{flange thickness}} = \frac{8}{.25} = 32 \leq 50$$

Inequalities 4.1 and 4.2 are satisfied since

$$\frac{I_{yL}}{I_{yS}}\left(\frac{\alpha\ell}{d_S}\right) = 0.91 \leq 1.30$$

$$\frac{I_{yL}}{I_{yS}} = 2.13 \leq 2.50$$

Following the steps in the proposed procedure:

Step 1. Basic case critical moment, using small end section properties is calculated for this singly symmetric section using Eq. 2.77:

$$M_{cr} = \frac{\pi^2(30x10^3)(33.33)(5.763)}{2(120)(120)}\left[1 \pm \sqrt{1 + \frac{4}{(5.763)^2}\left(\frac{1559.23}{33.33} + \frac{11200(.126)(120)^2}{\pi^2(30000)(33.33)}\right)}\right]$$

For large flange in compression,

M_{cr} = 7155k - in. = 596k - ft.

For small flange in compression,

M_{cr} = 3206k - in. = 276k - ft.

Step 2: Taper modification factor, C_a, is evaluated, using small end section properties and Eq. 3.6c, as

$$C_a = 1.0 - 1.458(.05)\sqrt{\frac{(11.2x10^3)(.126)(120)^2}{(30x10^3)(1559.23)}} + 44.6328\,\frac{(.05)(.126)}{33.33}$$

$$= 0.960$$

The calculations required in Steps 3 through 8 are made for each load case. For load Case I, the beam in single curvature:

Step 3: Extreme fiber stresses.

Small end: top flange stress (compressive) = 24.79 ksi

Large end: top flange stress (compressive) = 26.51 ksi

Reference end: large

Reference flange: top (large)

Step 4: Since the large end is referenced, R is evaluated as

$$R = \frac{S_{\text{top, large end}}}{S_{\text{top, small end}}} = \frac{63.38}{41.14} = 1.541$$

Step 5: The stress ratio, r, is evaluated as

$$r = \frac{\text{top flange stress, small end}}{\text{top flange stress, large end}} = \frac{24.79}{26.51} = 0.935$$

Step 6: Using Eq. 3.12 and large end section properties, C_b is evaluated as

$$C_b = 1.0 - .3867(.935-1) + .4739(.935-1)^2 + \frac{.9074(-0.05)(120)(.935-1)^2}{20.0}$$

$$= 1.028$$

Step 7: Omitted since the stress ratio is greater than -0.40.

Step 8: Using Eq. 3.4, the critical moments are evaluated as

$$(M_{cr})_L = 1.028(1.480)(596) = 907\text{k - ft.}$$

$$(M_{cr})_S = \frac{907(.935)}{1.541} = 550\text{k - ft.}$$

The critical moment for the large flange in compression from Step 1 is used as the basic case moment since the large flange is the referenced flange in this case.

The moment calculated by the theoretically correct procedure is 881k - ft., differing by 3.0% from that calculated by the simplified procedure.

For load case II, the beam is in double curvature:

Step 3: Extreme fiber stresses.

Small end: top flange stress (compressive) = 29.17 ksi

Large end: bottom flange stress (compressive) = 17.61 ksi

Reference end: small

Reference flange: large

Step 4: Omitted since the small end is referenced

Step 5: To evaluate the stress ratio, the large flange tensile stress at the large end is evaluated as -15.15 ksi. The stress ratio is then

$$r = \frac{\text{top flange stress, large end}}{\text{top flange stress, small end}} = \frac{-15.15}{29.17} = -0.519$$

Step 6: Omitted since r is less than -0.40.

Step 7: Using Eq. 3.12, small end section properties and a stress ratio of -0.40, C_b is evaluated as

$$C_{b,-.4} = 1.0 - .3867(-.4-1.0) + .4739(-.4-1.0)^2 + \frac{.9074(.05)(120)^2(-.4-1.0)^2}{14.0} = 3.232$$

Using Eq. 3.13b, C_b for a stress ratio of -1.00 is evaluated as

$$C_{b,-1} = 2.7596 - \frac{2.8152(5.763)}{14.0} - \frac{.6562(.05)(120)}{14.0} - \frac{15.653(.05)(5.763}{14.0}$$

$$= 0.998$$

By interpolation, C_b for a stress ratio of -.519 is

$$C_b = 3.232 + \frac{(.4-.519)}{.6}(3.232 - .998) = 2.789$$

Step 8: Using Eq. 3.3, the critical moments are evaluated as

$$(M_{cr})_S = 2.789(.960)(596) = 1595k - ft.$$

$$(M_{cr})_L = 1595(.519)(1.541) = 1275k - ft.$$

The critical moment for the large flange in compression from Step 1 is used as the basic case moment since the large flange is the referenced flange in this case.

The moment calculated by the theoretically correct procedure is 1516k - ft., differing by 5.2% from that calculated by the simplified procedure. This error is conservative, as anticipated because of the interpolation.

4.3 Conclusions

A method has been developed to determine the elastic critical lateral-torsional buckling moment of tapered beams with at least one plane of symmetry in the plane of loading, simply supported beams and subjected to bending moments at the ends. The governing differential equations were derived using the method of Trahair (21) and numerical solutions were obtained using the Galerkin method. Critical buckling moments determined using both four and five terms of a trigonometric displacement function showed that adequate convergence of the solution is assured with the use of only four terms, resulting in a savings of computer time.

The solutions obtained were compared with alternate solutions available in the literature for prismatic and doubly symmetric tapered beams, and agreement was excellent. Finite element solutions for prismatic and tapered, singly and doubly symmetric sections also showed excellent agreement with the solutions from the proposed method.

Using solutions generated by this method, and a step-wise multiple regression technique, a simplified design procedure was formulated. Using this procedure, critical buckling loads for simply supported tapered beams loaded by end moments will be predicted, at a 95% confidence level, with an accuracy of ±8% for single curvature cases and ±12% for double curvature cases. Limitations for the use of this procedure have been empirically determined, and must be observed. This proposed method is recommended for use with built up members composed of relatively thin plates, as are commonly in use in rigid frames of pre-engineered buildings. The method may also be applied to channel-capped sections if the ratio of large to small flange moments of inertia is less than 2.50.

REFERENCES

1. Amirikian, A., "Wedge-Beam Framing," Transactions of ASCE, Vol. 117, Paper No. 2508, 1952, pp. 596-631.

2. "Specification for the Design, Fabrication and Erection of Structural Steel for Buildings," Supplement No. 3, Appendix D, American Institute of Steel Construction, New York, 1974.

3. "Specification for the Design, Fabrication and Erection of Structural Steel for Buildings," American Institute of Steel Construction, New York, 1978.

4. Kuzmanovic, B. O., and Willems, N., Steel Design for Structural Engineers, Prentice-Hall, Inc., Englewood Cliffs, N.J., 1977.

5. Bleich, F., Buckling Strength of Metal Structures, McGraw-Hill Book Co., Inc., New York, N.Y., 1952.

6. Timoshenko, S. P., History of Strength of Materials, McGraw-Hill Book Co., Inc., New York, N.Y., 1953.

7. Timoshenko, S. P., and Gere, J. M., Theory of Elastic Stability, 2nd ed., McGraw-Hill Book Co., Inc., New York, N.Y., 1961.

8. Galambos, T. V., Structural Members and Frames, Prentice-Hall, Inc., Englewood Cliffs, N.J., 1968.

9. Guide to Stability Design Criteria for Metal Structures, Structural Stability Research Council, 3rd ed., B. G. Johnston, ed., John Wiley and Sons, Inc., New York, N.Y., 1976.

10. Wagner, H., "Verdrehung und Knickung von offenen Profilen," 25th Aniversary Publication, Technische Hochschule, Danzig, 1904-1929, Translated in National Advisory Committee for Aeronautics, Technical Memoir No. 807, 1936.

11. Timoshenko, S. P., "Theory of Bending, Torsion and Buckling of Thin-walled Members of Open Cross-section," Journal of the Franklin Institute, Vol. 239, 1945.

12. Vlasov, V. Z., Thin-Walled Elastic Beams, 2nd ed., Israel Program for Scientific Translations, Jerusalem, Israel, 1961.

13. Bleich, F., and Bleich, H., "Bending, Torsion and Buckling of Bars Composed of Thin Walls," Prelim. Pub. 2nd Cong. Intern. Assoc. Bridge and Structural Eng., English Edition, Berlin, 1936.

14. Lee, L. H. N., "Non-uniform Torsion of Tapered I-beams," Journal of the Franklin Institute, Vol. 262, 1956.

15. Preg, S. M., Jr., "Analytical Development of an Interaction Formula for the Design of Tapered Beam-Columns," Thesis presented to Carnegie Institute of Technology, at Pittsburg, Pa., in partial fulfillment of the requirements for the degree of Master of Science, 1967.

16. Culver, C. G., and Preg, S. M., Jr., "Elastic Stability of Tapered Beam-Columns," Journal of the Structural Division, ASCE, Vol. 94, No. ST2, Proc. Paper 5796, February, 1968, pp. 455-470.

17. Lee, G. C., Morrell, M. L., and Ketter, R. L., "Design of Tapered Members," Welding Research Council Bulletin, No. 173, June, 1972.

18. Chi, S., "Elastic Stability Analysis of Tapered Members," Thisis presented to the University of Oklahoma, Norman, Ok., in partial fulfillment of the requirements for the degree of Master of Science, 1978.

19. Trahair, N. S., and Kitipornchai, S., "Elastic Lateral Buckling of Stepped I-Beams," Journal of the Structural Division, ASCE, Vol. 97, No. ST10, Proc. Paper 8445, Oct., 1971, pp. 2535-2548.

20. Anderson, J. M., and Trahair, N. S., "Stability of Monosymmetric Beams and Cantilevers," Journal of the Structural Division, ASCE, Vol. 98, No. ST1, Proc. Paper 8646, Jan., 1972, pp. 269-286.

21. Kitipornchai, S., and Trahair, N. S., "Elastic Behavior of Tapered Monosymmetric I-beams," Journal of the Structural Division, ASCE, Vol. 101, No. ST8, Proc. Paper 11479, Aug., 1975, pp. 1661-1678.

22. Winter, G., "Lateral Stability of Unsymmetrical I-beams and Trusses in Bending," Transactions of ASCE, Vol. 108, Paper No. 2178, 1943, pp. 247-258.

23. de Vries, K., "Strength of Beams as Determined by Lateral Buckling," Transactions of ASCE, Vol. 112, Paper No. 2326, 1947, pp. 1245-1271.

24. Hall, D. B., discussion of "Strength of Beams as Determined by Lateral Buckling" by K. deVries, Transaction of ASCE, Vol. 112, 1947, pp. 1276-1279.

25. Salvadori, M. G., "Lateral Buckling of I-Beams," Transactions of ASCE, Vol. 120, Paper No. 2773, 1955, pp. 1165-1177.

26. Salvadori, M. G., "Lateral Buckling of Eccentrically Loaded I-Columns," Transactions of ASCE, Vol. 121, Paper No. 2836, 1956, pp. 1163-1178.

27. Clark, J. W., and Hill, H. N., "Lateral Buckling of Beams," Journal of the Structural Division, ASCE, Vol. 86, No. ST7, Proc. Paper 2559, July, 1960, pp. 175-196.

28. Morrell, M. L., and Lee, G. C., "Allowable Stress for Web-Tapered Beams with Lateral Restraints," Welding Research Council Bulletin, No. 192, February, 1974.

29. Trahair, N. S., The Behavior and Design of Steel Structures, Halsted Press, John Wiley and Sons, Inc., New York, N.Y., 1977.

30. Boley, B. A., "On the Accuracy of the Bernoulli-Euler Theory for Beams of Variable Section," Journal of Applied Mechanics, Vol. 30, September, 1963, pp. 373-378.

31. Lee, G. C., and Szabo, B. A., "Torsional Response of Tapered I-Girders," Journal of the Structural Division, ASCE, Vol. 93, No. ST5, Proc. Paper 5505, Oct., 1967, pp. 233-252.

32. Nethercot, D. A., and Rockey, K. C., "A Unified Approach to the Elastic Lateral Buckling of Beams," The Structural Engineer, Vol. 49, No. 7, July, 1971, pp. 321-330.

33. Barta, T. A., "On the Torsional-Flexural Buckling of Thin-Walled Elastic Bars with Monosymmetric Open Cross-Section," in Thin-Walled Structures, A. H. Chilver, ed., Chatto and Windus, London, England, pp. 60-86.

34. Akay, H. U., "Buckling Analysis of Stiffened Plates - BASP15," Computer Programming Series, The University of Texas at Austin, January, 1975.

35. Neter, J., and Wasserman, W., Applied Linear Statistical Models, Richard D. Irwin, Inc., Homewood, Ill., 1974.

36. "BMDP-77, Biomedical Computer Programs," W. J. Dixon, Series Ed., M. B. Brown, 1977 ed., University of California Press, Berkeley, Calif., 1977.

37. Nethercot, D. A., "Lateral Buckling of Tapered Beams," Publications, International Association of Bridge and Structural Engineering, Vol. 33-II, 1973, pp. 173-192.

APPENDIX A

Computer Program Listing and Sample Output

```
C**********************************************************************
C**********************************************************************
C**                                                                  **
C**                              LTBTB                               **
C**                                                                  **
C**                          A PROGRAM FOR THE                       **
C**                                                                  **
C**                     ELASTIC STABILITY ANALYSIS                   **
C**                                                                  **
C**                          OF WEDGE BEAMS                          **
C**                                                                  **
C**                     UNDER MOMENT GRADIENTS                       **
C**                                                                  **
C**                            B2                                    **
C**                        ============                              **
C**                    B1 ||    ||    || B1                         **
C**                       ||    ||    ||                            **
C**                             ||                                   **
C**                             ||                                   **
C**                             || B3                                **
C**                             ||                                   **
C**                             ||                                   **
C**                             ||                                   **
C**                          ==========                              **
C**                             B4                                   **
C**                                                                  **
C**      SUBMITTED BY PRISCILLA NELSON,IN PARTIAL COMPLETION OF THE  **
C**      REQUIREMENTS FOR THE MASTER'S DEGREE IN CIVIL/STRUCTURAL ENGINEERING **
C**      JULY,1979                                                   **
C**      MAJOR PROFESSOR:  DR. THOMAS M. MURRAY                      **
C**                                                                  **
C**********************************************************************
C**********************************************************************
C**                                                                  **
C**                          INPUT INSTRUCTIONS                      **
C**                                                                  **
C**            CARD ONE                                              **
C**                                                                  **
C**                 FULL EIGHTY COLUMNS AVAILABLE FOR LOAD AND GEOMETRY **
C**                 IDENTIFICATION. INFORMATION NOT USED IN PROGRAM.  **
C**                                                                  **
C**            CARD TWO                                              **
C**                                                                  **
C**                 IN 8F10 FORMAT, ENTER BEAM CROSS-SECTION DATA.   **
C**                                                                  **
C**                 B1  TOP FLANGE LIP LENGTH                        **
C**                 T1  TOP FLANGE LIP THICKNESS                     **
C**                 B2  TOP FLANGE LENGTH                            **
C**                 T2  TOP FLANGE THICKNESS                         **
C**                 B3  WEB LENGTH                                   **
C**                 T3  WEB THICKNESS                                **
C**                 B4  BOTTOM FLANGE LENGTH                         **
C**                 T4  BOTTOM FLANGE THICKNESS                      **
C**                                                                  **
C**            CARD THREE                                            **
C**                                                                  **
C**                 IN 4F10 FORMAT, ENTER BEAM GEOMETRY AND STRESS RATIOS. **
C**                                                                  **
C**                 ALPHA  TAPER                                     **
C**                 XL     LENGTH                                    **
C**                 ZL     RELATIVE STRESS AT LEFT END OF THE BEAM.  **
C**                        ZL=+1.0 COMPRESSION IN TOP FLANGE         **
C**                        ZL=-1.0  COMPRESSION IN BOTTOM FLANGE     **
C**                 ZR     RELATIVE STRESS AT RIGHT END OF THE BEAM. **
C**                        ZR=+1.0  COMPRESSION IN TOP FLANGE        **
C**                        ZR=-1.0  COMPRESSION IN BOTTOM FLANGE     **
C**                                                                  **
C**            LAST CARD                                             **
C**                                                                  **
C**                 "END OF DATA"   STARTING IN COLUMN 2.            **
C**                                                                  **
C**********************************************************************
C**********************************************************************
```

```
      EXTERNAL AMN,CMN,HMN,GMN
      DIMENSION A(8,8),C(8,8),S(4),ZZ(8,8),BETA(8),WK(128),X(8),ALFA(16)
      COMMON B1,T1,B2,T2,B3,T3,B4,T4,E,ALPHA,XL,XML,G,WIL,ARPA,M,N,YI
      COMMON AREA,GAM,NDD,YTL,YBL,EX
      COMPLEX ALFA,ZZ,X
      DOUBLE PRECISION ENDOF,ENDO
      DATA ENDOF/5HEND O/
C
C        DATA INPUT
C
 9999 READ(5,500) ENDO
  500 FORMAT(1X,A5,74H
     1                                )
      WRITE(6,501)
  501 FORMAT(1H1)
      IF(ENDOF.EQ.ENDO) STOP
      WRITE(6,500) ENDO
      READ(5,101)B1,T1,B2,T2,B3,T3,B4,T4
  101 FORMAT(8F10.4)
   25 READ(5,107)ALPHA,XL,ZL,ZR
  107 FORMAT(4F10.4)
      E=30000.
      G=11200.
C
C        NDD RECORDS IF TOP FLANGE AT REFERENCED END IS IN TENSION.
C
      NDD=-1
      IF(ZL.LT.0.0)NDD=+1
C
C        ITERN IS THE NUMBER OF TERMS INCLUDED IN THE DISPLACEMENT FUNCTION.
C
      ITERN=4
      WRITE(6,14)ITERN
   14 FORMAT(1H0,'THE NUMBER OF TERMS INCLUDED IN THE DISPLACEMENT FUNCT
     1ION IS',I4,' .')
C
C        SECTION PROPERTY CALCULATIONS
C
      BR=B3+ALPHA*XL
      AREA=B1*T1+B2*T2+B3*T3+B4*T4+B1*T1
      AREAR=AREA+ALPHA*XL*T3
      K=ITERN*2
      YBAL=(2.*B1*T1*(B3-B1/2.)+B2*T2*B3+B3*B3*T3/2.)/AREA
      YBAR=(2.*B1*T1*(BR-B1/2.)+B2*T2*BR+BR*BR*T3/2.)/AREAR
      YTOL=B3-YBAL
      YTOR=BR-YBAR
      XIL=(T1*B1**3*2.+B2*T2**3+T3*B3**3+B4*T4**3)/12.+2.*T1*B1*(YTOL-B1
     1/2.)**2+B2*T2*YTOL*YTOL+B3*T3*(B3/2.-YTOL)**2+B4*T4*YBAL*YBAL
      XIR=(T1*B1**3*2.+B2*T2**3+T3*BR**3+B4*T4**3)/12.+2.*T1*B1*(YTOR-B1
     1/2.)**2+B2*T2*YTOR*YTOR+BR*T3*(BR/2.-YTOR)**2+B4*T4*YBAR*YBAR
      TJL=(2.*B1*T1**3+B2*T2**3+B3*T3**3+B4*T4**3)/3.
      TJR=(2.*B1*T1**3+B2*T2**3+BR*T3**3+B4*T4**3)/3.
      YTL=2.*B1*T1*(B2/2.)**2+T2*B2**3/12.
      YBL=T4*B4**3/12.
      YI=YTL+YBL
      HL=(3.*B1*B1*B2*B2*T1-T4*B3*B4**3)/12./YI
      HR=(3.*B1*B1*B2*B2*T1-T4*BR*B4**3)/12./YI
      YOL=B3+HL-YBAL
      YOR=BR+HR-YBAR
      EX=B2*B2*B1*B1*T1/4./YTL
      WIL=YTL*YBL*(EX+B3)**2/YI
      WIR=YTL*YBL*(EX+BR)**2/YI
      ROL=(XIL+YI)/AREA+YOL**2
      ROR=(XIR+YI)/AREAR+YOR**2
      SL=XIL/YTOL
      SR=XIR/YTOR
      SBL=XIL/YBAL
      SBR=XIR/YBAR
      GAM=YTL*YBL/YI
```

```
      BXL=(YBAL*(T4*B4**3/12.+B4*T4*YBAL*YBAL)-YTOL*(T2*B2**3/12.+B2*T2*
     1YTOL*YTOL)-B2*B2*B1*T1*(YTOL/2.-B1/4.)-2.*B1*T1*(YTOL**3-1.5*B1*YT
     2OL*YTOL+B1*B1*YTOL-B1*B1*B1/4.)+YBAL**4*T3/4.-YTOL**4*T3/4.)/XIL+2
     3.*YOL
      BXR=(YBAR*(T4*B4**3/12.+B4*T4*YBAR*YBAR)-YTOR*(T2*B2**3/12.+B2*T2*
     1YTOR*YTOR)-B2*B2*B1*T1*(YTOR/2.-B1/4.)-2.*B1*T1*(YTOR**3-1.5*B1*YT
     2OR*YTOR+B1*B1*YTOR-B1*B1*B1/4.)+YBAR**4*T3/4.-YTOR**4*T3/4.)/XIR+2
     3.*YOR
C
C        CALCULATION OF MOMENT GRADIENT TERM
C
      ARFA=ZR*SR/ZL/SL*(-1.0)
      IF(NDD.GT.0)ARFA=ZR*SBR/ZL/SBL*(-1.0)
      IF(YOL.LE.1.E-4.AND.YOL.GE.-1.E-4)  YOL=0.0
      IF(YOR.LE.1.E-4.AND.YOR.GE.-1.E-4)  YOR=0.0
C
C        OUTPUT OF SECTION DATA
C
      WRITE(6,113)B1,T1,B2,T2,B3,T3,B4,T4,XL,ALPHA
  113 FORMAT(1H0,/' DIMENSIONS OF CROSS SECTION'//
     13X,'B1  =',F10.5,' IN',3X,'T1  =',F10.5,' IN'//
     13X,'B2  =',F10.5,' IN',3X,'T2  =',F10.5,' IN'//
     13X,'B3  =',F10.5,' IN',3X,'T3  =',F10.5,' IN'//
     13X,'B4  =',F10.5,' IN',3X,'T4  =',F10.5,' IN'//
     13X,'LENGTH=',F10.2,' IN.',//,3X,'ALPHA = ',F8.4)
      WRITE(6,111)ROL,ROR,YOL,YOR,ZL,ZR
  111 FORMAT(/,' RESULTS',///,10X,'LEFT END SECTION PROPERTIES',20X,'RIGH
     2T END SECTION PROPERTIES',//,7X,'RO   =',F11.4,' IN.',22X,'RO   =
     2',F10.4,' IN.',//,7X,'YO   = ',F10.4,' IN.',22X,'YO   = ',F10.4,'
     3IN.',///,7X,'RATIO  OF STRESSES IS,LEFT TO RIGHT ',F8.4,' :',F8.4)
      WRITE(6,103)AREA,AREAR,YBAL,YBAR,XIL,XIR
  103 FORMAT(//,7X,'AREA = ',F10.5,' IN**2',20X,'AREA = ',F10.5,' IN**2'
     1,//,7X,'YBAR = ',F10.5,' IN. FROM BOTTOM',10X,'YBAR = ',F10.5,' IN
     2. FROM BOTTOM',//,7X,'IX   = ',F15.5,' IN**4',15X,'IX   = ',F15.5,
     3' IN**4')
      WRITE(6,73)YI,YI,WIL,WIR,TJL,TJR,BXL,BXR
   73 FORMAT(//,7X,'IY   = ',F15.5,' IN**4',15X,'IY   = ',F15.5,' IN**4'
     1,//,7X,'CW   = ',F15.5,' IN**6',15X,'CW   = ',F15.5,' IN**6',//,7X
     2,'J    = ',F15.5,' IN**4',15X,'J    = ',F15.5,' IN**4',//,7X,'BX
     3 = ',F15.5,' IN.',17X,'BX   = ',F15.5,' IN.')
C
C        CHANGE TO UNITS OF FEET
C
      E=E*12**2
      G=G*12.**2
      WIL=WIL/12.**6
      YI=YI/12.**4
      XL=XL/12.
      AREA=AREA/12.**2
      GAM=GAM/12.**4
      B3=B3/12.
      T3=T3/12.
      B4=B4/12.
      T4=T4/12.
      B2=B2/12.
      T2=T2/12.
      B1=B1/12.
      T1=T1/12.
      YTL=YTL/(12.0**4)
      YBL=YBL/(12.0**4)
      EX=EX/12.
C
C        INITIALIZE MATRICES
C
      DO 205 I=1,K
      DO 205 J=1,K
      A(I,J)=0.0
      C(I,J)=0.0
  205 CONTINUE
```

```
C
C         INTEGRATE MATRIX ELEMENTS
C         I B M SUBROUTINE DCADRE USED
C
      STR=0.0
      END=1.0
      AERR=0.
      RERR=0.001
      DO 200 I=1,ITERN
      DO 200 J=1,ITERN
      M=I-1
      N=J-1
      A(I,J)=DCADRE(AMN,STR,END,AERR,RERR,ERROR,IER)
      A(I+ITERN,J+ITERN)=DCADRE(BMN,STR,END,AERR,RERR,ERROR,IER)
      C(I+ITERN,J+ITERN)=DCADRE(GMN,STR,END,AERR,RERR,ERROR,IER)
      C(I,ITERN+J)=DCADRE(CMN,STR,END,AERR,RERR,ERROR,IER)
  200 CONTINUE
C
C         COMPLETE MATRICES USING SYMMETRY
C
      DO 105 I=1,K
      DO 105 J=1,K
      A(J,I)=A(I,J)
      C(J,I)=C(I,J)
  105 CONTINUE
C
C         CALCULATE EIGENVALUES
C         I B M SUBROUTINE EIGZF USED
C
      IA=K
      IB=K
      IZ=K
      IJOB=0
  202 CALL EIGZF (A,IA,C,IB,K,IJOB,ALFA,BETA,ZZ,IZ,WK,IER)
      CR=10000000000.
      TD=10000000.
      DO 112 I=1,K
      IF(ABS(BETA(I)).LE.1.0E-8) X(I)=CR
      IF(ABS(BETA(I)).GT.1.E-8) X(I)=ALFA(I)/BETA(I)
      TT=REAL(X(I))
      IF(TT.LE.0.0) TD=ABS(TT)
C
C         FIND MINIMUM EIGENVALUE
C
      WRITE(6,3) X(I),ALFA(I),BETA(I)
    3 FORMAT(1X,5F15.6)
  112 CR=AMIN1(TD,CR)
C
C         CALCULATE MOMENT AT RIGHT END OF BEAM
C         SIGN CONVENTION AS PRESENTED IN THESIS
C
      OM=CR*NDD*(-1.0)
      CRM=OM*ARFA
      OM=OM*ZL/ABS(ZL)
C
C         OUTPUT FINAL RESULTS
C
  312 WRITE(6,300) OM,CRM
  300 FORMAT(//,' CRITICAL MOMENT AT LEFT END EQUALS',F15.5,' KIP-FT.',/
     1/,' CRITICAL MOMENT AT RIGHT END EQUALS',F14.5,' KIP-FT.')
      GOTO9999
  928 STOP
      END
```

```
      FUNCTION AMN(Z)
      COMMON B1,T1,B2,T2,B3,T3,B4,T4,E,ALPHA,XL,XML,G,WIL,ARFA,M,N,YI
      COMMON AREA,GAM,NDD,YTL,YBL,EX
      PP=3.14159
      IF(M.EQ.0) UMZ=-1.*PP**2*SIN(PP*Z)
      IF(M.EQ.1) UMZ=2.*PP*COS(PP*Z)-1.*PP**2*Z*SIN(PP*Z)
      IF(M.EQ.2) UMZ=2.*SIN(PP*Z)+4.*PP*Z*COS(PP*Z)-PP**2*Z**2*SIN(PP*Z)
      IF(M.GT.2) UMZ=M*(M-1)*Z**(M-2)*SIN(PP*Z)-PP**2*Z**M*SIN(PP*Z)+2.*P
     1P*M*Z**(M-1)*COS(PP*Z)
      IF(N.EQ.0) UNZ=-1.*PP**2*SIN(PP*Z)
      IF(N.EQ.1) UNZ=2.*PP*COS(PP*Z)-1.*PP**2*Z*SIN(PP*Z)
      IF(N.EQ.2) UNZ=2.*SIN(PP*Z)+4.*PP*Z*COS(PP*Z)-PP**2*Z**2*SIN(PP*Z)
      IF(N.GT.2) UNZ=N*(N-1)*Z**(N-2)*SIN(PP*Z)-PP**2*Z**N*SIN(PP*Z)+2.*P
     1P*N*Z**(N-1)*COS(PP*Z)
      AMN=UMZ*UNZ*E*YI/XL**3
      RETURN
      END
      FUNCTION CMN(Z)
      COMMON B1,T1,B2,T2,B3,T3,B4,T4,E,ALPHA,XL,XML,G,WIL,ARFA,M,N,YI
      COMMON AREA,GAM,NDD,YTL,YBL,EX
      PP=3.14159
      IF(M.EQ.0) UMZ=-1.*PP**2*SIN(PP*Z)
      IF(M.EQ.1) UMZ=2.*PP*COS(PP*Z)-1.*PP**2*Z*SIN(PP*Z)
      IF(M.EQ.2) UMZ=2.*SIN(PP*Z)+4.*PP*Z*COS(PP*Z)-PP**2*Z**2*SIN(PP*Z)
      IF(M.GT.2) UMZ=M*(M-1)*Z**(M-2)*SIN(PP*Z)-PP**2*Z**M*SIN(PP*Z)+2.*P
     1P*M*Z**(M-1)*COS(PP*Z)
      IF(N.EQ.0) UNI=SIN(PP*Z)
      IF(N.GT.0) UNI=Z**N*SIN(PP*Z)
      CMN=UNI*UMZ*(1.0-(1.0+ARFA)*Z)/XL*NDD
      RETURN
      END
      FUNCTION GMN(Z)
      COMMON B1,T1,B2,T2,B3,T3,B4,T4,E,ALPHA,XL,XML,G,WIL,ARFA,M,N,YI
      COMMON AREA,GAM,NDD,YTL,YBL,EX
      PP=3.14159
      IF(M.EQ.0) UMI=PP*COS(PP*Z)
      IF(N.EQ.0) UNI=PP*COS(PP*Z)
      IF(M.EQ.1) UMI=SIN(PP*Z)+PP*Z*COS(PP*Z)
      IF(N.EQ.1) UNI=SIN(PP*Z)+PP*Z*COS(PP*Z)
      IF(M.GT.1) UMI=M*Z**(M-1)*SIN(PP*Z)+PP*Z**M*COS(PP*Z)
      IF(N.GT.1) UNI=N*Z**(N-1)*SIN(PP*Z)+PP*Z**N*COS(PP*Z)
      IF(M.EQ.0) UP=SIN(PP*Z)
      IF(M.GT.0) UP=Z**M*SIN(PP*Z)
      BR=B3+ALPHA*XL*Z
      AREAR=AREA+ALPHA*XL*T3*Z
      YBAR=(2.*B1*T1*(BR-B1/2.)+B2*T2*BR+BR*BR*T3/2.)/AREAR
      HR=(3.*B1*B1*B2*B2*T1-T4*BR*B4**3)/12./YI
      YOR=BR+HR-YBAR
      IF(YOR.LE.1.E-4.AND.YOR.GE.-1.E-4)  YOR=0.0
      YTOR=BR-YBAR
      XIR=(T1*B1**3*2.+B2*T2**3+T3*BR**3+B4*T4**3)/12.+2.*T1*B1*(YTOR-B1
     1/2.)**2+B2*T2*YTOR*YTOR+BR*T3*(BR/2.-YTOR)**2+B4*T4*YBAR*YBAR
      BXR=(YBAR*(T4*B4**3/12.+B4*T4*YBAR*YBAR)-YTOR*(T2*B2**3/12.+B2*T2*
     1YTOR*YTOR)-B2*B2*B1*T1*(YTOR/2.-B1/4.)-2.*B1*T1*(YTOR**3-1.5*B1*YT
     2OR*YTOR+B1*B1*YTOR-B1*B1*B1/4.)+YBAR**4*T3/4.-YTOR**4*T3/4.)/XIR+2
     3.*YOR
      BX=BR+EX
      BBXR=(YTL*YTL/YI/YI*BX*ALPHA*YBAR*B4*T4-YBL*YBL/YI/YI*BX*ALPHA*YTO
     1R*B2*T2-2.0*(YBL*BX/YI-B1/2.0)*YBL/YI*ALPHA*(YTOR-B1/2.0)*B1*T1)/X
     2IR
      IF(BXR.LT.0.001.AND.BXR.GT.-0.001)BXR=0.0
      IF(BBXR.LT.0.001.AND.BBXR.GT.-0.001)BBXR=0.0
      GMN=(1.0-(1.0+ARFA)*Z)*(BXR*UMI*UNI/XL+BBXR*UP*UNI)*(NDD*(-1.0))
      RETURN
      END
```

```
      FUNCTION HMN(Z)
      COMMON B1,T1,B2,T2,B3,T3,B4,T4,E,ALPHA,XL,XML,G,WIL,ARFA,M,N,YI
      COMMON AREA,GAM,NDD,YTL,YBL,EX
      PP=3.14159
      IF(M.EQ.0) UMZ=-1.*PP**2*SIN(PP*Z)
      IF(N.EQ.0) UNZ=-1.*PP**2*SIN(PP*Z)
      IF(M.EQ.1) UMZ=2.*PP*COS(PP*Z)-1.*PP**2*Z*SIN(PP*Z)
      IF(N.EQ.1) UNZ=2.*PP*COS(PP*Z)-1.*PP**2*Z*SIN(PP*Z)
      IF(M.EQ.2) UMZ=2.*SIN(PP*Z)+4.*PP*Z*COS(PP*Z)-PP**2*Z**2*SIN(PP*Z)
      IF(N.EQ.2) UNZ=2.*SIN(PP*Z)+4.*PP*Z*COS(PP*Z)-PP**2*Z**2*SIN(PP*Z)
      IF(M.GT.2) UMZ=M*(M-1)*Z**(M-2)*SIN(PP*Z)-PP**2*Z**M*SIN(PP*Z)+2.*P
     1P*M*Z**(M-1)*COS(PP*Z)
      IF(N.GT.2) UNZ=N*(N-1)*Z**(N-2)*SIN(PP*Z)-PP**2*Z**N*SIN(PP*Z)+2.*P
     1P*N*Z**(N-1)*COS(PP*Z)
      IF(M.EQ.0) UMI=PP*COS(PP*Z)
      IF(N.EQ.0) UNI=PP*COS(PP*Z)
      IF(M.EQ.1) UMI=SIN(PP*Z)+PP*Z*COS(PP*Z)
      IF(N.EQ.1) UNI=SIN(PP*Z)+PP*Z*COS(PP*Z)
      IF(M.GT.1) UMI=M*Z**(M-1)*SIN(PP*Z)+PP*Z**M*COS(PP*Z)
      IF(N.GT.1) UNI=N*Z**(N-1)*SIN(PP*Z)+PP*Z**N*COS(PP*Z)
      BR=B3+ALPHA*XL*Z
      TJR=(2.*B1*T1**3+B2*T2**3+BR*T3**3+B4*T4**3)/3.
      BX=BR+EX
      WI=BX*BX*GAM
      WPSI=4.0*ALPHA*ALPHA*GAM
      WWPSI=2.0*ALPHA*GAM*BX
      HMN=G*TJR*UMI*UNI/XL+E*WI*UMZ*UNZ/XL/XL/XL+E*WWPSI/XL/XL*(UMZ*UNI+
     1UMI*UNZ)+E*WPSI/XL*UNI*UMI
      RETURN
      END
```

13. Bleich, F., and Bleich, H., "Bending, Torsion and Buckling of Bars Composed of Thin Walls," Prelim. Pub. 2nd Cong. Intern. Assoc. Bridge and Structural Eng., English Edition, Berlin, 1936.

14. Lee, L. H. N., "Non-uniform Torsion of Tapered I-beams," Journal of the Franklin Institute, Vol. 262, 1956.

15. Preg, S. M., Jr., "Analytical Development of an Interaction Formula for the Design of Tapered Beam-Columns," Thesis presented to Carnegie Institute of Technology, at Pittsburg, Pa., in partial fulfillment of the requirements for the degree of Master of Science, 1967.

16. Culver, C. G., and Preg, S. M., Jr., "Elastic Stability of Tapered Beam-Columns," Journal of the Structural Division, ASCE, Vol. 94, No. ST2, Proc. Paper 5796, February, 1968, pp. 455-470.

17. Lee, G. C., Morrell, M. L., and Ketter, R. L., "Design of Tapered Members," Welding Research Council Bulletin, No. 173, June, 1972.

18. Chi, S., "Elastic Stability Analysis of Tapered Members," Thisis presented to the University of Oklahoma, Norman, Ok., in partial fulfillment of the requirements for the degree of Master of Science, 1978.

19. Trahair, N. S., and Kitipornchai, S., "Elastic Lateral Buckling of Stepped I-Beams," Journal of the Structural Division, ASCE, Vol. 97, No. ST10, Proc. Paper 8445, Oct., 1971, pp. 2535-2548.

20. Anderson, J. M., and Trahair, N. S., "Stability of Monosymmetric Beams and Cantilevers," Journal of the Structural Division, ASCE, Vol. 98, No. ST1, Proc. Paper 8646, Jan., 1972, pp. 269-286.

21. Kitipornchai, S., and Trahair, N. S., "Elastic Behavior of Tapered Monosymmetric I-beams," Journal of the Structural Division, ASCE, Vol. 101, No. ST8, Proc. Paper 11479, Aug., 1975, pp. 1661-1678.

22. Winter, G., "Lateral Stability of Unsymmetrical I-beams and Trusses in Bending," Transactions of ASCE, Vol. 108, Paper No. 2178, 1943, pp. 247-258.

23. de Vries, K., "Strength of Beams as Determined by Lateral Buckling," Transactions of ASCE, Vol. 112, Paper No. 2326, 1947, pp. 1245-1271.

24. Hall, D. B., discussion of "Strength of Beams as Determined by Lateral Buckling" by K. deVries, Transaction of ASCE, Vol. 112, 1947, pp. 1276-1279.

25. Salvadori, M. G., "Lateral Buckling of I-Beams," Transactions of ASCE, Vol. 120, Paper No. 2773, 1955, pp. 1165-1177.

26. Salvadori, M. G., "Lateral Buckling of Eccentrically Loaded I-Columns," Transactions of ASCE, Vol. 121, Paper No. 2836, 1956, pp. 1163-1178.

27. Clark, J. W., and Hill, H. N., "Lateral Buckling of Beams," Journal of the Structural Division, ASCE, Vol. 86, No. ST7, Proc. Paper 2559, July, 1960, pp. 175-196.

28. Morrell, M. L., and Lee, G. C., "Allowable Stress for Web-Tapered Beams with Lateral Restraints," Welding Research Council Bulletin, No. 192, February, 1974.

29. Trahair, N. S., The Behavior and Design of Steel Structures, Halsted Press, John Wiley and Sons, Inc., New York, N.Y., 1977.

30. Boley, B. A., "On the Accuracy of the Bernoulli-Euler Theory for Beams of Variable Section," Journal of Applied Mechanics, Vol. 30, September, 1963, pp. 373-378.

31. Lee, G. C., and Szabo, B. A., "Torsional Response of Tapered I-Girders," Journal of the Structural Division, ASCE, Vol. 93, No. ST5, Proc. Paper 5505, Oct., 1967, pp. 233-252.

32. Nethercot, D. A., and Rockey, K. C., "A Unified Approach to the Elastic Lateral Buckling of Beams," The Structural Engineer, Vol. 49, No. 7, July, 1971, pp. 321-330.

33. Barta, T. A., "On the Torsional-Flexural Buckling of Thin-Walled Elastic Bars with Monosymmetric Open Cross-Section," in Thin-Walled Structures, A. H. Chilver, ed., Chatto and Windus, London, England, pp. 60-86.

34. Akay, H. U., "Buckling Analysis of Stiffened Plates - BASP15," Computer Programming Series, The University of Texas at Austin, January, 1975.

35. Neter, J., and Wasserman, W., Applied Linear Statistical Models, Richard D. Irwin, Inc., Homewood, Ill., 1974.

36. "BMDP-77, Biomedical Computer Programs," W. J. Dixon, Series Ed., M. B. Brown, 1977 ed., University of California Press, Berkeley, Calif., 1977.

37. Nethercot, D. A., "Lateral Buckling of Tapered Beams," Publications, International Association of Bridge and Structural Engineering, Vol. 33-II, 1973, pp. 173-192.

APPENDIX A

Computer Program Listing
and Sample Output

```
C**********************************************************************
C**********************************************************************
C**                                                                  **
C**                              LTBTB                               **
C**                                                                  **
C**                          A PROGRAM FOR THE                       **
C**                                                                  **
C**                    ELASTIC STABILITY ANALYSIS                    **
C**                                                                  **
C**                         OF WEDGE BEAMS                           **
C**                                                                  **
C**                      UNDER MOMENT GRADIENTS                      **
C**                                                                  **
C**                             B2                                   **
C**                          ==========                              **
C**                      B1 ||    ||   || B1                         **
C**                         ||    ||   ||                           **
C**                               ||                                 **
C**                               ||                                 **
C**                               || B3                              **
C**                               ||                                 **
C**                               ||                                 **
C**                               ||                                 **
C**                          ==========                              **
C**                             B4                                   **
C**                                                                  **
C**     SUBMITTED BY PRISCILLA NELSON,IN PARTIAL COMPLETION OF THE   **
C**     REQUIREMENTS FOR THE MASTER'S DEGREE IN CIVIL/STRUCTURAL ENGINEERING **
C**     JULY,1979                                                    **
C**     MAJOR PROFESSOR:  DR. THOMAS M. MURRAY                       **
C**                                                                  **
C**********************************************************************
C**********************************************************************
C**                                                                  **
C**                         INPUT INSTRUCTIONS                       **
C**                                                                  **
C**          CARD ONE                                                **
C**                                                                  **
C**               FULL EIGHTY COLUMNS AVAILABLE FOR LOAD AND GEOMETRY **
C**               IDENTIFICATION. INFORMATION NOT USED IN PROGRAM.   **
C**                                                                  **
C**          CARD TWO                                                **
C**                                                                  **
C**               IN 8F10 FORMAT, ENTER BEAM CROSS-SECTION DATA.     **
C**                                                                  **
C**               B1  TOP FLANGE LIP LENGTH                          **
C**               T1  TOP FLANGE LIP THICKNESS                       **
C**               B2  TOP FLANGE LENGTH                              **
C**               T2  TOP FLANGE THICKNESS                           **
C**               B3  WEB LENGTH                                     **
C**               T3  WEB THICKNESS                                  **
C**               B4  BOTTOM FLANGE LENGTH                           **
C**               T4  BOTTOM FLANGE THICKNESS                        **
C**                                                                  **
C**          CARD THREE                                              **
C**                                                                  **
C**               IN 4F10 FORMAT, ENTER BEAM GEOMETRY AND STRESS RATIOS. **
C**                                                                  **
C**               ALPHA  TAPER                                       **
C**               XL     LENGTH                                      **
C**               ZL     RELATIVE STRESS AT LEFT END OF THE BEAM.    **
C**                      ZL=+1.0 COMPRESSION IN TOP FLANGE           **
C**                      ZL=-1.0  COMPRESSION IN BOTTOM FLANGE       **
C**               ZR     RELATIVE STRESS AT RIGHT END OF THE BEAM.   **
C**                      ZR=+1.0  COMPRESSION IN TOP FLANGE          **
C**                      ZR=-1.0  COMPRESSION IN BOTTOM FLANGE       **
C**                                                                  **
C**          LAST CARD                                               **
C**                                                                  **
C**               "END OF DATA"   STARTING IN COLUMN 2.              **
C**                                                                  **
C**********************************************************************
C**********************************************************************
```

```
      EXTERNAL AMN,CMN,HMN,GMN
      DIMENSION A(8,8),C(8,8),S(4),ZZ(8,8),BETA(8),WK(128),X(8),ALFA(16)
      COMMON B1,T1,B2,T2,B3,T3,B4,T4,E,ALPHA,XL,XML,G,WIL,ARPA,M,N,YI
      COMMON AREA,GAM,NDD,YTL,YBL,EX
      COMPLEX ALFA,ZZ,X
      DOUBLE PRECISION ENDOF,ENDO
      DATA ENDOF/5HEND O/
C
C        DATA INPUT
C
 9999 READ(5,500) ENDO
  500 FORMAT(1X,A5,74H
     1                                )
      WRITE(6,501)
  501 FORMAT(1H1)
      IF(ENDOF.EQ.ENDO) STOP
      WRITE(6,500) ENDO
      READ(5,101)B1,T1,B2,T2,B3,T3,B4,T4
  101 FORMAT(8F10.4)
   25 READ(5,107)ALPHA,XL,ZL,ZR
  107 FORMAT(4F10.4)
      E=30000.
      G=11200.
C
C        NDD RECORDS IF TOP FLANGE AT REFERENCED END IS IN TENSION.
C
      NDD=-1
      IF(ZL.LT.0.0)NDD=+1
C
C        ITERN IS THE NUMBER OF TERMS INCLUDED IN THE DISPLACEMENT FUNCTION.
C
      ITERN=4
      WRITE(6,14)ITERN
   14 FORMAT(1H0,'THE NUMBER OF TERMS INCLUDED IN THE DISPLACEMENT FUNCT
     1ION IS',I4,' .')
C
C        SECTION PROPERTY CALCULATIONS
C
      BR=B3+ALPHA*XL
      AREA=B1*T1+B2*T2+B3*T3+B4*T4+B1*T1
      AREAR=AREA+ALPHA*XL*T3
      K=ITERN*2
      YBAL=(2.*B1*T1*(B3-B1/2.)+B2*T2*B3+B3*B3*T3/2.)/AREA
      YBAR=(2.*B1*T1*(BR-B1/2.)+B2*T2*BR+BR*BR*T3/2.)/AREAR
      YTOL=B3-YBAL
      YTOR=BR-YBAR
      XIL=(T1*B1**3*2.+B2*T2**3+T3*B3**3+B4*T4**3)/12.+2.*T1*B1*(YTOL-B1
     1/2.)**2+B2*T2*YTOL*YTOL+B3*T3*(B3/2.-YTOL)**2+B4*T4*YBAL*YBAL
      XIR=(T1*B1**3*2.+B2*T2**3+T3*BR**3+B4*T4**3)/12.+2.*T1*B1*(YTOR-B1
     1/2.)**2+B2*T2*YTOR*YTOR+BR*T3*(BR/2.-YTOR)**2+B4*T4*YBAR*YBAR
      TJL=(2.*B1*T1**3+B2*T2**3+B3*T3**3+B4*T4**3)/3.
      TJR=(2.*B1*T1**3+B2*T2**3+BR*T3**3+B4*T4**3)/3.
      YTL=2.*B1*T1*(B2/2.)**2+T2*B2**3/12.
      YBL=T4*B4**3/12.
      YI=YTL+YBL
      HL=(3.*B1*B1*B2*B2*T1-T4*B3*B4**3)/12./YI
      HR=(3.*B1*B1*B2*B2*T1-T4*BR*B4**3)/12./YI
      YOL=B3+HL-YBAL
      YOR=BR+HR-YBAR
      EX=B2*B2*B1*B1*T1/4./YTL
      WIL=YTL*YBL*(EX+B3)**2/YI
      WIR=YTL*YBL*(EX+BR)**2/YI
      ROL=(XIL+YI)/AREA+YOL**2
      ROR=(XIR+YI)/AREAR+YOR**2
      SL=XIL/YTOL
      SR=XIR/YTOR
      SBL=XIL/YBAL
      SBR=XIR/YBAR
      GAM=YTL*YBL/YI
```

```
      BXL=(YBAL*(T4*B4**3/12.+B4*T4*YBAL*YBAL)-YTOL*(T2*B2**3/12.+B2*T2*
     1YTOL*YTOL)-B2*B2*B1*T1*(YTOL/2.-B1/4.)-2.*B1*T1*(YTOL**3-1.5*B1*YT
     2OL*YTOL+B1*B1*YTOL-B1*B1*B1/4.)+YBAL**4*T3/4.-YTOL**4*T3/4.)/XIL+2
     3.*YOL
      BXR=(YBAR*(T4*B4**3/12.+B4*T4*YBAR*YBAR)-YTOR*(T2*B2**3/12.+B2*T2*
     1YTOR*YTOR)-B2*B2*B1*T1*(YTOR/2.-B1/4.)-2.*B1*T1*(YTOR**3-1.5*B1*YT
     2OR*YTOR+B1*B1*YTOR-B1*B1*B1/4.)+YBAR**4*T3/4.-YTOR**4*T3/4.)/XIR+2
     3.*YOR
C
C        CALCULATION OF MOMENT GRADIENT TERM
C
      ARFA=ZR*SR/ZL/SL*(-1.0)
      IF(NDD.GT.0)ARFA=ZR*SBR/ZL/SBL*(-1.0)
      IF(YOL.LE.1.E-4.AND.YOL.GE.-1.E-4) YOL=0.0
      IF(YOR.LE.1.E-4.AND.YOR.GE.-1.E-4) YOR=0.0
C
C        OUTPUT OF SECTION DATA
C
      WRITE(6,113)B1,T1,B2,T2,B3,T3,B4,T4,XL,ALPHA
  113 FORMAT(1H0,/' DIMENSIONS OF CROSS SECTION'//
     13X,'B1  =',F10.5,' IN',3X,'T1  =',F10.5,' IN'//
     13X,'B2  =',F10.5,' IN',3X,'T2  =',F10.5,' IN'//
     13X,'B3  =',F10.5,' IN',3X,'T3  =',F10.5,' IN'//
     13X,'B4  =',F10.5,' IN',3X,'T4  =',F10.5,' IN'//
     13X,'LENGTH=',F10.2,' IN.',//,3X,'ALPHA = ',F8.4)
      WRITE(6,111)ROL,ROR,YOL,YOR,ZL,ZR
  111 FORMAT(/,' RESULTS',///,10X,'LEFT END SECTION PROPERTIES',20X,'RIGH
     2T END SECTION PROPERTIES',///,7X,'RO   =',F11.4,' IN.',22X,'RO   =
     2',F10.4,' IN.',//,7X,'YO   = ',F10.4,' IN.',22X,'YO   = ',F10.4,'
     3IN.',///,7X,'RATIO  OF STRESSES IS,LEFT TO RIGHT ',F8.4,' :',F8.4)
      WRITE(6,103)AREA,AREAR,YBAL,YBAR,XIL,XIR
  103 FORMAT(//,7X,'AREA = ',F10.5,' IN**2',20X,'AREA = ',F10.5,' IN**2'
     1,//,7X,'YBAR = ',F10.5,' IN. FROM BOTTOM',10X,'YBAR = ',F10.5,' IN
     2. FROM BOTTOM',//,7X,'IX   = ',F15.5,' IN**4',15X,'IX   = ',F15.5,
     3' IN**4')
      WRITE(6,73)YI,YI,WIL,WIR,TJL,TJR,BXL,BXR
   73 FORMAT(//,7X,'IY   = ',F15.5,' IN**4',15X,'IY   = ',F15.5,' IN**4'
     1,//,7X,'CW   = ',F15.5,' IN**6',15X,'CW   = ',F15.5,' IN**6',//,7X
     2,'J    = ',F15.5,' IN**4',15X,'J    = ',F15.5,' IN**4',//,7X,'BX
     3 = ',F15.5,' IN.',17X,'BX   = ',F15.5,' IN.')
C
C        CHANGE TO UNITS OF FEET
C
      E=E*12**2
      G=G*12.**2
      WIL=WIL/12.**6
      YI=YI/12.**4
      XL=XL/12.
      AREA=AREA/12.**2
      GAM=GAM/12.**4
      B3=B3/12.
      T3=T3/12.
      B4=B4/12.
      T4=T4/12.
      B2=B2/12.
      T2=T2/12.
      B1=B1/12.
      T1=T1/12.
      YTL=YTL/(12.0**4)
      YBL=YBL/(12.0**4)
      EX=EX/12.
C
C        INITIALIZE MATRICES
C
      DO 205 I=1,K
      DO 205 J=1,K
      A(I,J)=0.0
      C(I,J)=0.0
  205 CONTINUE
```

```
C
C         INTEGRATE MATRIX ELEMENTS
C         I B M SUBROUTINE DCADRE USED
C
      STR=0.0
      END=1.0
      AERR=0.
      RERR=0.001
      DO 200 I=1,ITERN
      DO 200 J=1,ITERN
      M=I-1
      N=J-1
      A(I,J)=DCADRE(AMN,STR,END,AERR,RERR,ERROR,IER)
      A(I+ITERN,J+ITERN)=DCADRE(HMN,STR,END,AERR,RERR,ERROR,IER)
      C(I+ITERN,J+ITERN)=DCADRE(GMN,STR,END,AERR,RERR,ERROR,IER)
      C(I,ITERN+J)=DCADRE(CMN,STR,END,AERR,RERR,ERROR,IER)
  200 CONTINUE
C
C         COMPLETE MATRICES USING SYMMETRY
C
      DO 105 I=1,K
      DO 105 J=1,K
      A(J,I)=A(I,J)
      C(J,I)=C(I,J)
  105 CONTINUE
C
C         CALCULATE EIGENVALUES
C         I B M SUBROUTINE EIGZF USED
C
      IA=K
      IB=K
      IZ=K
      IJOB=0
  202 CALL EIGZF (A,IA,C,IB,K,IJOB,ALFA,BETA,ZZ,IZ,WK,IER)
      CR=10000000000.
      TD=10000000.
      DO 112 I=1,K
      IF(ABS(BETA(I)).LE.1.0E-8) X(I)=CR
      IF(ABS(BETA(I)).GT.1.E-8)X(I)=ALFA(I)/BETA(I)
      TT=REAL(X(I))
      IF(TT.LE.0.0) TD=ABS(TT)
C
C         FIND MINIMUM EIGENVALUE
C
      WRITE(6,3)X(I),ALFA(I),BETA(I)
    3 FORMAT(1X,5F15.6)
  112 CR=AMIN1(TD,CR)
C
C         CALCULATE MOMENT AT RIGHT END OF BEAM
C         SIGN CONVENTION AS PRESENTED IN THESIS
C
      OM=CR*NDD*(-1.0)
      CRM=OM*ARFA
      OM=OM*ZL/ABS(ZL)
C
C         OUTPUT FINAL RESULTS
C
  312 WRITE(6,300)OM,CRM
  300 FORMAT(//,' CRITICAL MOMENT AT LEFT END EQUALS',F15.5,' KIP-FT.',/
     1/,' CRITICAL MOMENT AT RIGHT END EQUALS',F14.5,' KIP-FT.')
      GOTO9999
  928 STOP
      END
```

```
      FUNCTION AMN(Z)
      COMMON B1,T1,B2,T2,B3,T3,B4,T4,E,ALPHA,XL,XML,G,WIL,ARFA,M,N,YI
      COMMON AREA,GAM,NDD,YTL,YBL,EX
      PP=3.14159
      IF(M.EQ.0) UMZ=-1.*PP**2*SIN(PP*Z)
      IF(M.EQ.1) UMZ=2.*PP*COS(PP*Z)-1.*PP**2*Z*SIN(PP*Z)
      IF(M.EQ.2) UMZ=2.*SIN(PP*Z)+4.*PP*Z*COS(PP*Z)-PP**2*Z**2*SIN(PP*Z)
      IF(M.GT.2) UMZ=M*(M-1)*Z**(M-2)*SIN(PP*Z)-PP**2*Z**M*SIN(PP*Z)+2.*P
     1P*M*Z**(M-1)*COS(PP*Z)
      IF(N.EQ.0) UNZ=-1.*PP**2*SIN(PP*Z)
      IF(N.EQ.1) UNZ=2.*PP*COS(PP*Z)-1.*PP**2*Z*SIN(PP*Z)
      IF(N.EQ.2) UNZ=2.*SIN(PP*Z)+4.*PP*Z*COS(PP*Z)-PP**2*Z**2*SIN(PP*Z)
      IF(N.GT.2) UNZ=N*(N-1)*Z**(N-2)*SIN(PP*Z)-PP**2*Z**N*SIN(PP*Z)+2.*P
     1P*N*Z**(N-1)*COS(PP*Z)
      AMN=UMZ*UNZ*E*YI/XL**3
      RETURN
      END
      FUNCTION CMN(Z)
      COMMON B1,T1,B2,T2,B3,T3,B4,T4,E,ALPHA,XL,XML,G,WIL,ARFA,M,N,YI
      COMMON AREA,GAM,NDD,YTL,YBL,EX
      PP=3.14159
      IF(M.EQ.0) UMZ=-1.*PP**2*SIN(PP*Z)
      IF(M.EQ.1) UMZ=2.*PP*COS(PP*Z)-1.*PP**2*Z*SIN(PP*Z)
      IF(M.EQ.2) UMZ=2.*SIN(PP*Z)+4.*PP*Z*COS(PP*Z)-PP**2*Z**2*SIN(PP*Z)
      IF(M.GT.2) UMZ=M*(M-1)*Z**(M-2)*SIN(PP*Z)-PP**2*Z**M*SIN(PP*Z)+2.*P
     1P*M*Z**(M-1)*COS(PP*Z)
      IF(N.EQ.0) UNI=SIN(PP*Z)
      IF(N.GT.0) UNI=Z**N*SIN(PP*Z)
      CMN=UNI*UMZ*(1.0-(1.0+ARFA)*Z)/XL*NDD
      RETURN
      END
      FUNCTION GMN(Z)
      COMMON B1,T1,B2,T2,B3,T3,B4,T4,E,ALPHA,XL,XML,G,WIL,ARFA,M,N,YI
      COMMON AREA,GAM,NDD,YTL,YBL,EX
      PP=3.14159
      IF(M.EQ.0) UMI=PP*COS(PP*Z)
      IF(N.EQ.0) UNI=PP*COS(PP*Z)
      IF(M.EQ.1) UMI=SIN(PP*Z)+PP*Z*COS(PP*Z)
      IF(N.EQ.1) UNI=SIN(PP*Z)+PP*Z*COS(PP*Z)
      IF(M.GT.1) UMI=M*Z**(M-1)*SIN(PP*Z)+PP*Z**M*COS(PP*Z)
      IF(N.GT.1) UNI=N*Z**(N-1)*SIN(PP*Z)+PP*Z**N*COS(PP*Z)
      IF(M.EQ.0) UP=SIN(PP*Z)
      IF(M.GT.0) UP=Z**M*SIN(PP*Z)
      BR=B3+ALPHA*XL*Z
      AREAR=AREA+ALPHA*XL*T3*Z
      YBAR=(2.*B1*T1*(BR-B1/2.)+B2*T2*BR+BR*BR*T3/2.)/AREAR
      HR=(3.*B1*B1*B2*B2*T1-T4*BR*B4**3)/12./YI
      YOR=BR+HR-YBAR
      IF(YOR.LE.1.E-4.AND.YOR.GE.-1.E-4)  YOR=0.0
      YTOR=BR-YBAR
      XIR=(T1*B1**3*2.+B2*T2**3+T3*BR**3+B4*T4**3)/12.+2.*T1*B1*(YTOR-B1
     1/2.)**2+B2*T2*YTOR*YTOR+BR*T3*(BR/2.-YTOR)**2+B4*T4*YBAR*YBAR
      BXR=(YBAR*(T4*B4**3/12.+B4*T4*YBAR*YBAR)-YTOR*(T2*B2**3/12.+B2*T2*
     1YTOR*YTOR)-B2*B2*B1*T1*(YTOR/2.-B1/4.)-2.*B1*T1*(YTOR**3-1.5*B1*YT
     2OR*YTOR+B1*B1*YTOR-B1*B1*B1/4.)+YBAR**4*T3/4.-YTOR**4*T3/4.)/XIR+2
     3.*YOR
      BX=BR+EX
      BBXR=(YTL*YTL/YI/YI*BX*ALPHA*YBAR*B4*T4-YBL*YBL/YI/YI*BX*ALPHA*YTO
     1R*B2*T2-2.0*(YBL*BX/YI-B1/2.0)*YBL/YI*ALPHA*(YTOR-B1/2.0)*B1*T1)/X
     2IR
      IF(BXR.LT.0.001.AND.BXR.GT.-0.001)BXR=0.0
      IF(BBXR.LT.0.001.AND.BBXR.GT.-0.001)BBXR=0.0
      GMN=(1.0-(1.0+ARFA)*Z)*(BXR*UMI*UNI/XL+BBXR*UP*UNI)*(NDD*(-1.0))
      RETURN
      END
```

```
      FUNCTION HMN(Z)
      COMMON B1,T1,B2,T2,B3,T3,B4,T4,E,ALPHA,XL,XML,G,WIL,ARFA,M,N,YI
      COMMON AREA,GAM,NDD,YTL,YBL,EX
      PP=3.14159
      IF(M.EQ.0) UMZ=-1.*PP**2*SIN(PP*Z)
      IF(N.EQ.0) UNZ=-1.*PP**2*SIN(PP*Z)
      IF(M.EQ.1) UMZ=2.*PP*COS(PP*Z)-1.*PP**2*Z*SIN(PP*Z)
      IF(N.EQ.1) UNZ=2.*PP*COS(PP*Z)-1.*PP**2*Z*SIN(PP*Z)
      IF(M.EQ.2) UMZ=2.*SIN(PP*Z)+4.*PP*Z*COS(PP*Z)-PP**2*Z**2*SIN(PP*Z)
      IF(N.EQ.2) UNZ=2.*SIN(PP*Z)+4.*PP*Z*COS(PP*Z)-PP**2*Z**2*SIN(PP*Z)
      IF(M.GT.2) UMZ=M*(M-1)*Z**(M-2)*SIN(PP*Z)-PP**2*Z**M*SIN(PP*Z)+2.*P
     1P*M*Z**(M-1)*COS(PP*Z)
      IF(N.GT.2) UNZ=N*(N-1)*Z**(N-2)*SIN(PP*Z)-PP**2*Z**N*SIN(PP*Z)+2.*P
     1P*N*Z**(N-1)*COS(PP*Z)
      IF(M.EQ.0) UMI=PP*COS(PP*Z)
      IF(N.EQ.0) UNI=PP*COS(PP*Z)
      IF(M.EQ.1) UMI=SIN(PP*Z)+PP*Z*COS(PP*Z)
      IF(N.EQ.1) UNI=SIN(PP*Z)+PP*Z*COS(PP*Z)
      IF(M.GT.1) UMI=M*Z**(M-1)*SIN(PP*Z)+PP*Z**M*COS(PP*Z)
      IF(N.GT.1) UNI=N*Z**(N-1)*SIN(PP*Z)+PP*Z**N*COS(PP*Z)
      BR=B3+ALPHA*XL*Z
      TJR=(2.*B1*T1**3+B2*T2**3+BR*T3**3+B4*T4**3)/3.
      BX=BR+EX
      WI=BX*BX*GAM
      WPSI=4.0*ALPHA*ALPHA*GAM
      WWPSI=2.0*ALPHA*GAM*BX
      HMN=G*TJR*UMI*UNI/XL+E*WI*UMZ*UNZ/XL/XL/XL+E*WWPSI/XL/XL*(UMZ*UNI+
     1UMI*UNZ)+E*WPSI/XL*UNI*UMI
      RETURN
      END
```

```
      EXTERNAL AMN,CMN,HMN,GMN
      DIMENSION A(8,8),C(8,8),S(4),ZZ(8,8),BETA(8),WK(128),X(8),ALFA(16)
      COMMON B1,T1,B2,T2,B3,T3,B4,T4,E,ALPHA,XL,XML,G,WIL,ARPA,M,N,YI
      COMMON AREA,GAM,NDD,YTL,YBL,EX
      COMPLEX ALFA,ZZ,X
      DOUBLE PRECISION ENDOF,ENDO
      DATA ENDOF/5HEND O/
C
C        DATA INPUT
C
 9999 READ(5,500) ENDO
  500 FORMAT(1X,A5,74H
     1                                )
      WRITE(6,501)
  501 FORMAT(1H1)
      IF(ENDOF.EQ.ENDO) STOP
      WRITE(6,500) ENDO
      READ(5,101)B1,T1,B2,T2,B3,T3,B4,T4
  101 FORMAT(8F10.4)
   25 READ(5,107)ALPHA,XL,ZL,ZR
  107 FORMAT(4F10.4)
      E=30000.
      G=11200.
C
C        NDD RECORDS IF TOP FLANGE AT REFERENCED END IS IN TENSION.
C
      NDD=-1
      IF(ZL.LT.0.0)NDD=+1
C
C        ITERN IS THE NUMBER OF TERMS INCLUDED IN THE DISPLACEMENT FUNCTION.
C
      ITERN=4
      WRITE(6,14)ITERN
   14 FORMAT(1H0,'THE NUMBER OF TERMS INCLUDED IN THE DISPLACEMENT FUNCT
     1ION IS',I4,' .')
C
C        SECTION PROPERTY CALCULATIONS
C
      BR=B3+ALPHA*XL
      AREA=B1*T1+B2*T2+B3*T3+B4*T4+B1*T1
      AREAR=AREA+ALPHA*XL*T3
      K=ITERN*2
      YBAL=(2.*B1*T1*(B3-B1/2.)+B2*T2*B3+B3*B3*T3/2.)/AREA
      YBAR=(2.*B1*T1*(BR-B1/2.)+B2*T2*BR+BR*BR*T3/2.)/AREAR
      YTOL=B3-YBAL
      YTOR=BR-YBAR
      XIL=(T1*B1**3*2.+B2*T2**3+T3*B3**3+B4*T4**3)/12.+2.*T1*B1*(YTOL-B1
     1/2.)**2+B2*T2*YTOL*YTOL+B3*T3*(B3/2.-YTOL)**2+B4*T4*YBAL*YBAL
      XIR=(T1*B1**3*2.+B2*T2**3+T3*BR**3+B4*T4**3)/12.+2.*T1*B1*(YTOR-B1
     1/2.)**2+B2*T2*YTOR*YTOR+BR*T3*(BR/2.-YTOR)**2+B4*T4*YBAR*YBAR
      TJL=(2.*B1*T1**3+B2*T2**3+B3*T3**3+B4*T4**3)/3.
      TJR=(2.*B1*T1**3+B2*T2**3+BR*T3**3+B4*T4**3)/3.
      YTL=2.*B1*T1*(B2/2.)**2+T2*B2**3/12.
      YBL=T4*B4**3/12.
      YI=YTL+YBL
      HL=(3.*B1*B1*B2*B2*T1-T4*B3*B4**3)/12./YI
      HR=(3.*B1*B1*B2*B2*T1-T4*BR*B4**3)/12./YI
      YOL=B3+HL-YBAL
      YOR=BR+HR-YBAR
      EX=B2*B2*B1*B1*T1/4./YTL
      WIL=YTL*YBL*(EX+B3)**2/YI
      WIR=YTL*YBL*(EX+BR)**2/YI
      ROL=(XIL+YI)/AREA+YOL**2
      ROR=(XIR+YI)/AREAR+YOR**2
      SL=XIL/YTOL
      SR=XIR/YTOR
      SBL=XIL/YBAL
      SBR=XIR/YBAR
      GAM=YTL*YBL/YI
```

```
      BXL=(YBAL*(T4*B4**3/12.+B4*T4*YBAL*YBAL)-YTOL*(T2*B2**3/12.+B2*T2*
     1YTOL*YTOL)-B2*B2*B1*T1*(YTOL/2.-B1/4.)-2.*B1*T1*(YTOL**3-1.5*B1*YT
     2OL*YTOL+B1*B1*YTOL-B1*B1*B1/4.)+YBAL**4*T3/4.-YTOL**4*T3/4.)/XIL+2
     3.*YOL
      BXR=(YBAR*(T4*B4**3/12.+B4*T4*YBAR*YBAR)-YTOR*(T2*B2**3/12.+B2*T2*
     1YTOR*YTOR)-B2*B2*B1*T1*(YTOR/2.-B1/4.)-2.*B1*T1*(YTOR**3-1.5*B1*YT
     2OR*YTOR+B1*B1*YTOR-B1*B1*B1/4.)+YBAR**4*T3/4.-YTOR**4*T3/4.)/XIR+2
     3.*YOR
C
C        CALCULATION OF MOMENT GRADIENT TERM
C
      ARFA=ZR*SR/ZL/SL*(-1.0)
      IF(NDD.GT.0)ARFA=ZR*SBR/ZL/SBL*(-1.0)
      IF(YOL.LE.1.E-4.AND.YOL.GE.-1.E-4) YOL=0.0
      IF(YOR.LE.1.E-4.AND.YOR.GE.-1.E-4) YOR=0.0
C
C        OUTPUT OF SECTION DATA
C
      WRITE(6,113)B1,T1,B2,T2,B3,T3,B4,T4,XL,ALPHA
  113 FORMAT(1H0,/' DIMENSIONS OF CROSS SECTION'//
     13X,'B1  =',F10.5,' IN',3X,'T1  =',F10.5,' IN'//
     13X,'B2  =',F10.5,' IN',3X,'T2  =',F10.5,' IN'//
     13X,'B3  =',F10.5,' IN',3X,'T3  =',F10.5,' IN'//
     13X,'B4  =',F10.5,' IN',3X,'T4  =',F10.5,' IN'//
     13X,'LENGTH=',F10.2,' IN.',//,3X,'ALPHA = ',F8.4)
      WRITE(6,111)ROL,ROR,YOL,YOR,ZL,ZR
  111 FORMAT(/,' RESULTS',//,10X,'LEFT END SECTION PROPERTIES',20X,'RIGH
     2T END SECTION PROPERTIES',//,7X,'RO   =',F11.4,' IN.',22X,'RO   =
     2',F10.4,' IN.',//,7X,'YO   = ',F10.4,' IN.',22X,'YO.  = ',F10.4,'
     3IN.',///,7X,'RATIO  OF STRESSES IS,LEFT TO RIGHT ',F8.4,' :',F8.4)
      WRITE(6,103)AREA,AREAR,YBAL,YBAR,XIL,XIR
  103 FORMAT(//,7X,'AREA = ',F10.5,' IN**2',20X,'AREA = ',F10.5,' IN**2'
     1,//,7X,'YBAR = ',F10.5,' IN. FROM BOTTOM',10X,'YBAR = ',F10.5,' IN
     2. FROM BOTTOM',//,7X,'IX   = ',F15.5,' IN**4',15X,'IX   = ',F15.5,
     3' IN**4')
      WRITE(6,73)YI,YI,WIL,WIR,TJL,TJR,BXL,BXR
   73 FORMAT(//,7X,'IY   = ',F15.5,' IN**4',15X,'IY   = ',F15.5,' IN**4'
     1,//,7X,'CW   = ',F15.5,' IN**6',15X,'CW   = ',F15.5,' IN**6',//,7X
     2,'J    = ',F15.5,' IN**4',15X,'J    = ',F15.5,' IN**4',//,7X,'BX
     3 = ',F15.5,' IN.',17X,'BX   = ',F15.5,' IN.')
C
C        CHANGE TO UNITS OF FEET
C
      E=E*12**2
      G=G*12.**2
      WIL=WIL/12.**6
      YI=YI/12.**4
      XL=XL/12.
      AREA=AREA/12.**2
      GAM=GAM/12.**4
      B3=B3/12.
      T3=T3/12.
      B4=B4/12.
      T4=T4/12.
      B2=B2/12.
      T2=T2/12.
      B1=B1/12.
      T1=T1/12.
      YTL=YTL/(12.0**4)
      YBL=YBL/(12.0**4)
      EX=EX/12.
C
C        INITIALIZE MATRICES
C
      DO 205 I=1,K
      DO 205 J=1,K
      A(I,J)=0.0
      C(I,J)=0.0
  205 CONTINUE
```

```
C
C         INTEGRATE MATRIX ELEMENTS
C         I B M SUBROUTINE DCADRE USED
C
      STR=0.0
      END=1.0
      AERR=0.
      RERR=0.001
      DO 200 I=1,ITERN
      DO 200 J=1,ITERN
      M=I-1
      N=J-1
      A(I,J)=DCADRE(AMN,STR,END,AERR,RERR,ERROR,IER)
      A(I+ITERN,J+ITERN)=DCADRE(HMN,STR,END,AERR,RERR,ERROR,IER)
      C(I+ITERN,J+ITERN)=DCADRE(GMN,STR,END,AERR,RERR,ERROR,IER)
      C(I,ITERN+J)=DCADRE(CMN,STR,END,AERR,RERR,ERROR,IER)
  200 CONTINUE
C
C         COMPLETE MATRICES USING SYMMETRY
C
      DO 105 I=1,K
      DO 105 J=1,K
      A(J,I)=A(I,J)
      C(J,I)=C(I,J)
  105 CONTINUE
C
C         CALCULATE EIGENVALUES
C         I B M SUBROUTINE EIGZF USED
C
      IA=K
      IB=K
      IZ=K
      IJOB=0
  202 CALL EIGZF (A,IA,C,IB,K,IJOB,ALFA,BETA,ZZ,IZ,WK,IER)
      CR=10000000000.
      TD=10000000.
      DO 112 I=1,K
      IF(ABS(BETA(I)).LE.1.0E-8) X(I)=CR
      IF(ABS(BETA(I)).GT.1.E-8)X(I)=ALFA(I)/BETA(I)
      TT=REAL(X(I))
      IF(TT.LE.0.0) TD=ABS(TT)
C
C         FIND MINIMUM EIGENVALUE
C
      WRITE(6,3)X(I),ALFA(I),BETA(I)
    3 FORMAT(1X,5F15.6)
  112 CR=AMIN1(TD,CR)
C
C         CALCULATE MOMENT AT RIGHT END OF BEAM
C         SIGN CONVENTION AS PRESENTED IN THESIS
C
      OM=CR*NDD*(-1.0)
      CRM=OM*ARFA
      OM=OM*ZL/ABS(ZL)
C
C         OUTPUT FINAL RESULTS
C
  312 WRITE(6,300)OM,CRM
  300 FORMAT(//,' CRITICAL MOMENT AT LEFT END EQUALS',F15.5,' KIP-FT.',/
     1/,' CRITICAL MOMENT AT RIGHT END EQUALS',F14.5,' KIP-FT.')
      GOTO9999
  928 STOP
      END
```

```
      FUNCTION AMN(Z)
      COMMON B1,T1,B2,T2,B3,T3,B4,T4,E,ALPHA,XL,XML,G,WIL,ARFA,M,N,YI
      COMMON AREA,GAM,NDD,YTL,YBL,EX
      PP=3.14159
      IF(M.EQ.0) UMZ=-1.*PP**2*SIN(PP*Z)
      IF(M.EQ.1) UMZ=2.*PP*COS(PP*Z)-1.*PP**2*Z*SIN(PP*Z)
      IF(M.EQ.2) UMZ=2.*SIN(PP*Z)+4.*PP*Z*COS(PP*Z)-PP**2*Z**2*SIN(PP*Z)
      IF(M.GT.2) UMZ=M*(M-1)*Z**(M-2)*SIN(PP*Z)-PP**2*Z**M*SIN(PP*Z)+2.*P
     1P*M*Z**(M-1)*COS(PP*Z)
      IF(N.EQ.0) UNZ=-1.*PP**2*SIN(PP*Z)
      IF(N.EQ.1) UNZ=2.*PP*COS(PP*Z)-1.*PP**2*Z*SIN(PP*Z)
      IF(N.EQ.2) UNZ=2.*SIN(PP*Z)+4.*PP*Z*COS(PP*Z)-PP**2*Z**2*SIN(PP*Z)
      IF(N.GT.2) UNZ=N*(N-1)*Z**(N-2)*SIN(PP*Z)-PP**2*Z**N*SIN(PP*Z)+2.*P
     1P*N*Z**(N-1)*COS(PP*Z)
      AMN=UMZ*UNZ*E*YI/XL**3
      RETURN
      END
      FUNCTION CMN(Z)
      COMMON B1,T1,B2,T2,B3,T3,B4,T4,E,ALPHA,XL,XML,G,WIL,ARFA,M,N,YI
      COMMON AREA,GAM,NDD,YTL,YBL,EX
      PP=3.14159
      IF(M.EQ.0) UMZ=-1.*PP**2*SIN(PP*Z)
      IF(M.EQ.1) UMZ=2.*PP*COS(PP*Z)-1.*PP**2*Z*SIN(PP*Z)
      IF(M.EQ.2) UMZ=2.*SIN(PP*Z)+4.*PP*Z*COS(PP*Z)-PP**2*Z**2*SIN(PP*Z)
      IF(M.GT.2) UMZ=M*(M-1)*Z**(M-2)*SIN(PP*Z)-PP**2*Z**M*SIN(PP*Z)+2.*P
     1P*M*Z**(M-1)*COS(PP*Z)
      IF(N.EQ.0) UNI=SIN(PP*Z)
      IF(N.GT.0) UNI=Z**N*SIN(PP*Z)
      CMN=UNI*UMZ*(1.0-(1.0+ARFA)*Z)/XL*NDD
      RETURN
      END
      FUNCTION GMN(Z)
      COMMON B1,T1,B2,T2,B3,T3,B4,T4,E,ALPHA,XL,XML,G,WIL,ARFA,M,N,YI
      COMMON AREA,GAM,NDD,YTL,YBL,EX
      PP=3.14159
      IF(M.EQ.0) UMI=PP*COS(PP*Z)
      IF(N.EQ.0) UNI=PP*COS(PP*Z)
      IF(M.EQ.1) UMI=SIN(PP*Z)+PP*Z*COS(PP*Z)
      IF(N.EQ.1) UNI=SIN(PP*Z)+PP*Z*COS(PP*Z)
      IF(M.GT.1) UMI=M*Z**(M-1)*SIN(PP*Z)+PP*Z**M*COS(PP*Z)
      IF(N.GT.1) UNI=N*Z**(N-1)*SIN(PP*Z)+PP*Z**N*COS(PP*Z)
      IF(M.EQ.0) UP=SIN(PP*Z)
      IF(M.GT.0) UP=Z**M*SIN(PP*Z)
      BR=B3+ALPHA*XL*Z
      AREAR=AREA+ALPHA*XL*T3*Z
      YBAR=(2.*B1*T1*(BR-B1/2.)+B2*T2*BR+BR*BR*T3/2.)/AREAR
      HR=(3.*B1*B1*B2*B2*T1-T4*BR*B4**3)/12./YI
      YOR=BR+HR-YBAR
      IF(YOR.LE.1.E-4.AND.YOR.GE.-1.E-4)  YOR=0.0
      YTOR=BR-YBAR
      XIR=(T1*B1**3*2.+B2*T2**3+T3*BR**3+B4*T4**3)/12.+2.*T1*B1*(YTOR-B1
     1/2.)**2+B2*T2*YTOR*YTOR+BR*T3*(BR/2.-YTOR)**2+B4*T4*YBAR*YBAR
      BXR=(YBAR*(T4*B4**3/12.+B4*T4*YBAR*YBAR)-YTOR*(T2*B2**3/12.+B2*T2*
     1YTOR*YTOR)-B2*B2*B1*T1*(YTOR/2.-B1/4.)-2.*B1*T1*(YTOR**3-1.5*B1*YT
     2OR*YTOR+B1*B1*YTOR-B1*B1*B1/4.)+YBAR**4*T3/4.-YTOR**4*T3/4.)/XIR+2
     3.*YOR
      BX=BR+EX
      BBXR=(YTL*YTL/YI/YI*BX*ALPHA*YBAR*B4*T4-YBL*YBL/YI/YI*BX*ALPHA*YTO
     1R*B2*T2-2.0*(YBL*BX/YI-B1/2.0)*YBL/YI*ALPHA*(YTOR-B1/2.0)*B1*T1)/X
     2IR
      IF(BIR.LT.0.001.AND.BXR.GT.-0.001)BXR=0.0
      IF(BBXR.LT.0.001.AND.BBXR.GT.-0.001)BBXR=0.0
      GMN=(1.0-(1.0+ARFA)*Z)*(BXR*UMI*UNI/XL+BBXR*UP*UNI)*(NDD*(-1.0))
      RETURN
      END
```

```
      FUNCTION HMN(Z)
      COMMON B1,T1,B2,T2,B3,T3,B4,T4,E,ALPHA,XL,XML,G,WIL,ARFA,M,N,YI
      COMMON AREA,GAM,NDD,YTL,YBL,EX
      PP=3.14159
      IF(M.EQ.0) UMZ=-1.*PP**2*SIN(PP*Z)
      IF(N.EQ.0) UNZ=-1.*PP**2*SIN(PP*Z)
      IF(M.EQ.1) UMZ=2.*PP*COS(PP*Z)-1.*PP**2*Z*SIN(PP*Z)
      IF(N.EQ.1) UNZ=2.*PP*COS(PP*Z)-1.*PP**2*Z*SIN(PP*Z)
      IF(M.EQ.2) UMZ=2.*SIN(PP*Z)+4.*PP*Z*COS(PP*Z)-PP**2*Z**2*SIN(PP*Z)
      IF(N.EQ.2) UNZ=2.*SIN(PP*Z)+4.*PP*Z*COS(PP*Z)-PP**2*Z**2*SIN(PP*Z)
      IF(M.GT.2) UMZ=M*(M-1)*Z**(M-2)*SIN(PP*Z)-PP**2*Z**M*SIN(PP*Z)+2.*P
     1P*M*Z**(M-1)*COS(PP*Z)
      IF(N.GT.2) UNZ=N*(N-1)*Z**(N-2)*SIN(PP*Z)-PP**2*Z**N*SIN(PP*Z)+2.*P
     1P*N*Z**(N-1)*COS(PP*Z)
      IF(M.EQ.0) UMI=PP*COS(PP*Z)
      IF(N.EQ.0) UNI=PP*COS(PP*Z)
      IF(M.EQ.1) UMI=SIN(PP*Z)+PP*Z*COS(PP*Z)
      IF(N.EQ.1) UNI=SIN(PP*Z)+PP*Z*COS(PP*Z)
      IF(M.GT.1) UMI=M*Z**(M-1)*SIN(PP*Z)+PP*Z**M*COS(PP*Z)
      IF(N.GT.1) UNI=N*Z**(N-1)*SIN(PP*Z)+PP*Z**N*COS(PP*Z)
      BR=B3+ALPHA*XL*Z
      TJR=(2.*B1*T1**3+B2*T2**3+BR*T3**3+B4*T4**3)/3.
      BX=BR+EX
      WI=BX*BX*GAM
      WPSI=4.0*ALPHA*ALPHA*GAM
      WWPSI=2.0*ALPHA*GAM*BX
      HMN=G*TJR*UMI*UNI/XL+E*WI*UMZ*UNZ/XL/XL/XL+E*WWPSI/XL/XL*(UMZ*UNI+
     1UMI*UNZ)+E*WPSI/XL*UNI*UMI
      RETURN
      END
```

EXAMPLE USING A WIDE-FLANGED BEAM WITH A CHANNEL CAP

THE NUMBER OF TERMS INCLUDED IN THE DISPLACEMENT FUNCTION IS 4 .

DIMENSIONS OF CROSS SECTION

B1 =	1.66800 IN	T1 =	0.34300 IN
B2 =	5.65700 IN	T2 =	0.50400 IN
B3 =	7.79000 IN	T3 =	0.23000 IN
B4 =	5.25000 IN	T4 =	0.30800 IN

LENGTH= 60.00 IN.

ALPHA = 0.0

RESULTS

LEFT END SECTION PROPERTIES		RIGHT END SECTION PROPERTIES	
RC =	16.3793 IN.	RC =	16.3793 IN.
YC =	1.7324 IN.	YC =	1.7324 IN.

RATIO OF STRESSES IS,LEFT TO RIGHT 1.0000 : 1.0000

AREA =	7.40407 IN**2	AREA =	7.40407 IN**2
YBAR =	5.01728 IN. FROM BOTTOM	YBAR =	5.01728 IN. FROM BOTTOM
IX =	78.58081 IN**4	IX =	78.58081 IN**4
IY =	20.47188 IN**4	IY =	20.47188 IN**4
CW =	206.70523 IN**6	CW =	206.70523 IN**6
J =	0.36901 IN**4	J =	0.36901 IN**4
BX =	5.32799 IN.	BX =	5.32799 IN.

CRITICAL MOMENT AT LEFT END EQUALS 995.75830 KIP-FT.

CRITICAL MOMENT AT RIGHT END EQUALS -995.75830 KIP-FT.

APPENDIX B

Calculation of Section Properties

$$J = \frac{2b_1t_1^3 + b_2t_2^3 + b_3t_3^3 + b_4t_4^3}{3}$$

$$I_{y,top} = 2b_1t_1\left(\frac{b_2}{2}\right)^2 + \frac{t_2b_2^3}{12}$$

$$I_{y,bottom} = \frac{t_4b_4^3}{12}$$

$$I_y = I_{y,top} + I_{y,bottom}$$

$$y_o = b_3 + \frac{3b_1^2b_2^2t_1 - t_4b_3b_4^3}{12\ I_y} - \bar{y}_b$$

$$e = \frac{b_2^2b_1^2t_1}{4I_{y,top}} = \text{location of shear center of channel}$$

$$I_w = \frac{I_{y,top}\ I_{y,bottom}\ (e + b_3)^2}{I_y}$$

$$\beta_x = \frac{1}{I_x}\left[\bar{y}_b\left(\frac{t_4b_4^3}{12} + b_4t_4\,\bar{y}_b^2\right) - \bar{y}_t\left(\frac{t_2b_2^3}{12} + b_2t_2\,\bar{y}_t^2\right)\right.$$

$$- b_2^2b_1t_1\left(\frac{\bar{y}_t}{2} - \frac{b_1}{4}\right) - 2b_1t_1\left(\bar{y}_t^3 - \frac{3b_1\bar{y}_t^2}{2} + b_1^2\bar{y}_t - \frac{b_1^3}{4}\right)$$

$$\left. + \frac{\bar{y}_b^4t_3}{4} - \frac{\bar{y}_t^4t_3}{4}\right] + 2y_o$$

APPENDIX C

Data and Results of Comparisons

TABLE C.1 Results of Critical Moment Calculations SECTION I

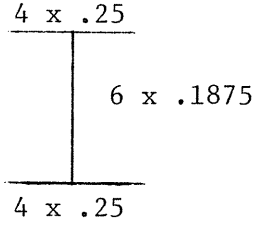

Taper α Radians	Length ℓ Inches	Stress Ratio r	Polynomial Functions (CHI) 4 terms (K-ft)	Polynomial Functions (CHI) 5 terms (K-ft)	Trigonometric Functions (Proposed) 4 terms (K-ft)	Trigonometric Functions (Proposed) 5 terms (K-ft)	Finite Element BASP 15 4 x 8 (K-ft)	Finite Element BASP 15 2 x 25 (K-ft)	Finite Element BASP 15 4 x 16 (K-ft)
0.00	60.0	+1.0*	62.82	62.79	62.79	62.79	63.91		63.08
		+0.5	82.83	82.79	82.92	82.92	84.25		83.09
		0.0	114.85	114.84	116.21	116.19	116.59		116.40
		-0.5	155.89	155.76	163.73	163.40		164.83	
		-1.0	156.43	156.06	172.61	171.95		175.80	
0.01	180.0	+1.0	10.67	10.67	10.63	10.63		10.82	
		+0.5	14.64	14.63	14.77	14.77	16.12		15.08
		0.0	20.71	20.69	22.37	22.35	24.74	22.65	22.85
		-0.5	25.28	25.15	33.38	33.21	37.78	33.71	
		-1.0	19.79	19.74	26.58	26.46	29.59	27.20	27.08

*exact solution = 62.79 K-ft.

TABLE C.2 Results of Critical Moment Calculations SECTION II

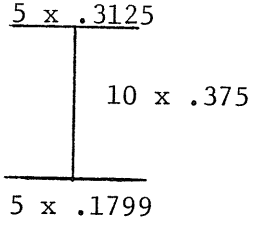

Taper α Radians	Length ℓ Inches	Stress Ratio r	Polynomial Functions (CHI) 4 terms (K-ft)	Polynomial Functions (CHI) 5 terms (K-ft)	Trigonometric Functions (Proposed) 4 terms (K-ft)	Trigonometric Functions (Proposed) 5 terms (K-ft)	Finite Element BASP 15 4 x 8 (K-ft)	Finite Element BASP 15 2 x 25 (K-ft)	Finite Element BASP 15 4 x 16 (K-ft)
0.00	120.0	+1.0*	71.94	71.91	71.91	71.91	76.27		74.01
		+0.5	94.47	94.44	94.90	94.90	100.71		97.67
		0.0	127.62	127.62	132.31	132.29	140.98		136.11
		-0.5	156.98	156.82	181.82	181.38	195.79	185.60	186.24
		-1.0	127.89	127.31	160.44	159.08	173.30	159.98	161.47
0.05	120.0	+1.0	62.74	62.69	61.07	61.04	64.28		62.87
		+0.5	89.33	89.31	89.38	89.37	94.10		91.94
		0.0	138.75	138.58	151.45	151.26	159.82		154.87
		-0.5	168.87	167.31	204.84	204.15	213.50		201.99
		-1.0	90.63	90.53	94.09	94.00	97.67		93.86

*exact solution = 71.91 K-ft.

TABLE C.3 Results of Critical Moment Calculations SECTION III

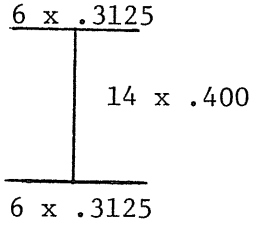

Taper α Radians	Length ℓ Inches	Stress Ratio r	Polynomial Functions (CHI) 4 terms (K-ft)	Polynomial Functions (CHI) 5 terms (K-ft)	Trigonometric Functions (Proposed) 4 terms (K-ft)	Trigonometric Functions (Proposed) 5 terms (K-ft)	Finite Element BASP 15 4 x 8 (K-ft)	Finite Element BASP 15 2 x 25 (K-ft)	Finite Element BASP 15 4 x 16 (K-ft)
0.00	180.0	+1.0*	83.47	83.43	83.43	83.53	88.34		85.32
		+0.5	109.69	109.65	110.11	110.11	116.65		112.58
		0.0	149.06	149.06	153.66	153.63	163.39		156.98
		-0.5	191.44	191.21	215.09	214.48	230.71		218.69
		-1.0	182.96	182.52	228.76	227.57	247.39		231.33
0.05	180.0	+1.0	70.16	70.12	68.47	68.46	71.61		69.81
		+0.5	101.33	101.31	101.32	101.32	106.15		103.31
		0.0	163.02	162.73	176.51	176.30	185.90		179.16
		-0.5	221.96	219.38	272.75	271.07	287.40		269.96
		-1.0	138.92	183.43	143.57	143.55	150.24		144.42

*exact solution = 83.43 K-ft.

TABLE C.4 Results of Critical Moment Calculations SECTION IV

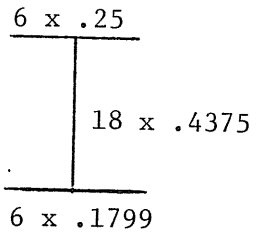

Taper α Radians	Length ℓ Inches	Stress Ratio r	Polynomial Functions (CHI) 4 terms (K-ft)	Polynomial Functions (CHI) 5 terms (K-ft)	Trigonometric Functions (Proposed) 4 terms (K-ft)	Trigonometric Functions (Proposed) 5 terms (K-ft)	Finite Element BASP 15 4 x 8 (K-ft)	Finite Element BASP 15 2 x 25 (K-ft)	Finite Element BASP 15 4 x 16 (K-ft)
0.00	240	+1.0*	54.95	54.93	54.93	54.93	59.89		56.93
		+0.5	71.94	71.92	72.45	72.45	79.08		75.10
		0.0	95.54	95.54	100.75	100.72	110.60		104.47
		-0.5	114.47	114.34	139.38	138.91	155.27		144.48
		-1.0	97.86	97.55	136.01	134.93	153.98		140.53
0.05	240	+1.0	43.23	43.20	42.10	42.09	45.12		43.59
		+0.5	63.83	63.81	63.50	63.50	68.21		65.75
		0.0	104.41	104.22	115.26	115.11	125.25		119.18
		-0.5	118.08	117.40	155.03	154.01	170.00		159.05
		-1.0	63.02	62.93	68.27	68.09	73.63		70.25

*exact solution = 54.93 K-ft.

TABLE C.5 Results of Critical Moment Calculations SECTION V

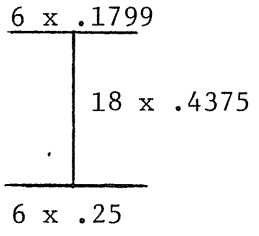

Taper α Radians	Length ℓ Inches	Stress Ratio r	Polynomial Functions (CHI) 4 terms (K-ft)	Polynomial Functions (CHI) 5 terms (K-ft)	Trigonometric Functions (Proposed) 4 terms (K-ft)	Trigonometric Functions (Proposed) 5 terms (K-ft)	Finite Element BASP 15 4 x 8 (K-ft)	Finite Element BASP 15 2 x 25 (K-ft)	Finite Element BASP 15 4 x 16 (K-ft)
0.00	240.0	+1.0*	46.50	46.48	46.48	46.48	51.12		48.23
		+0.5	60.85	60.83	61.27	61.27	67.46		63.57
		0.0	80.83	80.82	84.91	84.87	94.12		88.09
		-0.5	99.83	99.59	118.01	117.45	132.65		122.06
		-1.0	97.86	97.53	136.01	134.92	153.98		140.53
0.05	240.0	+1.0	35.02	34.99	34.31	34.31	36.96		35.52
		+0.5	52.33	52.32	52.13	52.13	56.36		53.99
		0.0	87.94	87.71	96.06	95.93	105.55		99.35
		-0.5	113.52	111.97	154.69	153.22	173.44		159.03
		-1.0	71.10	70.79	79.46	79.31	86.02		82.16

*exact solution = 46.49 K-ft.

TABLE C.1 Results of Critical Moment Calculations SECTION I

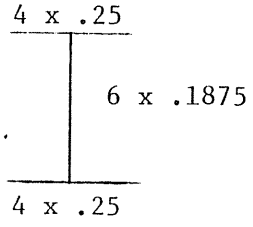

Taper α Radians	Length ℓ Inches	Stress Ratio r	Polynomial Functions (CHI) 4 terms (K-ft)	Polynomial Functions (CHI) 5 terms (K-ft)	Trigonometric Functions (Proposed) 4 terms (K-ft)	Trigonometric Functions (Proposed) 5 terms (K-ft)	Finite Element BASP 15 4 x 8 (K-ft)	Finite Element BASP 15 2 x 25 (K-ft)	Finite Element BASP 15 4 x 16 (K-ft)
0.00	60.0	+1.0*	62.82	62.79	62.79	62.79	63.91		63.08
		+0.5	82.83	82.79	82.92	82.92	84.25		83.09
		0.0	114.85	114.84	116.21	116.19	116.59		116.40
		-0.5	155.89	155.76	163.73	163.40		164.83	
		-1.0	156.43	156.06	172.61	171.95		175.80	
0.01	180.0	+1.0	10.67	10.67	10.63	10.63		10.82	
		+0.5	14.64	14.63	14.77	14.77	16.12		15.08
		0.0	20.71	20.69	22.37	22.35	24.74	22.65	22.85
		-0.5	25.28	25.15	33.38	33.21	37.78	33.71	
		-1.0	19.79	19.74	26.58	26.46	29.59	27.20	27.08

*exact solution = 62.79 K-ft.

TABLE C.2 Results of Critical Moment Calculations SECTION II

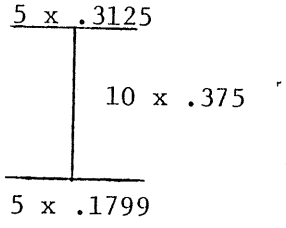

Taper α Radians	Length ℓ Inches	Stress Ratio r	Polynomial Functions (CHI) 4 terms (K-ft)	Polynomial Functions (CHI) 5 terms (K-ft)	Trigonometric Functions (Proposed) 4 terms (K-ft)	Trigonometric Functions (Proposed) 5 terms (K-ft)	Finite Element BASP 15 4 x 8 (K-ft)	Finite Element BASP 15 2 x 25 (K-ft)	Finite Element BASP 15 4 x 16 (K-ft)
0.00	120.0	+1.0*	71.94	71.91	71.91	71.91	76.27		74.01
		+0.5	94.47	94.44	94.90	94.90	100.71		97.67
		0.0	127.62	127.62	132.31	132.29	140.98		136.11
		-0.5	156.98	156.82	181.82	181.38	195.79	185.60	186.24
		-1.0	127.89	127.31	160.44	159.08	173.30	159.98	161.47
0.05	120.0	+1.0	62.74	62.69	61.07	61.04	64.28		62.87
		+0.5	89.33	89.31	89.38	89.37	94.10		91.94
		0.0	138.75	138.58	151.45	151.26	159.82		154.87
		-0.5	168.87	167.31	204.84	204.15	213.50		201.99
		-1.0	90.63	90.53	94.09	94.00	97.67		93.86

*exact solution = 71.91 K-ft.

TABLE C.3 Results of Critical Moment Calculations SECTION III

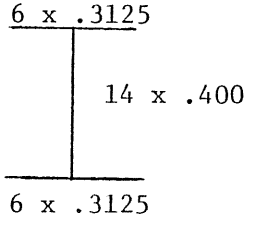

Taper α Radians	Length ℓ Inches	Stress Ratio r	Polynomial Functions (CHI) 4 terms (K-ft)	Polynomial Functions (CHI) 5 terms (K-ft)	Trigonometric Functions (Proposed) 4 terms (K-ft)	Trigonometric Functions (Proposed) 5 terms (K-ft)	Finite Element BASP 15 4 x 8 (K-ft)	Finite Element BASP 15 2 x 25 (K-ft)	Finite Element BASP 15 4 x 16 (K-ft)
0.00	180.0	+1.0*	83.47	83.43	83.43	83.53	88.34		85.32
		+0.5	109.69	109.65	110.11	110.11	116.65		112.58
		0.0	149.06	149.06	153.66	153.63	163.39		156.98
		-0.5	191.44	191.21	215.09	214.48	230.71		218.69
		-1.0	182.96	182.52	228.76	227.57	247.39		231.33
0.05	180.0	+1.0	70.16	70.12	68.47	68.46	71.61		69.81
		+0.5	101.33	101.31	101.32	101.32	106.15		103.31
		0.0	163.02	162.73	176.51	176.30	185.90		179.16
		-0.5	221.96	219.38	272.75	271.07	287.40		269.96
		-1.0	138.92	183.43	143.57	143.55	150.24		144.42

*exact solution = 83.43 K-ft.

TABLE C.4 Results of Critical Moment Calculations SECTION IV

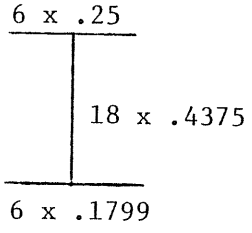

Taper α Radians	Length ℓ Inches	Stress Ratio r	Polynomial Functions (CHI) 4 terms (K-ft)	Polynomial Functions (CHI) 5 terms (K-ft)	Trigonometric Functions (Proposed) 4 terms (K-ft)	Trigonometric Functions (Proposed) 5 terms (K-ft)	Finite Element BASP 15 4 x 8 (K-ft)	Finite Element BASP 15 2 x 25 (K-ft)	Finite Element BASP 15 4 x 16 (K-ft)
0.00	240	+1.0*	54.95	54.93	54.93	54.93	59.89		56.93
		+0.5	71.94	71.92	72.45	72.45	79.08		75.10
		0.0	95.54	95.54	100.75	100.72	110.60		104.47
		-0.5	114.47	114.34	139.38	138.91	155.27		144.48
		-1.0	97.86	97.55	136.01	134.93	153.98		140.53
0.05	240	+1.0	43.23	43.20	42.10	42.09	45.12		43.59
		+0.5	63.83	63.81	63.50	63.50	68.21		65.75
		0.0	104.41	104.22	115.26	115.11	125.25		119.18
		-0.5	118.08	117.40	155.03	154.01	170.00		159.05
		-1.0	63.02	62.93	68.27	68.09	73.63		70.25

*exact solution = 54.93 K-ft.

TABLE C.5 Results of Critical Moment Calculations SECTION V

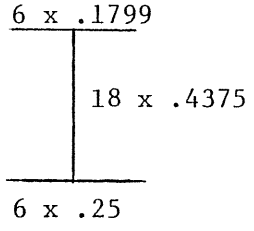

Taper α Radians	Length ℓ Inches	Stress Ratio r	Polynomial Functions (CHI) 4 terms (K-ft)	Polynomial Functions (CHI) 5 terms (K-ft)	Trigonometric Functions (Proposed) 4 terms (K-ft)	Trigonometric Functions (Proposed) 5 terms (K-ft)	Finite Element BASP 15 4 x 8 (K-ft)	Finite Element BASP 15 2 x 25 (K-ft)	Finite Element BASP 15 4 x 16 (K-ft)
0.00	240.0	+1.0*	46.50	46.48	46.48	46.48	51.12		48.23
		+0.5	60.85	60.83	61.27	61.27	67.46		63.57
		0.0	80.83	80.82	84.91	84.87	94.12		88.09
		-0.5	99.83	99.59	118.01	117.45	132.65		122.06
		-1.0	97.86	97.53	136.01	134.92	153.98		140.53
0.05	240.0	+1.0	35.02	34.99	34.31	34.31	36.96		35.52
		+0.5	52.33	52.32	52.13	52.13	56.36		53.99
		0.0	87.94	87.71	96.06	95.93	105.55		99.35
		-0.5	113.52	111.97	154.69	153.22	173.44		159.03
		-1.0	71.10	70.79	79.46	79.31	86.02		82.16

*exact solution = 46.49 K-ft.

$$J = \frac{2b_1t_1^3 + b_2t_2^3 + b_3t_3^3 + b_4t_4^3}{3}$$

$$I_{y,top} = 2b_1t_1\left(\frac{b_2}{2}\right)^2 + \frac{t_2b_2^3}{12}$$

$$I_{y,bottom} = \frac{t_4b_4^3}{12}$$

$$I_y = I_{y,top} + I_{y,bottom}$$

$$y_o = b_3 + \frac{3b_1^2b_2^2t_1 - t_4b_3b_4^3}{12\ I_y} - \bar{y}_b$$

$$e = \frac{b_2^2b_1^2t_1}{4I_{y,top}} = \text{location of shear center of channel}$$

$$I_w = \frac{I_{y,top}\ I_{y,bottom}\ (e + b_3)^2}{I_y}$$

$$\beta_x = \frac{1}{I_x}\left[\bar{y}_b\left(\frac{t_4b_4^3}{12} + b_4t_4\,\bar{y}_b^2\right) - \bar{y}_t\left(\frac{t_2b_2^3}{12} + b_2t_2\,\bar{y}_t^2\right)\right.$$

$$- b_2^2b_1t_1\left(\frac{\bar{y}_t}{2} - \frac{b_1}{4}\right) - 2b_1t_1\left(\bar{y}_t^3 - \frac{3b_1\bar{y}_t^2}{2} + b_1^2\bar{y}_t - \frac{b_1^3}{4}\right)$$

$$\left. + \frac{\bar{y}_b^4t_3}{4} - \frac{\bar{y}_t^4t_3}{4}\right] + 2y_o$$

APPENDIX B

CALCULATION OF SECTION PROPERTIES

Section Properties required are calculated using the equations which follow. All calculations are made with reference to the line element figures below.

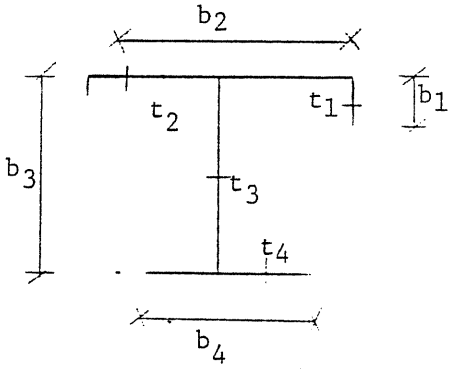

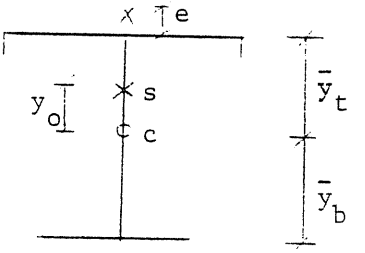

$$\text{AREA} = 2b_1t_1 + b_2t_2 + b_3t_3 + b_4t_4$$

$$\bar{y}_b = \frac{2b_1t_1(b_3 - \frac{b_1}{2}) + b_2t_2b_3 + b_3t_3\frac{b_3}{2}}{\text{AREA}}$$

$$\bar{y}_t = b_3 - \bar{y}_b$$

$$I_x = \frac{2t_1b_1^3 + b_2t_2^3 + t_3b_3^3 + b_4t_4^3}{12} + 2t_1b_1(\bar{y}_t - \frac{b_1}{2})^2$$

$$+ b_2t_2\bar{y}_t^2 + b_3t_3(\frac{b_3}{2} - \bar{y}_t)^2 + b_yt_y\bar{y}_b^2$$

EXAMPLE USING A WIDE-FLANGED BEAM WITH A CHANNEL CAP

THE NUMBER OF TERMS INCLUDED IN THE DISPLACEMENT FUNCTION IS 4 .

DIMENSIONS OF CROSS SECTION

B1 = 1.66800 IN T1 = 0.34300 IN

B2 = 5.65700 IN T2 = 0.50400 IN

B3 = 7.79000 IN T3 = 0.23000 IN

B4 = 5.25000 IN T4 = 0.30800 IN

LENGTH= 60.00 IN.

ALPHA = 0.0

RESULTS

LEFT END SECTION PROPERTIES			RIGHT END SECTION PROPERTIES		
RC	=	16.3793 IN.	RC	=	16.3793 IN.
YC	=	1.7324 IN.	YC	=	1.7324 IN.
RATIO OF STRESSES IS,LEFT TO RIGHT		1.0000 : 1.0000			
AREA	=	7.40407 IN**2	AREA	=	7.40407 IN**2
YBAR	=	5.01728 IN. FROM BOTTOM	YBAR	=	5.01728 IN. FROM BOTTOM
IX	=	78.58081 IN**4	IX	=	78.58081 IN**4
IY	=	20.47188 IN**4	IY	=	20.47188 IN**4
CW	=	206.70523 IN**6	CW	=	206.70523 IN**6
J	=	0.36901 IN**4	J	=	0.36901 IN**4
BX	=	5.32799 IN.	BX	=	5.32799 IN.

CRITICAL MOMENT AT LEFT END EQUALS 998.75830 KIP-FT.

CRITICAL MOMENT AT RIGHT END EQUALS -998.75830 KIP-FT.

```
C**********************************************************************
C**********************************************************************
C**                                                                  **
C**                              LIBT3                               **
C**                                                                  **
C**                          A PROGRAM FOR THE                       **
C**                                                                  **
C**                     ELASTIC STABILITY ANALYSIS                   **
C**                                                                  **
C**                          OF WEDGE BEAMS                          **
C**                                                                  **
C**                       UNDER MOMENT GRADIENTS                     **
C**                                                                  **
C**                              B2                                  **
C**                          ============                            **
C**                       B1 ||    ||    || B1                       **
C**                          ||    ||    ||                          **
C**                                ||                                **
C**                                ||                                **
C**                                || B3                             **
C**                                ||                                **
C**                                ||                                **
C**                                ||                                **
C**                           ==========                             **
C**                              B4                                  **
C**                                                                  **
C**      SUBMITTED BY PRISCILLA NELSON,IN PARTIAL COMPLETION OF THE  **
C**      REQUIREMENTS FOR THE MASTER'S DEGREE IN CIVIL/STRUCTURAL ENGINEERING **
C**      JULY,1979                                                   **
C**      MAJOR PROFESSOR:  DR. THOMAS M. MURRAY                      **
C**                                                                  **
C**********************************************************************
C**********************************************************************
C**                                                                  **
C**                          INPUT INSTRUCTIONS                      **
C**                                                                  **
C**           CARD ONE                                               **
C**                                                                  **
C**                FULL EIGHTY COLUMNS AVAILABLE FOR LOAD AND GEOMETRY **
C**                IDENTIFICATION. INFORMATION NOT USED IN PROGRAM.  **
C**                                                                  **
C**           CARD TWO                                               **
C**                                                                  **
C**                IN 8F10 FORMAT, ENTER BEAM CROSS-SECTION DATA.    **
C**                                                                  **
C**                B1  TOP FLANGE LIP LENGTH                         **
C**                T1  TOP FLANGE LIP THICKNESS                      **
C**                B2  TOP FLANGE LENGTH                             **
C**                T2  TOP FLANGE THICKNESS                          **
C**                B3  WEB LENGTH                                    **
C**                T3  WEB THICKNESS                                 **
C**                B4  BOTTOM FLANGE LENGTH                          **
C**                T4  BOTTOM FLANGE THICKNESS                       **
C**                                                                  **
C**           CARD THREE                                             **
C**                                                                  **
C**                IN 4F10 FORMAT, ENTER BEAM GEOMETRY AND STRESS RATIOS. **
C**                                                                  **
C**                ALPHA  TAPER                                      **
C**                XL     LENGTH                                     **
C**                ZL     RELATIVE STRESS AT LEFT END OF THE BEAM.   **
C**                       ZL=+1.0 COMPRESSION IN TOP FLANGE          **
C**                       ZL=-1.0  COMPRESSION IN BOTTOM FLANGE      **
C**                ZR     RELATIVE STRESS AT RIGHT END OF THE BEAM.  **
C**                       ZR=+1.0  COMPRESSION IN TOP FLANGE         **
C**                       ZR=-1.0  COMPRESSION IN BOTTOM FLANGE      **
C**                                                                  **
C**           LAST CARD                                              **
C**                                                                  **
C**                "END OF DATA"   STARTING IN COLUMN 2.             **
C**                                                                  **
C**********************************************************************
C**********************************************************************
```

TABLE 3.10

Summary of Error Statistics
Equations 3.6c, 3.12, 3.13 and 3.14 used in Prediction

Stress Ratio	Equations Used	Average Absolute Error, %	Mean Error, %	Standard Deviation of Error, %	No. of sections with >5% error Unconservative	conservative	Maximum Error, % Unconservative	Conservative
Wide Flange Sections								
1.00		1.89	0.57	3.05	3	3	8.1	10.9
0.50		1.99	-.19	3.32	3	4	10.9	11.0
0.00		2.07	1.10	3.21	3	2	12.7	12.2
-.50	3.13a	5.03	-.62	6.77	7	11	21.1	15.6
-1.00	3.14a	10.69	4.47	15.58	25	9	50.2	46.0
-.50	3.13b	4.92	-.64	6.73	7	11	20.9	15.5
-1.00	3.14b	10.72	4.69	15.66	25	9	49.2	46.0
Channel-Capped Sections								
1.00		2.08	2.08	2.36	9	0	9.4	
0.50		3.08	1.92	3.11	11	0	9.1	
0.00		2.76	2.65	2.41	10	0	9.1	
-.50	3.13a	13.65	8.74	22.87	25	9	100.0	16.7
-1.00	3.14a	18.47	8.85	26.27	27	9	73.8	79.3
-.50	3.13b	11.79	8.46	21.65	22	8	100.0	15.3
-1.00	3.14b	20.15	0.23	36.31	27	11	52.7	100.0

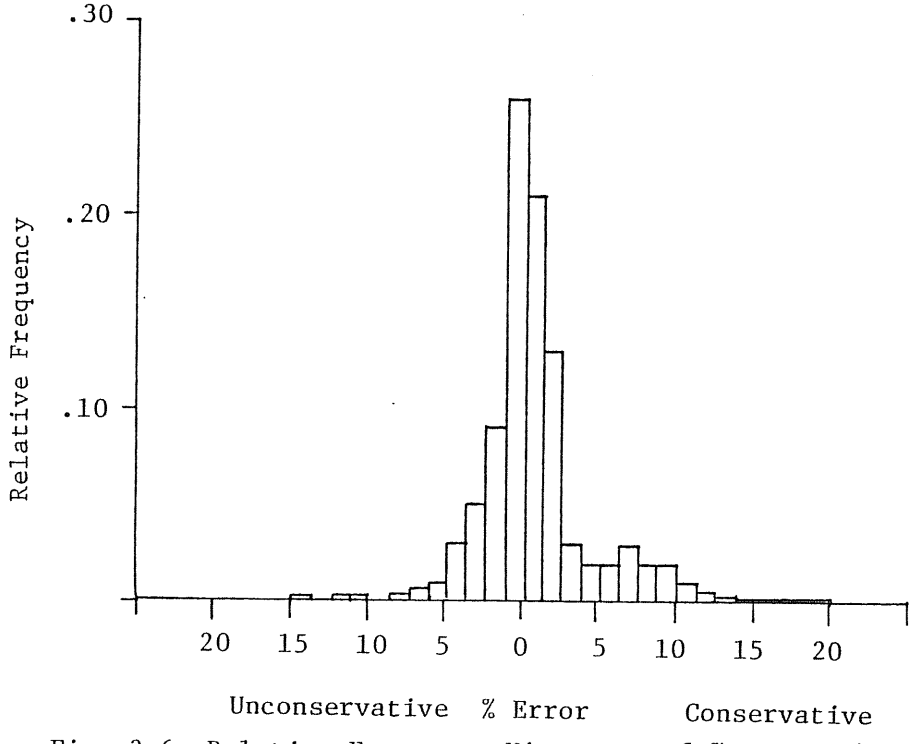

Fig. 3.6 Relative Frequency Histogram of % Errors in Prediction Using Eqs. 3.6c, 3.12, 3.13a and 3.14a

TABLE 3.8

Sections Deviating by More Than 5% From
Expected Critical Moment
Equations 3.6c and 3.12

Small End Depth	Taper	Length	Reference End	Symmetry	Flange in Compression	Stress Ratio	Error (+ Uncons.)
9.5	.05	120	Small	Single	Small	-.40	-5.5
9.5	.10	60	Small	Single	Small	-.40	-6.2
9.5	.01	240	Large	Single	Small	0.0	5.1
9.5	.01	240	Large	Single	Small	-.20	5.2
9.5	.01	240	Large	Single	Small	-.40	5.6
17.375	.05	180	Small	Single	Large	-.40	5.9
17.375	.05	240	Small	Single	Large	-.40	7.9
17.375	.10	60	Small	Single	Large	-.40	5.8
17.375	.10	120	Small	Single	Large	-.40	7.8
17.375	.05	180	Small	Single	Small	-.40	-5.3
17.375	.05	240	Small	Single	Small	-.40	-6.2
17.375	.10	120	Small	Single	Small	-.40	-7.5
17.375	.10	120	Large	Single	Large	-4.0	-5.3

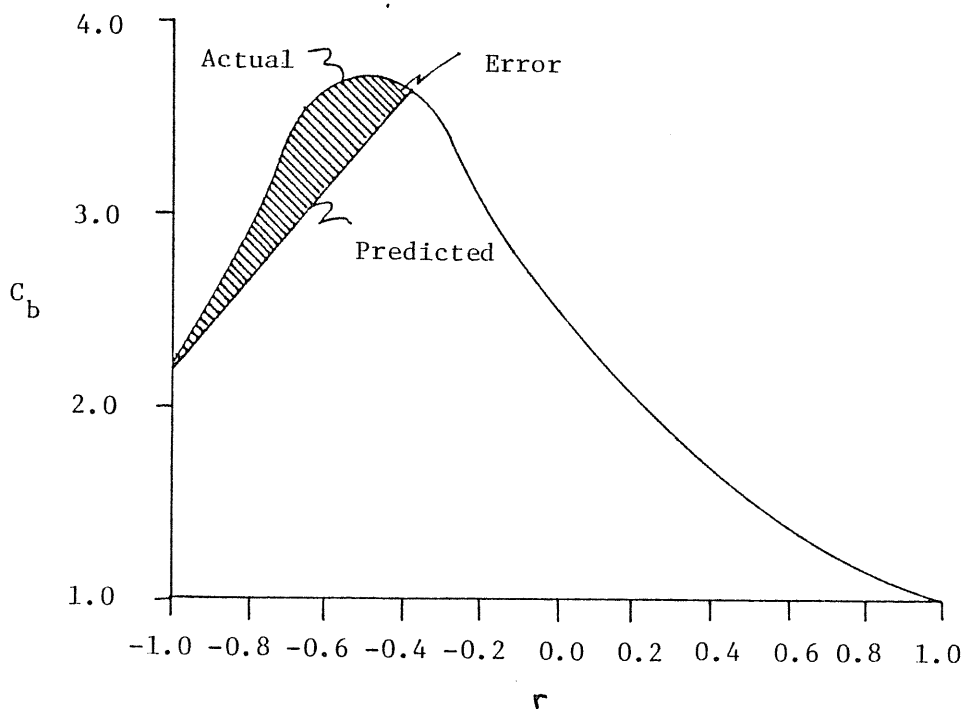

Fig. 3.5 Illustration of the Conservative Nature of the Proposed Interpolation 120" Length Doubly Symmetric Section 9.5" Depth

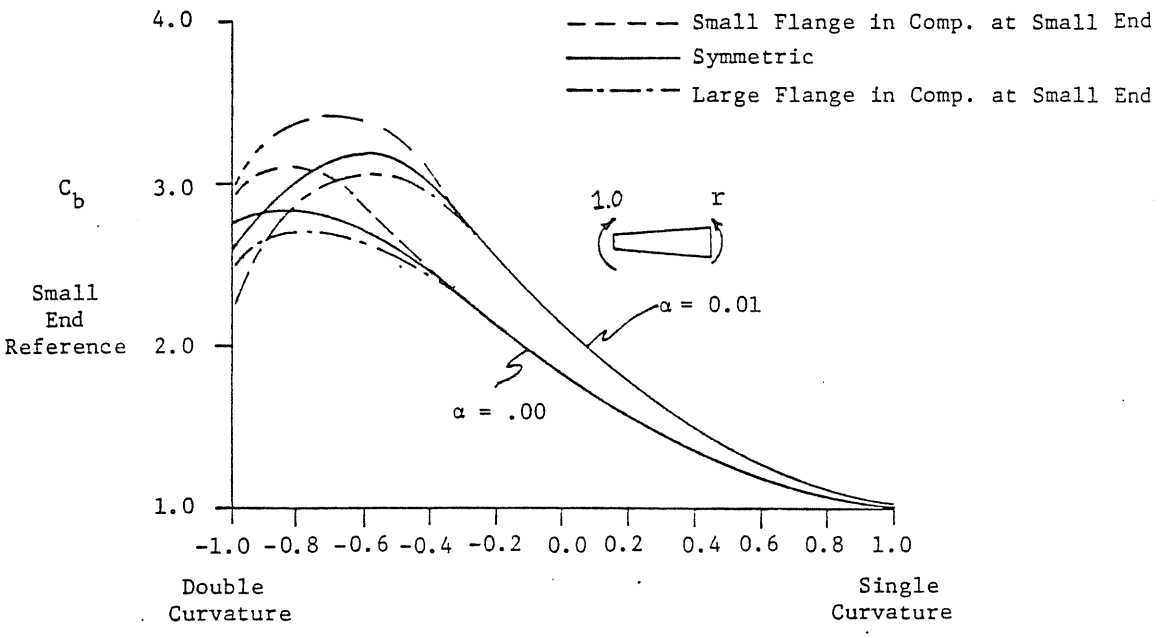

Fig. 3.3 C_b vs. r, 240" beam length

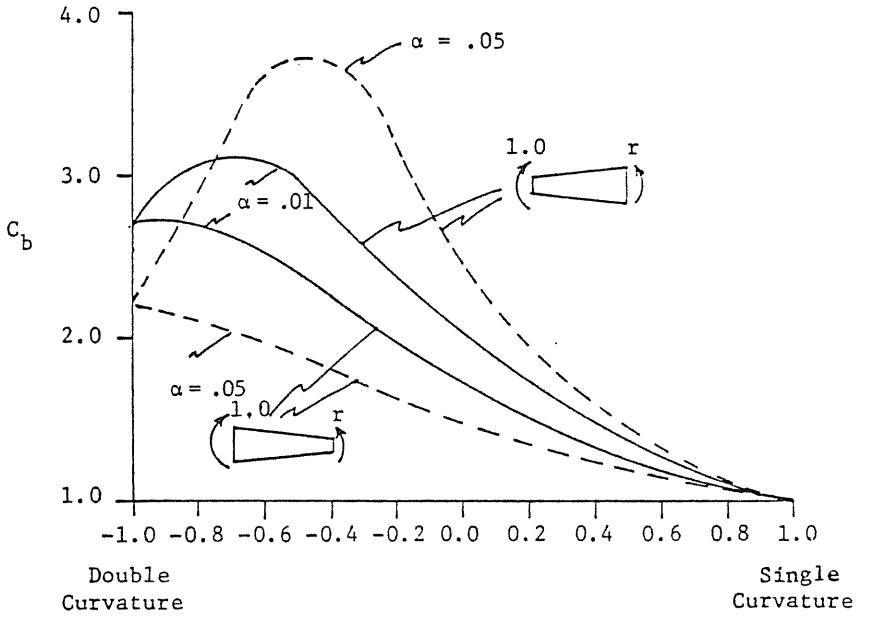

Fig. 3.4 C_b vs. r, 240" Beam Doubly Symmetric Cross Section 17.25 Depth

Table 3.4

Section Data for Determining C_b

Small End Depth in	Flange Width in	Comp. Flange Thickness in	Tension Flange Thickness in	Taper α radians	Unbraced length, in			
					60	120	180	240
9.5	6.0	0.25	0.25	0.00	X	X	X	X
				0.01	x	X	X	X
				0.05	X	X		
				0.10	X			
9.5	6.0	0.25	0.1875	0.00	X	X	X	X
				0.01	X	X	X	X
				0.05	X	X		
				0.10	X			
9.5	6.0	0.1875	0.25	0.00	X	X	X	X
				0.01	X	X	X	X
				0.05	X	X		
				0.10	X			
17.25	10.0	0.375	0.375	0.00	X	X	X	X
				0.01	X	X	X	X
				0.05	X	X	X	X
				0.10	X	X		
17.375	10.0	0.375	0.25	0.00	X	X	X	X
				0.01	X	X	X	X
				0.05	X	X	X	X
				0.10	X	X		
17.375	10.0	0.25	0.375	0.00	X	X	X	X
				0.01	X	X	X	X
				0.05	X	X	X	X
				0.10	X	X		

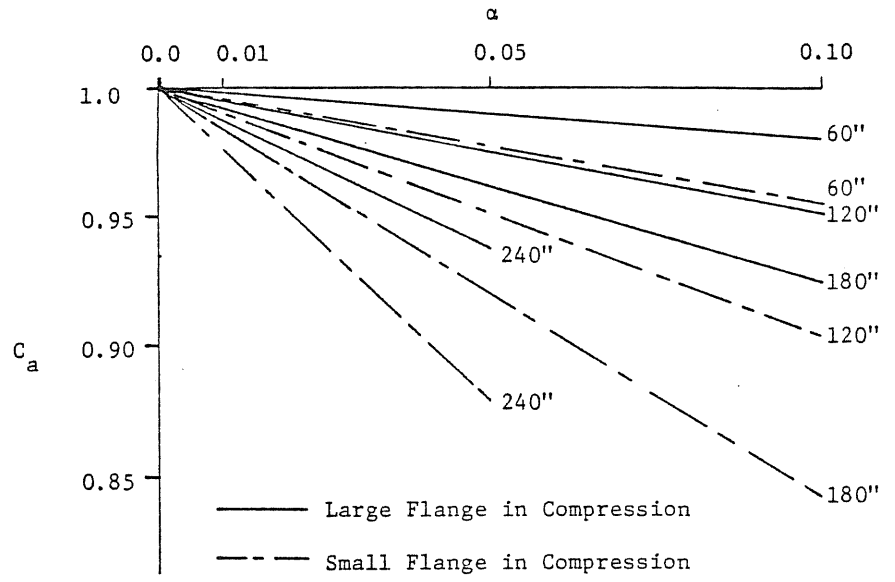

Fig. 3.1 C_α vs. α for Various Lengths, Singly Symmetric 18 in. Deep Section

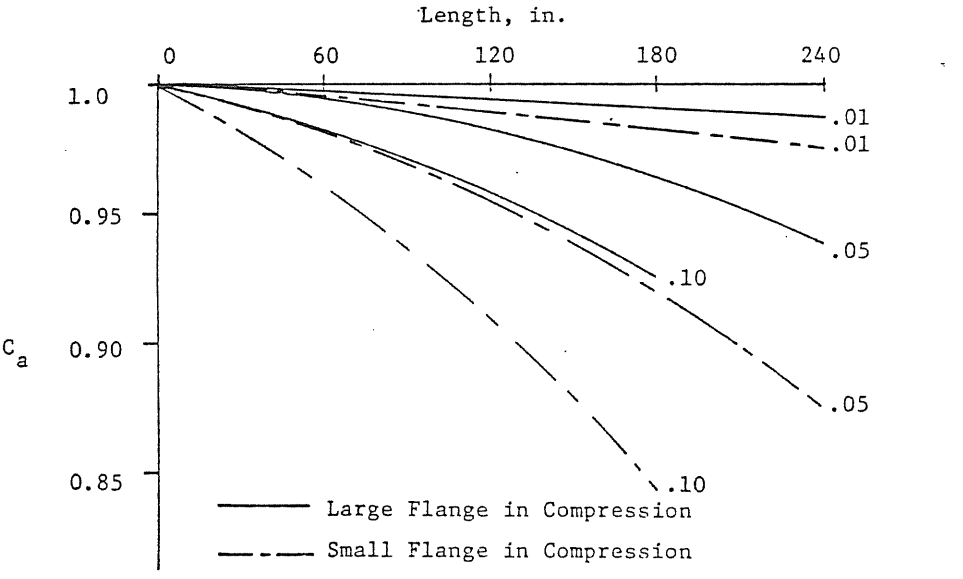

Fig. 3.2 C_α vs. Length for Various Tapers Singly Symmetric Section

Table 3.1b

Unsymmetrical Section Data
for
Determining C_a

Small End Depth in	Flange Width in	Large Flange Thickness, in				Small Flange Thickness, in				Taper α Radians	Unbraced Length, in			
		3/16	1/4	5/16	3/8	3/16	1/4	5/16	3/8		60	120	180	240
8.0	5.0		X			X				0.00	X	X	X	
										0.01	X	X	X	
										0.05	X	X		
										0.10	X			
12.0	5.0		X			X				0.00	X	X	X	X
										0.01	X	X	X	X
										0.05	X			
	6.0		X			X				0.00	X	X	X	X
										0.01	X	X	X	X
										0.05	X	X		
										0.10	X			
	8.0		X			X				0.00	X	X	X	X
										0.01	X	X	X	X
										0.05	X	X	X	X
										0.10	X	X		
18.0	6.0		X			X				0.00	X	X	X	X
	8.0		X			X				0.00	X	X	X	X
										0.01	X	X	X	X
										0.05	X	X		
										0.10	X			
	10.0				X		X	X		0.00	X	X	X	X
										0.01	X	X	X	X
										0.05	X	X	X	X
										0.10	X	X		
	12.0				X		X	X		0.00	X	X	X	X
										0.01	X	X	X	X
										0.05	X	X	X	X
										0.10	X	X	X	
24.0	8.0		X			X				0.00	X	X	X	X
	10.0				X		X	X		0.00	X	X	X	X
										0.01	X	X	X	X
										0.05	X	X		
										0.10	X			
	12.0				X		X	X		0.00	X	X	X	X
										0.01	X	X	X	X
										0.05	X	X	X	X
										0.10	X	X		

Table 3.1a

Symmetrical Section Data
for
Determining C_a

Small End Depth in	Flange Width in	Flange Thickness, in							Taper α radians	Unbraced Length, in			
		3/16	1/4	5/16	3/8	1/2	5/8	3/4		60	120	180	240
6.0	3.0	X							0.00	X	X		
									0.01	X	X		
									0.05	X			
	4.0	X	X						0.00	X	X		
									0.01	X	X		
									0.05	X	X		
8.0	3.0	X							0.00	X	X	X	
									0.01	X			
	4.0	X	X						0.00	X	X	X	
									0.01	X	X	X	
									0.05	X			
	5.0	X	X	X					0.00	X	X	X	
									0.01	X	X	X	
									0.05	X	X		
									0.10	X			
12.0	4.0	X	X						0.00	X	X	X	X
	5.0	X	X	X					0.00	X	X	X	X
									0.01	X	X	X	X
									0.05	X			
	6.0	X	X	X	X				0.00	X	X	X	X
									0.01	X	X	X	X
									0.05	X	X		
									0.10	X			
	8.0	X	X	X	X	X			0.00	X	X	X	X
									0.01	X	X	X	X
									0.05	X	X	X	X
									0.10	X	X		
18.0	6.0	X	X	X	X				0.00	X	X	X	X
	8.0	X	X	X	X	X			0.00	X	X	X	X
									0.01	X	X	X	X
									0.05	X	X		
									0.10	X			
	10.0		X	X	X	X	X		0.00	X	X	X	X
									0.01	X	X	X	X
									0.05	X	X	X	X
									0.10	X	X		
	12.0		X	X	X	X	X	X	0.00	X	X	X	X
									0.01	X	X	X	X
									0.05	X	X	X	X
									0.10	X	X	X	
24.0	8.0	X	X	X	X	X			0.00	X	X	X	X
	10.0		X	X	X	X	X		0.00	X	X	X	X
									0.01	X	X	X	X
									0.05	X	X		
									0.10	X			
	12.0		X	X	X	X	X	X	0.00	X	X	X	X
									0.01	X	X	X	X
									0.05	X	X	X	X
									0.10	X	X		

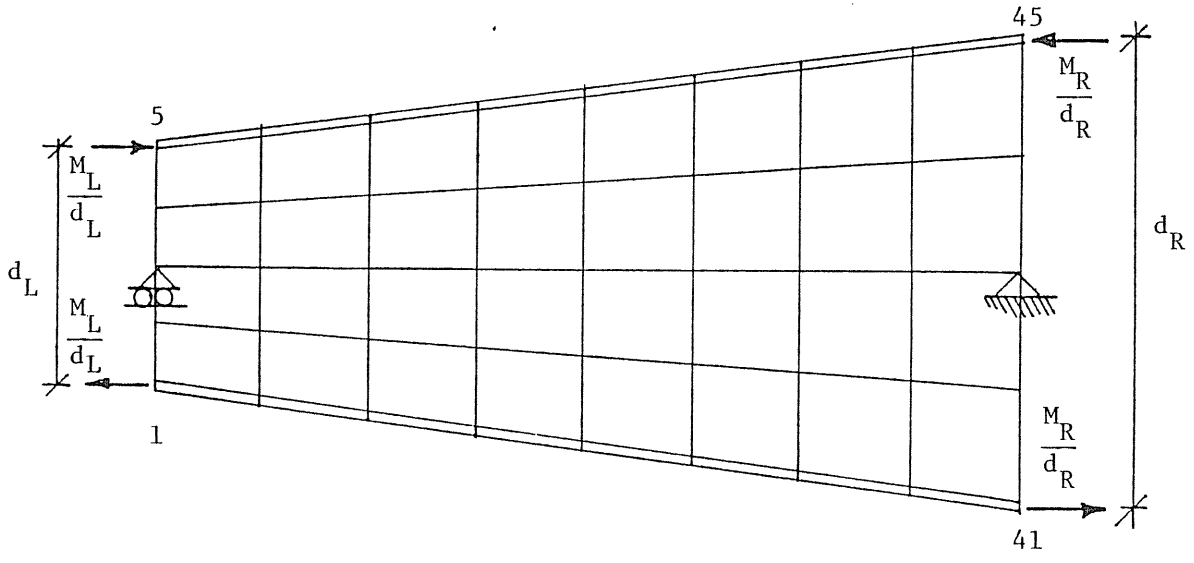

In-plane Boundary Conditions
at 3 u = 0

at 43 u = 0

v = 0

Out-of-Plane Boundary Conditions at
1, 2, 3, 4, 5, 41, 42, 43, 44, 45 w = 0

$\theta_k = 0$

Fig. 2.14 4 x 8 Finite Element Mesh

TABLE 2.3

"C" Values for Prismatic
Doubly Symmetric Members

Section	Stress Ratio	Chi(18)	Culver and Preg(10)	Proposed
I — 4 x .25 / 6 x .1875 / 4 x .25, Length = 60"	+1.0	1.00	1.00	1.00
	+0.5	1.32	1.32	1.32
	0.0	1.83	1.85	1.85
	-0.5	2.48	2.60	2.61
	-1.0	2.49	2.74	2.75
III — 6 x .3125 / 14 x .400 / 6 x .3125, Length = 180"	+1.0	1.00	1.00	1.00
	+0.5	1.32	1.32	1.32
	0.0	1.79	1.84	1.84
	-0.5	2.29	2.57	2.58
	-1.0	2.19	2.72	2.72

TABLE 2.2

Percent Differences Observed Between the Proposed Method, Exact Solutions and the Method of Chi (18).

Section	Taper	Length	Stress Ratio	% Differences* Exact.	% Differences* Chi	Taper	Length	Stress Ratio	% Differences* Chi
I: 4 x .25 / 6 x .1875 / 4 x .25	0.0	60"	+1.0	0.00	+0.05	0.01	180"	+1.0	+0.38
			+0.5		-0.11			+0.5	-0.88
			0.0		-1.17			0.0	-7.42
			-0.5		-4.79			-.5	-24.27
			-1.0		-9.37			-1.0	-25.55
II: 5 x .3125 / 10 x .375 / 5 x .1799	0.0	120"	+1.0	0.00	+0.04	0.05	120"	+1.0	+2.73
			+0.5		-0.57			0.5	-0.06
			0.0		-3.54			0.0	-8.39
			-0.5		-13.66			-0.5	-17.56
			-1.0		-20.29			-1.0	-3.68
III: 6 x .3125 / 14 x .400 / 6 x .3125	0.0	180"	+1.0	0.00	+0.05	0.05	180"	+1.0	+2.47
			+0.5		-0.38			+0.5	+0.01
			0.0		-2.99			0.0	-7.64
			-0.5		-11.00			-0.5	-18.62
			-1.0		-20.02			-1.0	-3.24
IV: 6 x .25 / 18 x .4375 / 6 x .1799	0.0	240"	+1.0	0.00	+0.04	0.05	240"	+1.0	+2.68
			+0.5		-0.70			+0.5	+0.52
			0.0		-5.17			0.0	-9.41
			-0.5		-17.87			-0.5	-23.83
			-1.0		-28.05			-1.0	-7.69
V: 6 x .1799 / 18 x .4375 / 6 x .25	0.0	240"	+1.0	-0.02	+0.04	0.05	240"	+1.0	+2.07
			+0.5		-0.69			+0.5	+0.38
			0.0		-4.81			0.0	-8.45
			-0.5		-15.41			-0.5	-26.61
			-1.0		-28.05			-1.0	-10.52

*% Differences based on comparison of 4-term displacement function solutions. Minus sign indicates solution less than proposed method solution.

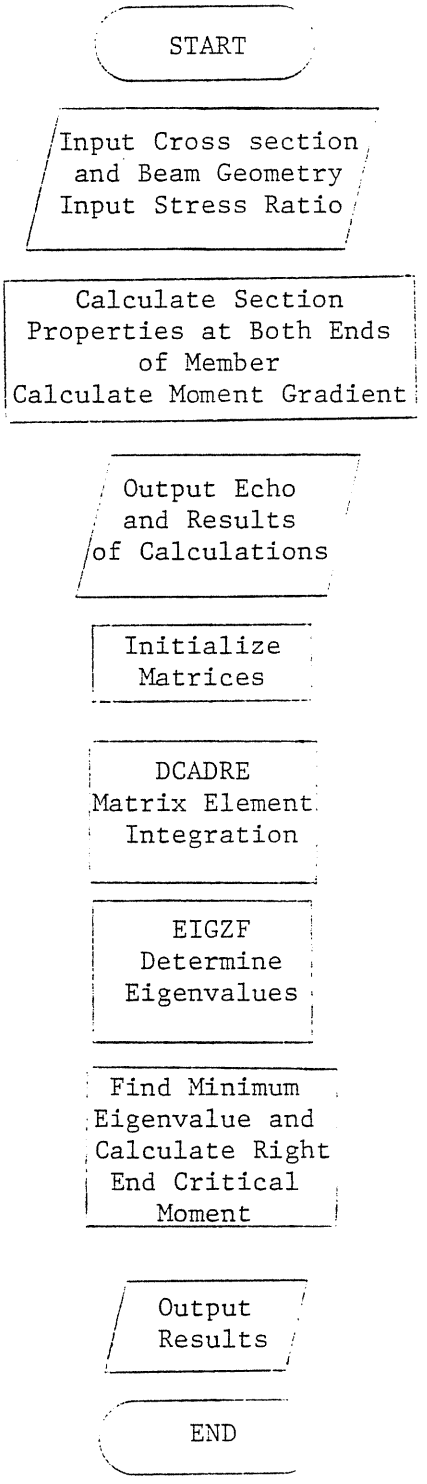

Fig. 2.13 Macro-Flowchart for Computer Program

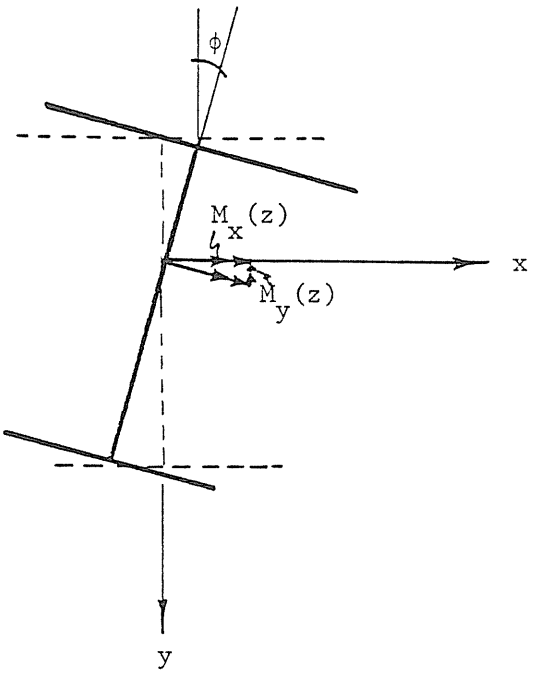

Fig. 2.11 Applied Minor Axis Moment

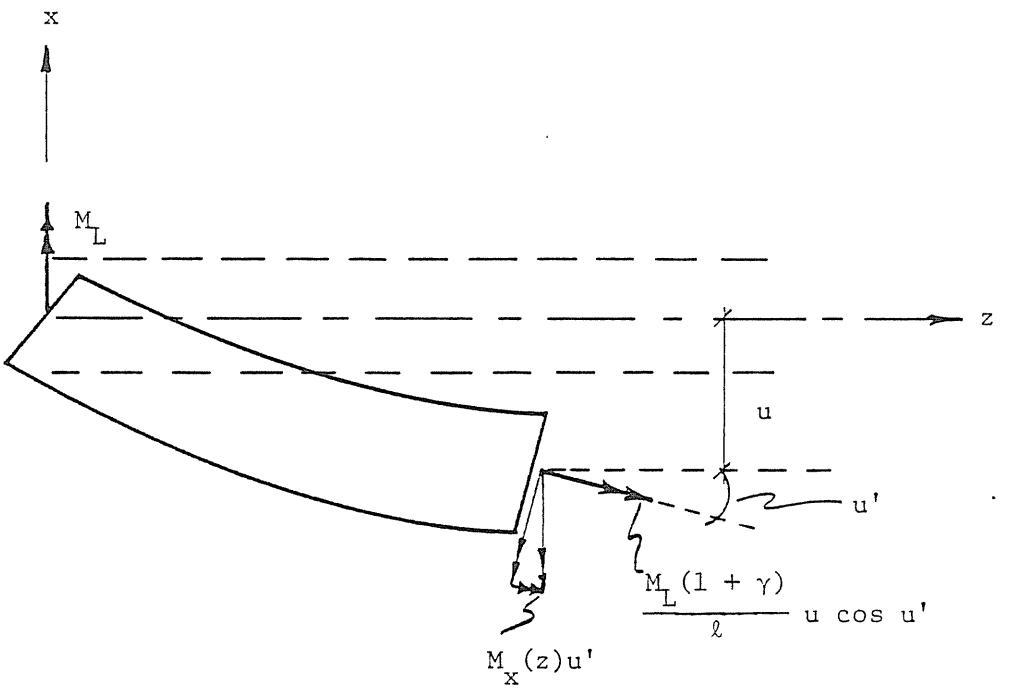

Fig. 2.12 External Applied Torque (plan view)

where γ is the end moment ratio

$$\gamma = \frac{M_R}{M_L} \tag{2.37}$$

Referring to Fig. 2.11, and assuming that ϕ is small, so that $\sin\phi$ may be approximated as ϕ, the y-axis moment can be written as

$$M_y(z) = -M_x(z)\phi = -M_L\phi(1 - (\gamma + 1)\frac{z}{\ell}) \tag{2.38}$$

With reference to Fig. 2.12, it can be seen that external torque is supplied from two sorces: (1) The reaction, indicated in Fig. 2.10, produces a torsional component as it acts through the out-of-plane displacement, u. (2) This displacement also generates a torsional component from the major axis bending. Thus, the total external torque, again assuming small angles so that $\cos u'$ may be approximated as 1.0, may be written as

$$T_{sc} = M_L(1 - (1 + \gamma)\frac{z}{\ell})u' + M_L(\frac{1 + \gamma}{\ell})u \tag{2.39}$$

and if I_y is assumed constant for a beam tapered in depth only, the complete equations become:

In-plane Bending

$$M_L(1 - (1 + \gamma)\frac{z}{\ell}) = -EI_x(z)v'' \tag{2.40}$$

Out of Plane Bending

$$-M_L\phi(1 - (1 + \gamma)\frac{z}{\ell}) = EI_y u'' \tag{2.41}$$

Torsion

$$M_L u'(1 - (1 + \gamma)\frac{z}{\ell}) + M_L(\frac{1 + \gamma}{\ell})u = GJ(z)\phi' - \frac{d}{dz}(EI_w(z)\phi'') - \frac{d}{dz}(EI_{w\psi}(z)\phi')$$

$$+ EI_{w\psi}(z)\phi'' + EI_{\psi}(z)\phi' + M_L(1 - (1 + \gamma)\frac{z}{\ell})[\beta_x(z)\phi' + \bar{\beta}_x(z)\phi] \tag{2.42}$$

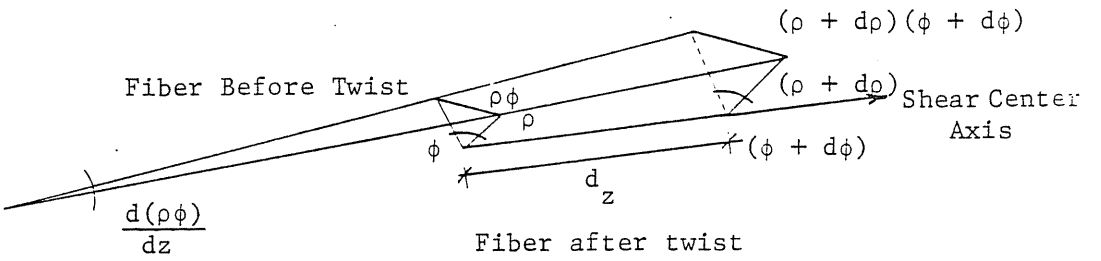

Fig. 2.8 Displacement of Longitudinal Fiber During Twisting (after Trahair, (21))

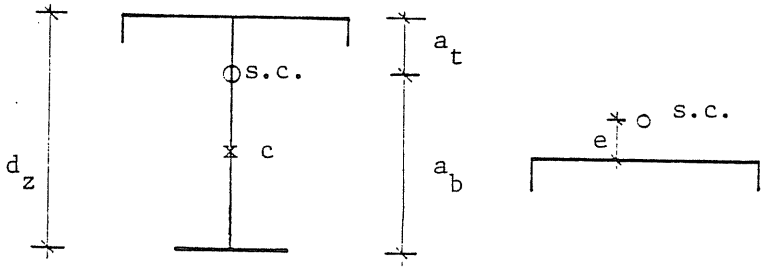

Fig. 2.9 Generalized Mono-Symmetric Cross-Section

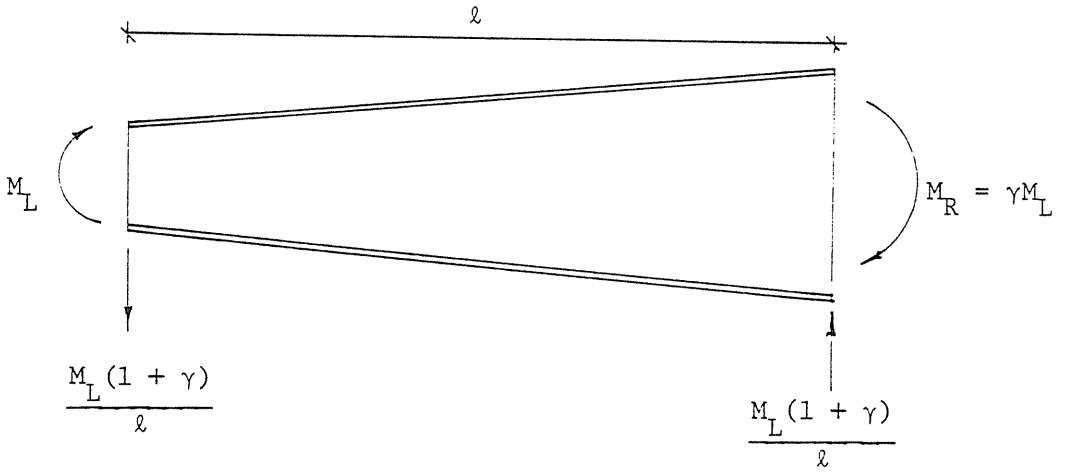

Fig. 2.10 Applied Major Axis Loading Condition

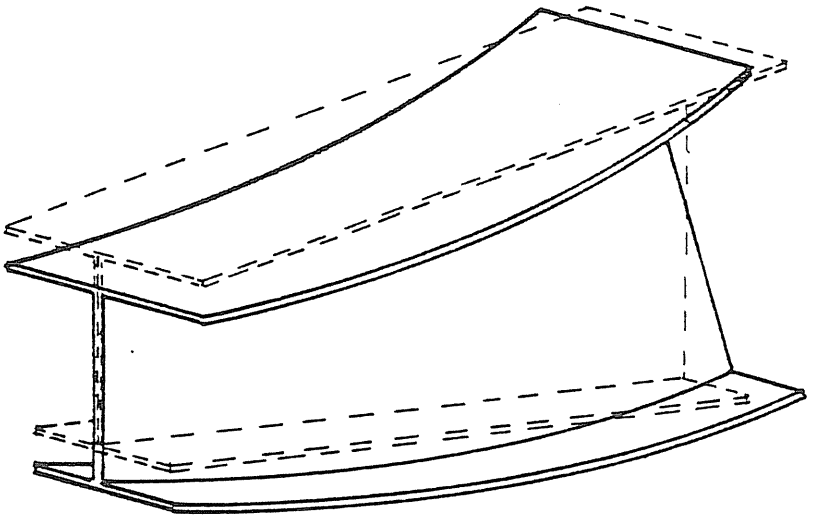

Fig. 2.7a The Wagner Effect - Major Axis Bending of a Singly Symmetric Beam

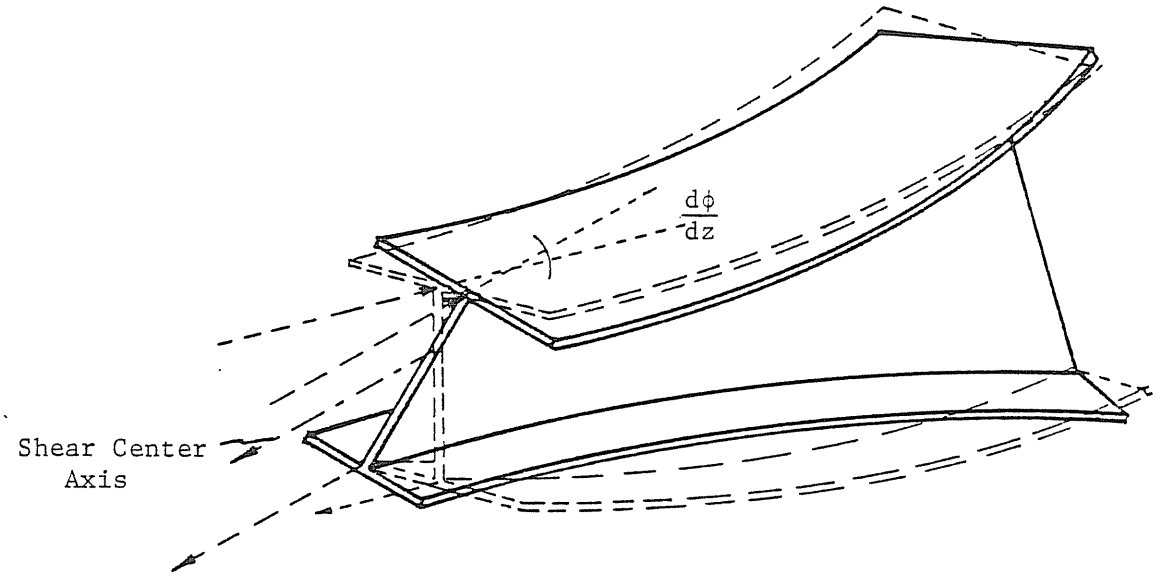

Fig. 2.7b The Wagner Effect - Shear Center Twist Producing a Disturbing Torque as Flange Force Vectors Are Rotated

$$\frac{-d}{dz}(a_t M_{ft} - a_b M_{fb}) = \frac{-Ed}{dz}[\frac{I_{fb}I_{ft}}{I_y}d_z u'' - \frac{I_{ft}I_{fb}}{I_y}d_z u'' + \frac{I_{fb}d_z}{I_y}\frac{d^2}{dz^2}(a_t\phi) + \frac{I_{ft}d_z}{I_y}\frac{d^2}{dz^2}(a_b\phi)] \qquad (2.19)$$

Noting that the u" terms cancel, expanding and neglecting second order derivatives of "a" as small, this term becomes

$$\frac{-d}{dz}(a_t M_{ft} - a_b M_{fb}) = \frac{-Ed}{dz}[a_t^2 I_{ft}\phi'' + a_b^2 I_{fb}\phi'' - 2(a_t I_{ft} a_t' + a_b I_{fb} a_b')\phi'] \qquad (2.20)$$

A similar sequence of substitutions into the second term of equation 2.18 results in the following equation for the flange warping component of torsion,

$$T_f = \frac{-d}{dz}(EI_w\phi'')\frac{-d}{dz}(EI_{w\psi}\phi') + EI_{\psi x}u'' + EI_{w\psi}\phi'' + EI_{\psi}\phi' \qquad (2.21)$$

where the additional beam properties are defined as

$$I_w = a_t^2 I_{ft} + a_b^2 I_{fb} \qquad (2.22a)$$

$$I_{w\psi} = 2(a_t I_{ft} a_t' + a_b I_{fb} a_b') \qquad (2.22b)$$

$$I_{wx} = a_t' I_{ft} - a_b' I_{fb} \qquad (2.22c)$$

$$I = 4[(a_t')^2 I_{ft} + (a_b')^2 I_{fb}] \qquad (2.22d)$$

When a monosymmetric thin-walled beam loaded in its plane of symmetry is twisted, as in the case of lateral torsional buckling, normal stresses present will exert an additional disturbing torque.

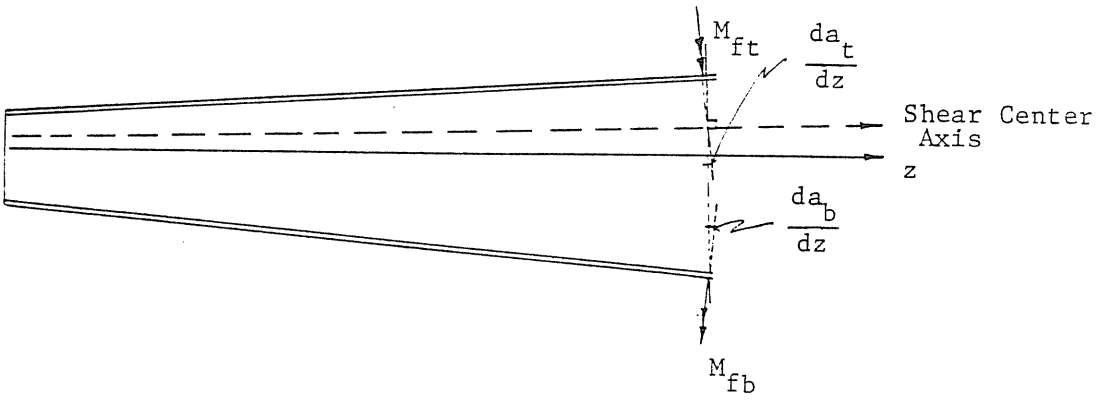

Fig. 2.5 Inclination of Flange Moments

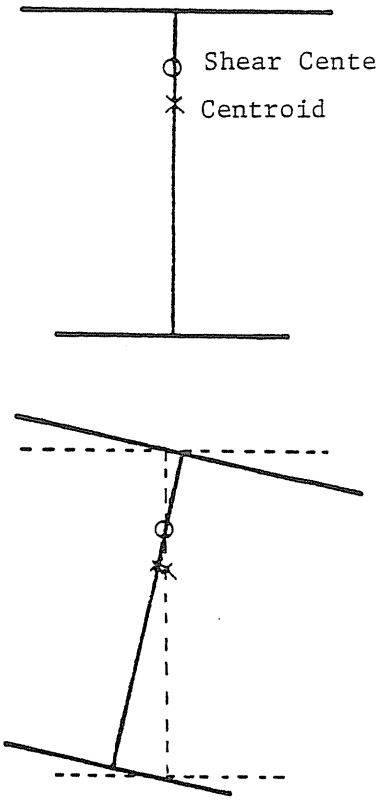

Fig. 2.6 Displacement and Rotation of a Mono-Symmetric Cross Section

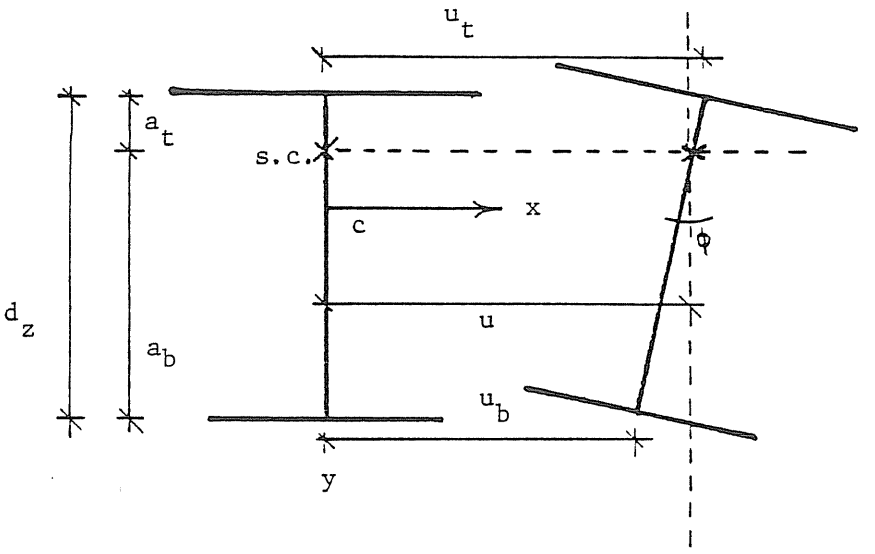

Fig. 2.3 Out-of-Plane Deflection Coupled with Twisting

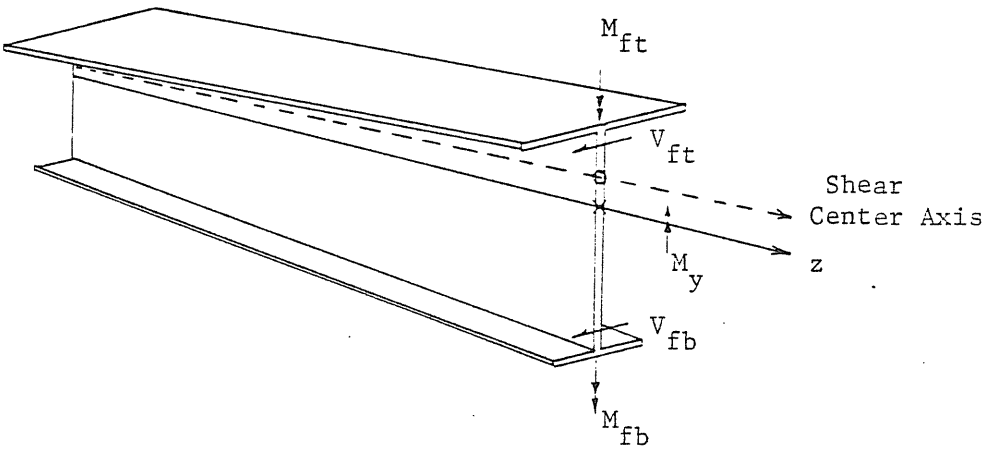

Fig. 2.4 Relationship of Flange Shears and Flange Moments

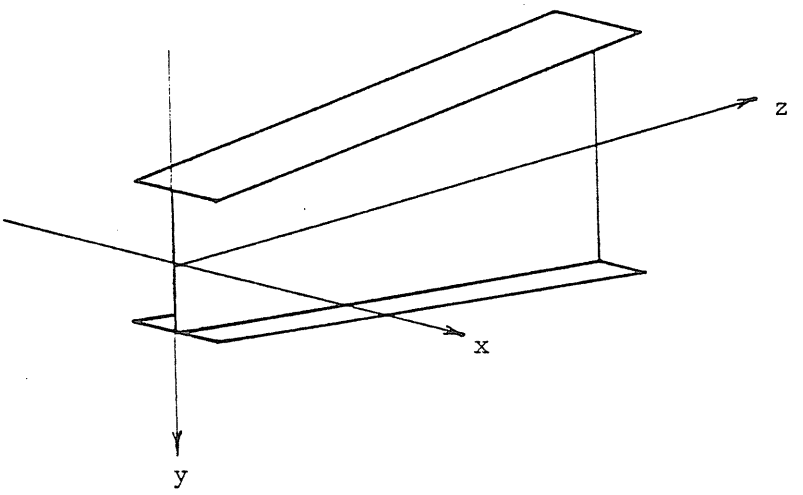

Fig 2.1 Centroidal Coordinate System

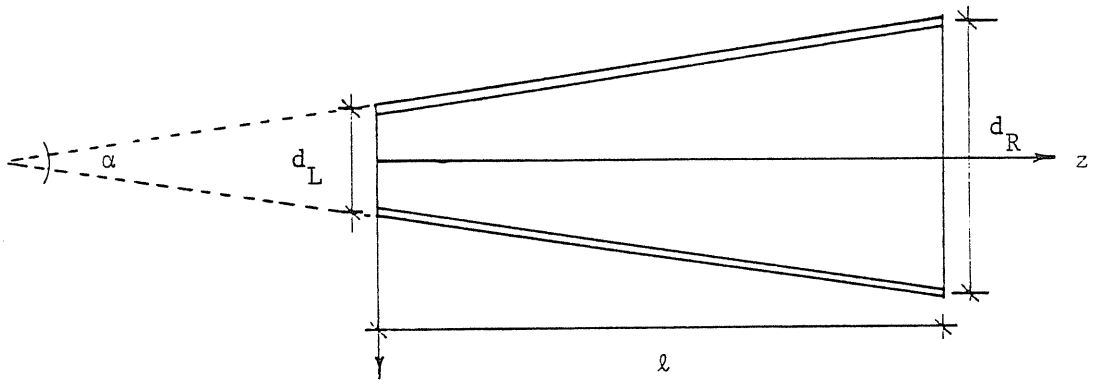

Fig. 2.2 Tapered Beam Geometry